

EFFECT OF PICK BLUNTING ON CUTTING PERFORMANCE
FOR WEAK-MODERATE ROCKS

A THESIS SUBMITTED TO
THE GRADUATE SCHOOL OF NATURAL AND APPLIED SCIENCES
OF
MIDDLE EAST TECHNICAL UNIVERSITY

BY

CİHAN DOĞRUÖZ

IN PARTIAL FULFILLMENT OF THE REQUIREMENTS
FOR
THE DEGREE OF DOCTOR OF PHILOSOPHY
IN
MINING ENGINEERING

SEPTEMBER 2010

Approval of the thesis:

**EFFECT OF PICK BLUNTING ON CUTTING PERFORMANCE
FOR WEAK-MODERATE ROCKS**

submitted by **CİHAN DOĞRUÖZ** in partial fulfillment of the requirements
for the degree of **Doctor of Philosophy in Mining Engineering Department,**
Middle East Technical University by,

Prof. Dr. Canan Özgen
Dean, Graduate School of **Natural and Applied Sciences**

Prof. Dr. Ali İhsan Arol
Head of Department, **Mining Engineering**

Prof. Dr. Naci Bölükbaşı
Supervisor, **Mining Engineering Dept., METU**

Examining Committee Members:

Prof. Dr. Tevfik Güyagüler
Mining Engineering Dept., METU

Prof. Dr. Naci Bölükbaşı
Mining Engineering Dept., METU

Prof. Dr. Bahtiyar Ünver
Mining Engineering Dept., Hacettepe University

Assoc. Prof. Dr. H. Aydın Bilgin
Mining Engineering Dept., METU

Prof. Dr. Kaan Erarlan
Mining Engineering Dept., Dumlupınar University

Date: 17.09.2010

I hereby declare that all information in this document has been obtained and presented in accordance with academic rules and ethical conduct. I also declare that, as required by these rules and conduct, I have fully cited and referenced all material and results that are not original to this work.

Name, Last name : Cihan Doğruöz

Signature :

ABSTRACT

EFFECT OF PICK BLUNTING ON CUTTING PERFORMANCE FOR WEAK-MODERATE ROCKS

DOĞRUÖZ, Cihan

Ph.D., Department of Mining Engineering

Supervisor: Prof. Dr. Naci BÖLÜKBAŞI

September 2010, 144 pages

The laboratory cutting specific energy is widely used to estimate the cuttability of rocks by a roadheader fitted with sharp picks. Sharp picks on the other hand become blunt due to wear in time and require replacement. Although it is known that the pick blunting affects adversely the rock cuttability, no study exists to show the relationships between the degree of pick wear and the cutting specific energy obtained by standard cutting tests. In this study, standard cutting tests were carried out on different rock types, with picks having varying degrees of blunting. The relationships between wear flats and the cutting forces, specific energies and size distribution for various rock properties such as uniaxial compressive strength, tensile strength, cone indenter number, shore hardness, schmidth hammer hardness, density and grain size were established. The mean cutting force and the cutting specific energy have been found to increase 2-3 times and 4-5 times respectively with 4 mm wear flat as compared to sharp picks as the strength and density of rocks increase. No relation exists between mineral grain size and the cutting performance. A definite relation could not be established between the wear land and the size distribution of the product. Charts have been produced to predict critical wear flats for different rock property values considering 25 MJ/m³ as the limiting specific

energy above which poor cutting performance occurs. Nine prediction models have been developed by statistical analysis to estimate the laboratory cutting specific energy from various rock properties and wear rates.

Keywords: Laboratory Cutting Specific Energy, Wear Flat, Roadheader Cutting Tool, Standard Cutting Test

ÖZ

ZAYIF VE ORTA SERTLİKTEKİ KAYAÇLAR İÇİN KESİCİ UÇLARDAKİ KÖRLENMENİN KESME PERFORMANSINA ETKİSİ

DOĞRUÖZ, Cihan

Doktora, Maden Mühendisliği Bölümü

Tez Yöneticisi: Prof. Dr. Naci BÖLÜKBAŞI

Eylül 2010, 144 sayfa

Kayaçların keskin uçlarla donatılmış galeri açma makinaları ile kesilebilirliğini tahmin etmek için laboratuvar kesme enerjisi yaygın bir şekilde kullanılmaktadır. Keskin uçlar ise aşınmaya bağlı olarak zamanla körleşmekte ve değiştirilmeleri gerekmektedir. Kesici uçlardaki körleşmenin kayaçların kesilebilirliğini olumsuz etkilediği bilinmekle birlikte, körleşme derecesi ile standart kesme deneyleri sonucu elde edilen kesme özgül enerjisi arasındaki ilişki üzerine bir çalışma henüz bulunmamaktadır. Bu çalışmada, değişik körleşme derecelerindeki kesici uçlar kullanılarak değişik kayaçlar üzerinde standart kesme deneyleri yapılmıştır. Aşınma yüzeyi genişliği ile kesme özgül enerjisi, kesme kuvveti ve parça tane büyüklüğü dağılımı arasındaki ilişkiler, tek eksenli basma dayanımı, çekme dayanımı, koni delici sertliği, shore sertliği, schmidth çekici sertliği, birim hacim ağırlığı ve mineral tane büyüklüğü gibi kayaç özellikleri için saptanmıştır. Ortalama kesme kuvveti ve kesme enerjisinin, kaya dayanımı ve yoğunluğu arttıkça, keskin uçlara göre sırasıyla 2-3 kat ve 4-5 kat arttığı saptanmıştır. Mineral tane büyüklüğü ile kesme performansı arasında bir ilişki bulunmamaktadır. Aşınma yüzeyi ile malzeme tane büyüklüğü arasında belirli bir ilişki saptanamamıştır. Kötü kesme performansını belirleyen sınır özgül enerji değeri 25 MJ/m^3 kabul edilerek, değişik kaya özelliği

değerlerinde kritik aşınma yüzey genişliklerinin tahmini için grafikler oluşturulmuştur. Laboratuvar kesme özgül enerjisini, çeşitli kaya özellikleri ve aşınma derecelerinden tahmin etmek üzere istatistiksel analiz yöntemi ile dokuz model geliştirilmiştir.

Anahtar Kelimeler: Laboratuvar Kesme Özgül Enerjisi, Aşınma Yüzeyi Genişliği, Galeri Açma Makinesi Kesme Ucu, Standart Kesme Deneyi

To My Family

ACKNOWLEDGEMENTS

I would like to express my deepest gratitude to my supervisor, Prof. Dr. Naci Bölükbaşı, for his guidance, helpful comments and advice throughout thesis.

I want to thank to the examining committee members, Prof. Dr. Tevfik Güyagüler, Assoc. Prof. Dr. H. Aydın Bilgin, Prof. Dr. Bahtiyar Ünver and Prof. Dr. Kaan Erarslan for their valuable comments and suggestions.

I wish to express my appreciation to Tahsin Işıksal, İsmail Kaya and Hakan Uysal for their help with the experiments.

I would like to show my gratitude to my best friends Cemil Acar, İlker Acar, Barış Çakmak, Barış Arslan and Emrah Bakır. Also I want to express my appreciation to my special friend Burcu Erkmen for her supports.

Finally, I want to express my deepest appreciation to my family, especially my elder brother Mustafa Doğruöz, for their patience, care and support.

TABLE OF CONTENTS

ABSTRACT.....	iv
ÖZ.....	vi
ACKNOWLEDGEMENTS.....	ix
TABLE OF CONTENTS.....	x
LIST OF TABLES.....	xiv
LIST OF FIGURES.....	xvi
LIST OF SYMBOLS.....	xx

CHAPTERS

1. INTRODUCTION

1.1. General.....	1
1.2.Objective and Scope of the Thesis.....	2

2. LITERATURE REVIEW

2.1.Boom Type Roadheaders.....	6
2.1.1. Introduction.....	6
2.1.2.Classification.....	6
2.1.2.1. Classification According to Times of Production.....	6
2.1.2.2.Classification According to Weight.....	7
2.1.3.Basic Components.....	10
2.1.3.1.Boom, Cutting Head and Cutting Picks.....	10
2.1.3.2.Loading Unit.....	12
2.1.3.3.Haulage Unit.....	13
2.2.Roadheader Performance Prediction.....	13
2.2.1.Uniaxial Compressive Strength.....	14
2.2.2.Tensile Strength and Shear Strength.....	21
2.2.3.Cone Indenter Hardness.....	21
2.2.4.Shore Hardness.....	22

2.2.5. Schmidt Rebound Hardness.....	23
2.2.6. Laboratory Cutting Specific Energy.....	24
2.3. Wear Mechanisms in Rock Cutting.....	28
2.3.1. Abrasive Wear.....	28
2.3.2. Rock Abrasiveness.....	28
2.3.3. Tool Material and Manufacturing Techniques.....	30
2.3.4. Micro Chipping.....	32
2.3.5. Gross Failure.....	33
2.3.6. Thermal Cracking.....	34
2.4. Effect of Pick Blunting on Cutting Performance.....	34
3. EXPERIMENTAL PROCEDURE	
3.1. Rock Property Tests.....	39
3.1.1. Uniaxial Compressive and Tensile Strength Tests.....	39
3.1.2. Cone Indenter Test.....	39
3.1.2.1. Apparatus.....	39
3.1.2.2. Procedure.....	40
3.1.2.3. Calculation.....	40
3.1.3. Shore Hardness Test.....	41
3.1.4. Schmidt Rebound Hardness Test.....	42
3.1.5. Petrographic Analyses.....	42
3.1.6. Density Determination.....	43
3.2. Laboratory Cutting Tests.....	43
3.2.1. The Rock Cutting Set-Up.....	43
3.2.1.1. Shaping Machine.....	44
3.2.1.2. Triaxial Dynamometer.....	44
3.2.1.3. Recording Unit.....	45
3.2.1.4. Calibration.....	45
3.2.1.5. Standard Conditions for a Cutting Test and the Degrees of Blunting.....	46
3.3. Size Distribution and Coarseness Index.....	48

4. EXPERIMENTAL RESULTS AND DISCUSSIONS

4.1. Rock Property Test Results.....	49
4.2. Thin Section Results.....	50
4.3. Cutting Test Results.....	52
4.4. Relationships Between Laboratory Cutting Specific Energy, Mean Cutting Force and Wear Flats With Uniaxial Compressive Strengths.....	55
4.5. Relationships Between Laboratory Cutting Specific Energy, Mean Cutting Force and Wear Flats With Tensile Strengths.....	59
4.6. Relationships Between Laboratory Cutting Specific Energy, Mean Cutting Force and Wear Flats with Cone Indenter Hardness.....	63
4.7. Relationships Between Laboratory Cutting Specific Energy, Mean Cutting Force and Wear Flats With Shore Hardness.....	67
4.8. Relationships Between Laboratory Cutting Specific Energy, Mean Cutting Force and Wear Flats With Schmidt Hammer Hardness.....	71
4.9. Relationships Between Laboratory Cutting Specific Energy, Mean Cutting Force and Wear Flats With Density.....	75
4.10. Effect of Mineral Grain Size on Cutting Specific Energy.....	79
4.11. Effect of Breakout Angle.....	81
4.12. Effect of Wear Flat on Size Distribution and Coarseness Index.....	82
4.13. Rock Property Value Limits Causing Poor Cutting Performance at Different Wear Flats.....	103

5. EVALUATION OF RESULTS AND ESTABLISHING MODELS BY STATISTICAL ANALYSES

5.1. MODEL 1.....	105
5.2. MODEL 2.....	107
5.3. MODEL 3.....	109
5.4. MODEL 4.....	111
5.5. MODEL 5.....	113
5.6. MODEL 6.....	115
5.7. MODEL 7.....	117

5.8. MODEL 8.....	119
5.9. MODEL 9.....	121
5.10.COMPARISON OF MODELS.....	123
6. CONCLUSIONS AND RECOMMENDATIONS.....	131
REFERENCES.....	135
VITA.....	144

LIST OF TABLES

TABLES

Table 2.1. Classification According to Weight.....	7
Table 2.2. Properties of Typical Roadheaders.....	8
Table 2.3. Factors Influencing Roadheader Performance and Tool Consumption Rates.....	13
Table 2.4. Correlations Between Cone Indenter Number and Machine Performance.....	22
Table 2.5. Roadheader Performance Relative to Laboratory Specific Energy.....	26
Table 2.6. The Effect of Systematic Blunting on the Forces Required to Cut Grooves in Cwmtillery, Graw Coal.....	36
Table 3.1. Calculation of Coarseness Index.....	48
Table 4.1. Rock Property Test Results.....	50
Table 4.2. Petrographic Characteristics.....	51
Table 4.3. Mineral Grain Sizes.....	52
Table 4.4. Cutting Test Results.....	53
Table 4.4. Cutting Test Results (continued).....	54
Table 4.5. Breakout Angles With Sharp Picks.....	81
Table 4.6. Critical Limits for Various Rock Properties.....	103
Table 5.1. Summary of the First Statistical Model.....	106
Table 5.2. Analyse of Variance (ANOVA) for First Model.....	106
Table 5.3. Coefficients of First Model.....	106
Table 5.4. Summary of the Second Statistical Model.....	108
Table 5.5. Analyse of Variance (ANOVA) for Second Model.....	108
Table 5.6. Coefficients of Second Model.....	108
Table 5.7. Summary of the Third Statistical Model.....	110
Table 5.8. Analyse of Variance (ANOVA) for Third Model.....	110
Table 5.9. Coefficients of Third Model.....	110
Table 5.10. Summary of the Fourth Statistical Model.....	112

Table 5.11. Analyse of Variance (ANOVA) for Fourth Model.....	112
Table 5.12. Coefficients of Fourth Model.....	112
Table 5.13. Summary of the Fifth Statistical Model.....	114
Table 5.14. Analyse of Variance (ANOVA) for Fifth Model.....	114
Table 5.15. Coefficients of Fifth Model.....	114
Table 5.16. Summary of the Sixth Statistical Model.....	116
Table 5.17. Analyse of Variance (ANOVA) for Sixth Model.....	116
Table 5.18. Coefficients of Sixth Model.....	116
Table 5.19. Summary of the Seventh Statistical Model.....	118
Table 5.20. Analyse of Variance (ANOVA) for Seventh Model.....	118
Table 5.21. Coefficients of Seventh Model.....	118
Table 5.22. Summary of the Eighth Statistical Model.....	120
Table 5.23. Analyse of Variance (ANOVA) for Eighth Model.....	120
Table 5.24. Coefficients of Eighth Model.....	120
Table 5.25. Summary of the Ninth Statistical Model.....	122
Table 5.26. Analyse of Variance (ANOVA) for Ninth Model.....	122
Table 5.27. Coefficients of Ninth Model.....	122
Table 5.28. Laboratory and Predicted Specific Energy Results for Nine Different Statistical Models and for All Rock Types.....	127
Table 5.28. Laboratory and Predicted Specific Energy Results for Nine Different Statistical Models and for All Rock Types (continued).....	128
Table 5.28. Laboratory and Predicted Specific Energy Results for Nine Different Statistical Models and for All Rock Types (continued).....	129
Table 5.28. Laboratory and Predicted Specific Energy Results for Nine Different Statistical Models and for All Rock Types (continued).....	130

LIST OF FIGURES

FIGURES

Figure 1.1. The Flowsheet of the Testing Methodology.....	4
Figure 2.1. Typical Light (Mk-2A), Medium (Mk-2B) and Heavy Weight (Mk-3) Roadheading Machines.....	9
Figure 2.2. Ripping (a) and Milling (b) Type Cutting Heads	11
Figure 2.3. Radial, Forward-Attack and Point-Attack Picks.....	12
Figure 2.4. Typical ICR Curves for Axial Roadheaders.....	14
Figure 2.5. Comparison of Cutting Performance.....	15
Figure 2.6. The Variation of Instantaneous Cutting Rate with Uniaxial Compressive Strength of Rock, RQD > 50.....	16
Figure 2.7. The Variation of Instantaneous Cutting Rate with Uniaxial Compressive Strength of Rock, RQD < 50.....	16
Figure 2.8. The Variation of Instantaneous Cutting Rate with RQD, $\sigma_c = 90-100$ MPa.....	17
Figure 2.9. Plot of ICR (Instantaneous cutting rate) vs. UCS at Different Geological Conditions Encountered and All Types of Roadheaders.....	18
Figure 2.10. Plot of ICR vs. RPI for Sedimentary Rocks and Transverse Roadheaders.....	19
Figure 2.11. Plot of ICR vs. RPI for Evaporitic Rocks and Transverse Roadheaders.....	19
Figure 2.12. Cutting Performance Correlated with Compressive Strength of 26 Rock Samples.....	20
Figure 2.13. Cutting Performance Correlated with Destruction Work of 26 Rock Samples.....	20
Figure 2.14. Relationship Between Schmidt Hammer Rebound Values and Net Cutting Rate.....	23
Figure 2.15. Prediction of Cutting Rate From Laboratory Specific Energy.....	25

Figure 2.16. Comparison of the Performance Prediction Curve for the Medium-Weight Machines with Those of Light-Weight and Heavy Weight Machines.....	27
Figure 2.17. Sharp (a) and Blunt (b) Cutting Tools.....	35
Figure 2.18. Systematic Blunting of Wedges Used to Groove Coal.....	36
Figure 2.19. Relationship Between Specific Energy and Wear Flat.....	38
Figure 2.20. Relationship Between Mean Cutting Force and Wear Flat.....	38
Figure 3.1. NCB Cone Indenter.....	40
Figure 3.2. Model C-2 Type Shore Scleroscope.....	41
Figure 3.3. L-Type Schmithammer.....	42
Figure 3.4. Rock Cutting Setup.....	44
Figure 3.5. Typical Records of Direct and Mean Cutting Forces on an Ultraviolet Paper.....	45
Figure 3.6. Sharp (a) and Blunted (b) Standard Cutting Picks.....	47
Figure 3.7. Blunting of a Standard Pick by Using Diamond Grinding Disc.....	47
Figure 3.8. Sharp and Blunted Picks Used in the Tests.....	48
Figure 4.1. Relationships Between Uniaxial Compressive Strength and Laboratory Cutting Specific Energy at Different Wear Flats.....	56
Figure 4.2. Critical Wear Flats for Varying Uniaxial Compressive Strengths.....	57
Figure 4.3. Relationships Between Uniaxial Compressive Strength and Mean Cutting Force at Different Wear Flats.....	58
Figure 4.4. Relationships Between Brazilian Tensile Strength and Laboratory Specific Cutting Energy at Different Wear Flats.....	60
Figure 4.5. Critical Wear Flats for Varying Brazilian Tensile Strengths.....	61
Figure 4.6. Relationships Between Brazilian Tensile Strength and Mean Cutting Force at Different Wear Flats.....	62
Figure 4.7. Relationships Between Cone Indenter Number and Laboratory Specific Cutting Energy at Different Wear Flats.....	64
Figure 4.8. Critical Wear Flats for Varying Standard Cone Indenter Numbers.....	65
Figure 4.9. Relationships Between Cone Indenter Number and Mean Cutting Force at Different Wear Flats.....	66
Figure 4.10. Relationships Between Shore Hardness and Laboratory Specific Cutting Energy at Different Wear Flats.....	68

Figure 4.11. Critical Wear Flats for Varying Shore Hardness Values.....	69
Figure 4.12. Relationships Between Shore Hardness and Mean Cutting Force at Different Wear Flats.....	70
Figure 4.13. Relationships Between Schmidth Hammer Hardness and Laboratory Specific Cutting Energy at Different Wear Flats.....	72
Figure 4.14. Critical Wear Flats for Varying Schmidth Hammer Hardness.....	73
Figure 4.15. Relationships Between Schmidth Hammer Hardness and Mean Cutting Force at Different Wear Flats.....	74
Figure 4.16. Relationships Between Density and Laboratory Specific Cutting Energy at Different Wear Flats.....	76
Figure 4.17. Critical Wear Flats for Varying Density.....	77
Figure 4.18. Relationships Between Density and Mean Cutting Force at Different Wear Flats.....	78
Figure 4.19. Relationships Between the Mineral Grain Size and the Laboratory Cutting Specific Energy at Various Wear Flats.....	79
Figure 4.20. Relationships Between the Mineral Grain Size and the Mean Cutting Force at Various Wear Flats.....	80
Figure 4.21. Effect of Wear Flat on Size Distribution (a) and Coarseness Index (b)for Limestone 1.....	83
Figure 4.22. Effect of Wear Flat on Size Distribution (a) and Coarseness Index (b)for Limestone 2.....	84
Figure 4.23. Effect of Wear Flat on Size Distribution (a) and Coarseness Index (b) for Limestone 3.....	85
Figure 4.24. Effect of Wear Flat on Size Distribution (a) and Coarseness Index (b) for Limestone 4.....	86
Figure 4.25. Effect of Wear Flat on Size Distribution (a) and Coarseness Index (b) for Clayey-Limestone.....	87
Figure 4.26. Effect of Wear Flat on Size Distribution (a) and Coarseness Index (b) for Mudstone 1.....	88
Figure 4.27. Effect of Wear Flat on Size Distribution (a) and Coarseness Index (b) for Mudstone 2.....	89

Figure 4.28. Effect of Wear Flat on Size Distribution (a) and Coarseness Index (b) for Mudstone 3.....	90
Figure 4.29. Effect of Wear Flat on Size Distribution (a) and Coarseness Index (b) for Mudstone 4.....	91
Figure 4.30. Effect of Wear Flat on Size Distribution (a) and Coarseness Index (b) for Mudstone-siltstone.....	92
Figure 4.31. Effect of Wear Flat on Size Distribution (a) and Coarseness Index (b) for Marl 1.....	93
Figure 4.32. Effect of Wear Flat on Size Distribution (a) and Coarseness Index (b) for Marl 2.....	94
Figure 4.33. Effect of Wear Flat on Size Distribution (a) and Coarseness Index (b) for Altered Tuff.....	95
Figure 4.34. Effect of Wear Flat on Size Distribution (a) and Coarseness Index (b) for Lithic Tuff 1.....	96
Figure 4.35. Effect of Wear Flat on Size Distribution (a) and Coarseness Index (b) for Lithic Tuff 2.....	97
Figure 4.36. Effect of Wear Flat on Size Distribution (a) and Coarseness Index (b) for Claystone.....	98
Figure 4.37. Effect of Wear Flat on Size Distribution (a) and Coarseness Index (b) for Siltstone 1.....	99
Figure 4.38. Effect of Wear Flat on Size Distribution (a) and Coarseness Index (b) for Siltstone 2.....	100
Figure 4.39. Effect of Wear Flat on Size Distribution (a) and Coarseness Index (b) for Andesite.....	101
Figure 4.40. Effect of Wear Flat on Size Distribution (a) and Coarseness Index (b) for Travertine.....	102
Figure 5.1. Comparisons of The Predicted and Laboratory Cutting Specific Energies for Statistical Models 1, 2, 3.....	124
Figure 5.2. Comparisons of The Predicted and Laboratory Cutting Specific Energies for Statistical Models 4, 5, 6.....	125
Figure 5.3. Comparisons of The Predicted and Laboratory Cutting Specific Energies for Statistical Models 7, 8, 9.....	126

LIST OF SYMBOLS AND ABBREVIATIONS

ANOVA	: analyse of variance
BTS	: brazilian tensile strength
D	: density
F_c	: cutting force
F_n	: normal force
ICR	: instantaneous cutting rate
Is	: standard cone indenter hardness
ISRM	: International Society for Rock Mechanics
in	: inch
kJ/m^3	: kilojoule/cubic meter
kJ/kg	: kilojoule/kilogram
kN	: kilonewton
kW	: kilowatt
lbf	: pound-force
SE_L	: laboratory cutting specific energy
M	: model
MJ/m^3	: megajoule/cubicmeter
MPa	: megapascal
MRDE	: Mining Research and Development Establishment
P	: power
RMCI	: rock mass cuttability index
RPI	: roadheader penetration index
RQD	: rock quality designation
SCH	: schmidth hammer hardness
SH	: shore hardness
UCS	: uniaxial compressive strength
W	: roadheader weight
W_F	: wear flat
W_Z	: specific destruction work

CHAPTER 1

INTRODUCTION

1.1. General

Roadheaders have been applied in a wide range of rock types and structures in addition to coal measures strata since the early 1960's. The major improvements achieved in the last 50 years consist of steadily increased machine weight, size and cutterhead power, improved design of boom, muck pick-up and loading system, more efficient cutterhead design and metallurgical developments of cutting picks.

The maximum drivage rates from roadheaders can and will only be obtained if these machines are matched to the geological characteristics and rock properties of the rocks to be excavated. An essential prerequisite of any mechanical excavation programme is the need to know the mechanical cutting or excavation characteristics of the coal or rocks to be cut. Failure to determine these characteristics may result in failure to reach production objectives and in breakdown of machines which will require expensive replacements. Therefore, before installing costly roadway driving machines, it is essential to determine the machinability characteristics of rock materials. These characteristics can be studied in the laboratory and at the field to determine the specifications of machines and the type of cutting tools best suited to the type of rock.

The performance of mine excavation machinery depends upon a variety of factors, including strength properties of rocks, shape, size and geometry of cutting tools, type and configuration of cutting picks on the excavating heads, the cutting specific energies (MJ/m^3) and the mean cutting forces (kN) available in the excavation machinery, rock mechanics parameters, abrasiveness and weariness of the rocks and the cutting materials. The abrasive wear of cutting tools due to rock pick interaction is important as the cost and delays incurred for the replacement of the worn out parts reflects upon overall machine performance.

Studies have been mainly carried out to establish the relationships between the cutting performance and the rock properties (McFeat-Smith and Fowell, 1977; Gehring, 1989; Bilgin et.al, 1996; Çopur et.al, 1998; Thuro and Plinninger, 1999; Göktañ and Güneş, 2005 and Keleş, 2005).

McFeat Smith and Fowell developed standard cutting tests and established a good relationship between the laboratory cutting specific energy and the in-situ cutting performance of rocks by roadheaders (Fowell and McFeat Smith,1976; McFeat Smith and Fowell,1977; Fowell and Pycroft,1980; Fowell and Johnson,1982). Similar relationships have also been found by other researchers for different size roadheaders (Keleş, 2005; Balcı and Bilgin, 2005).

In case where laboratory facilities for rock cutting tests are not available, some empirical models regarding some intact rock properties are used to predict the specific energy. McFeat Smith studied the relationships and established a correlation between the laboratory cutting specific energy (SE) and some rock properties (McFeat Smith,1975).

1.2. Objective and Scope of the Thesis

Sharp cutting picks on a roadheader cutting head become blunt in time and require replacement. It is important to replace the picks at the critical degree of blunting at which considerable increase in cutting forces and specific energies start. All researchers consider that the cutting picks are sharp whereas in practice blunting develops due to several causes when rock cutting starts. On the other hand, the degree of variation in cutting forces and specific energies with the increase in pick blunting is unknown.

Up to now, no investigation has been carried out to establish the effects of degree of blunting on laboratory cutting forces and specific energies. In this study, standard rock cutting tests have been carried out on different types of rocks with sharp and artificially blunted picks and variation in cutting forces and specific energies were determined at different wear flats for different rock types.

The main objectives of this thesis are as follows:

- a) To determine the relationships between laboratory cutting specific energies, cutting forces and:
 - Wear flats
 - Rock Properties; Uniaxial Compressive Strength (UCS), Brazilian Tensile Strength (BTS), Cone Indenter Hardness (Is), Shore Hardness, Schmidt Hammer Hardness, Rock Density, Mineral Grain Size.
- b) To establish the effect of pick blunting on size distribution and coarseness index.
- c) To determine critical wear flats at different rock properties above which poor cutting performance is expected.
- d) To develop models by statistical analysis to predict the laboratory cutting specific energy for different rock properties and wear flats.

Figure 1.1 shows the flowsheet of the testing methodology.

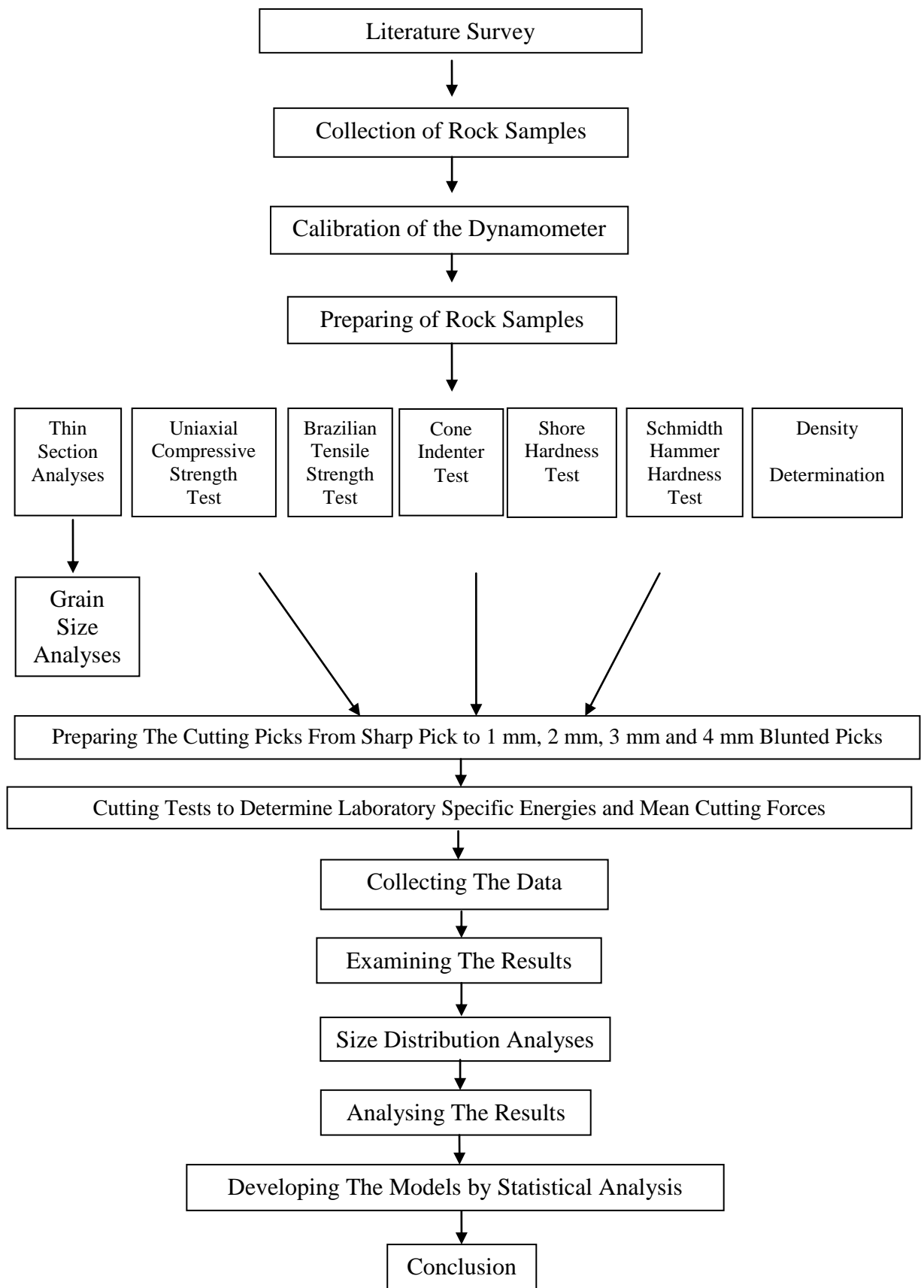


Figure 1.1. The Flowsheet of the Testing Methodology

This thesis is divided into six chapters including the Introduction Chapter 1. Literature Review is presented in Chapter 2. Experimental Procedure is given in Chapter 3. Experimental Results and Discussions are given in Chapter 4. Evaluation of Results and Establishing Models by Statistical Analyses are given in Chapter 5. Conclusions and Recommendations are given in Chapter 6.

CHAPTER 2

LITERATURE REVIEW

2.1. Boom Type Roadheaders

2.1.1. Introduction

Boom type roadheaders are mechanical excavation machines that break rock by utilizing tungsten carbide tipped cutting tools faced in a specific geometry on a rotating cutting head. The cutter head is driven by an electric motor through a heavy duty gearbox for either milling or ripping cutting actions. Boom movement is controlled by hydraulic cylinders sized to provide sufficient force to maintain the cutting head in contact with the face, and the machine is track mounted to allow tramming from one work face to another. Roadheaders have traditionally operated in sedimentary rock with an unconfined compressive strength of less than 100 MPa (Neil et.al,1994). Occasionally harder rocks can be excavated where joints, bedding planes, fractures or other planes of weakness are present.

2.1.2. Classification

The roadheaders can be classified according to their times of production, their rock-cutting abilities and their weights (Bölükbaşı, 1986).

2.1.2.1. Classification According to Times of Production

a) First Generation

First generation machines were introduced in Western Europe in the 1960's. The lighter models of these early boom miners weighed about 9 tons and could cut soft rocks having compressive strength up to about 40 MPa.

b) Second Generation

Second generation machines were developed around 1970. These machines generally weigh between 22-37 tons. Some of these machines can cut competent rock with compressive strength as high as 85 MPa if the silica content of the rock is low.

c) Third Generation

The third generation, heavy-weight machines became available in 1976. These machines weigh between 45-70 tons and can cut competent rock with compressive strength of 100 MPa.

d) Fourth Generation

Machine weights have reached up to 120 tons about 2000 which can be considered as fourth generation machines. Such machines can cut economically most rock formations up to 100 MPa uniaxial compressive strength (UCS) and rocks up to 160 MPa UCS if favorable jointing or bedding is present with low RQD numbers (Çopur et. al, 1998; Thuro and Plinninger, 1999; Neil et. al, 1994).

2.1.2.2. Classification According to Weight

Tucker (1985) classified roadheaders according to weight as:

- Light Duty; weight up to 30 t, cutting capabilities up to 70 MPa
- Medium Duty; weight between 34-45 t, cutting capabilities up to 100 MPa
- Heavy Duty; weight over 45 t, cutting capabilities up to 120 MPa

Table 2.1. Classification According to Weight by Atlas Copco – Eickhoff (Schneider, 1988);

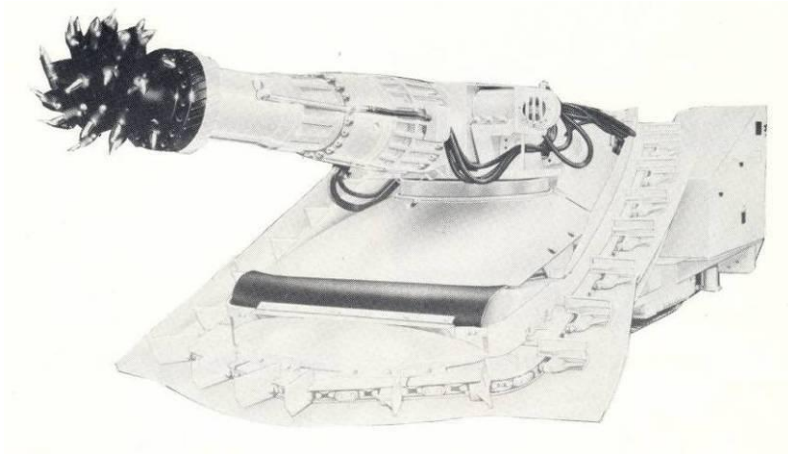
Class	Weight
0	<20 t
I	20-30 t
II	30-50 t
III	50-75 t
IV	>75 t

Neil et. al (1994) refer roadheaders as small size up to 30 t, midsize between 30-70 t and large size between 70-120 t.

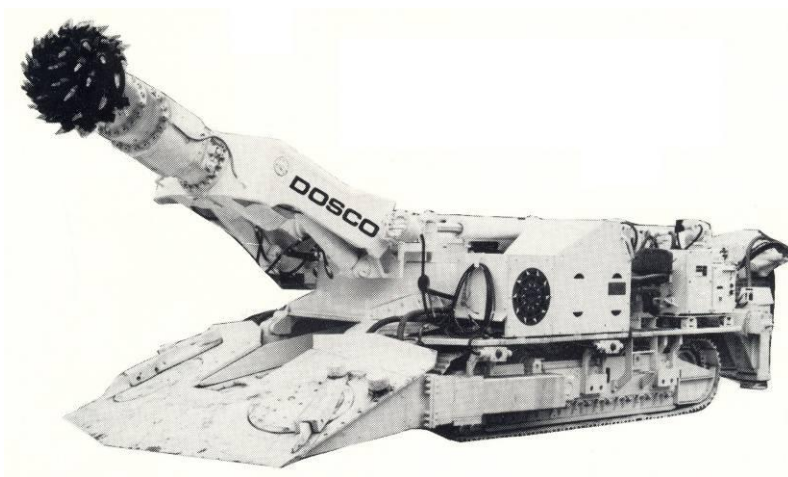
Table 2.1 shows the main types of roadheaders and Figure 2.1 shows Mk-2A, Mk-2B and Mk-3 machines which are the typical light, medium and heavy weight machines, respectively.

Table 2.2. Properties of Typical Roadheaders (Pearse, 1987)

Machine Type	Weight (t)	Head Drive (kW)	Total Power (kW)
ANDERSON STRATCLYDE (UK)			
Boom Miner	22.0	60	120
RH25	25.4	82	157
RH22	35.0	112	187
RH1/3	50.0	90	190
RH1/4	66.0	112	234
RH90	90.0	150	300
DOSCO (UK)			
D.R.C.L.	17.0	37	75
MK2A	23.0-26.0	67	149
SL120	35.0	82	164
MK.2B	38.0	82-112	194-224
LH 1300	43.0	140	286
TB600	81.6	2x190	604
MK3	85.2	140	293
ATLAS COPCO-EICKHOFF (GERMANY)			
ET-100 Series	27.0-34.0	110-132	190/212
ET-200 Series	52.0	200	360
ET-300 Series	78.0-95.0	200/250	380/430
ET-400 Series	97.0-110.0	300	460/480
MACHINE EXPORT (USSR)			
Pk-3	10.8	32	78
Pk-9r	32.0	90	173
MANNESMAN-DEMAG (GERMANY)			
VS3	63.0	160/200	265
VS3/2	75.0	160/200	300
VS4	95.0	132/200	300
MITSUI-MIIKE (JAPAN)			
MRH-S50 13	18.5	50	80
MRH-S100 40	25.0	60/100	145
MRH-S125 23	30.0	75/125	170
VOEST-ALPINE (GERMANY)			
F6-A	12.0	30	60
AM 30	14.5	45	75
AM 45	20.0	75	135
AM 50	22.0	100	155
AM 95	80.0	300	445
AM 100	79.8	235	450
PAURAT (GERMANY)			
E169	44.0	100	185
E1 95	46.0	170	263
E134	70.0	115/230	353
E200	115.0	350	512
SALZGITTER (GERMANY)			
STM 100	25.0	100	200
STM 160	45.0	160	257
STM 200	65.0	200	330
WESTFALIA (GERMANY)			
Furchs	6.0	45	52
Luchs	24.0	90	150
WA300 Bison	73.0	300	437



Dosco Mk-2A



Dosco Mk-2B



Dosco Mk-3

Figure 2.1. Typical Light (Mk-2A), Medium (Mk-2B) and Heavy Weight (Mk-3) Roadheading Machines

2.1.3. Basic Components

Boom type roadheaders consist mainly of the following units:

2.1.3.1. Boom, Cutting Head and Cutting Picks

a) Boom

Roadheaders can have either fixed or telescopic booms. Telescopic boom is advantageous especially on soft floors since sumping can be achieved without moving the machine forward.

b) Types of Cutting Heads

All boom miners utilize cutter bits fixed on a rotary cutterhead that is powered by an electric motor. Sumping of the boom-miner cutterhead into the face usually utilizes a forward thrust on its crawlers. This initial cut is then enlarged using vertical, horizontal, or spiral cuts. The two significantly different cutting actions are milling and ripping.

i) Milling: For milling type cutting, the cutterhead rotates in line with the axis of the cutter boom; the primary cutting force is exerted sideways. The milling action rips the rock from the face and throws the rock across the floor parallel to the front of the loader head (in comparison, a ripping action throws the rock onto the loader head). However, due to the relatively simple in-line gearing between the milling cutterhead and the drive motor, milling heads can have smaller diameters than comparable ripper-head machines. This, milling miners are better suited for selective mining.

ii) Ripping Type Roadheader: cutterhead rotates at an axis which is parallel to the face. The ripper head utilize three forces to break the rock. The principle cutting torque is provided by the rotary motion of the cutterhead, and downward vertical thrust is provided by the boom. Horizontal force is provided by the slewing of the cutter boom. If the rock is soft, a ripping miner takes a deep cut so that several bit spirals are cutting simultaneously and the machine produces at its maximum rate. If the rock is very hard, only one bit spiral is utilized. In such a case, when the cutting

becomes tough, approximately the full power developed by the cutter motor can be applied to a single bit. That is the reason these boom miners can cut far harder rock at a given power than can standard continuous miners. Figure 2.2 shows the milling and ripping type cutting heads.

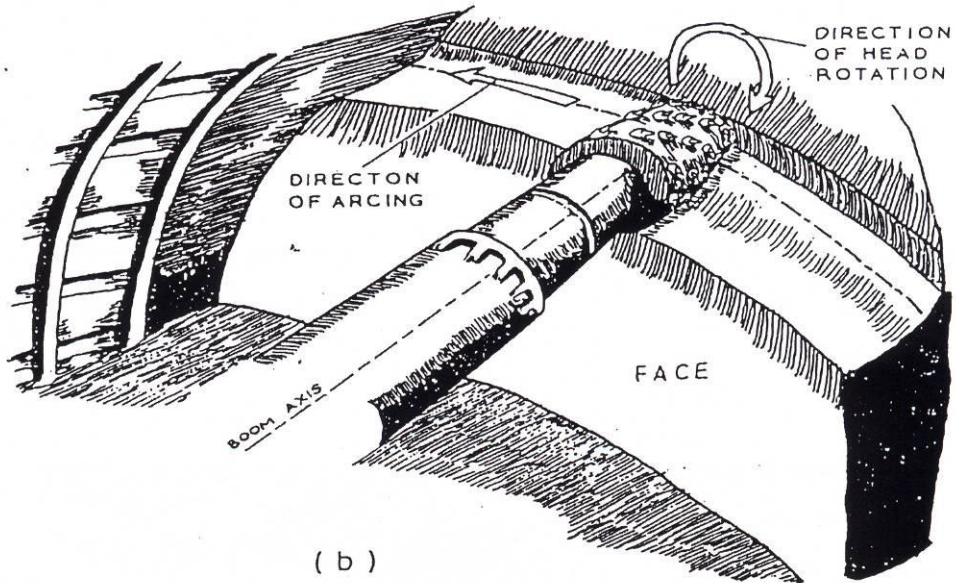
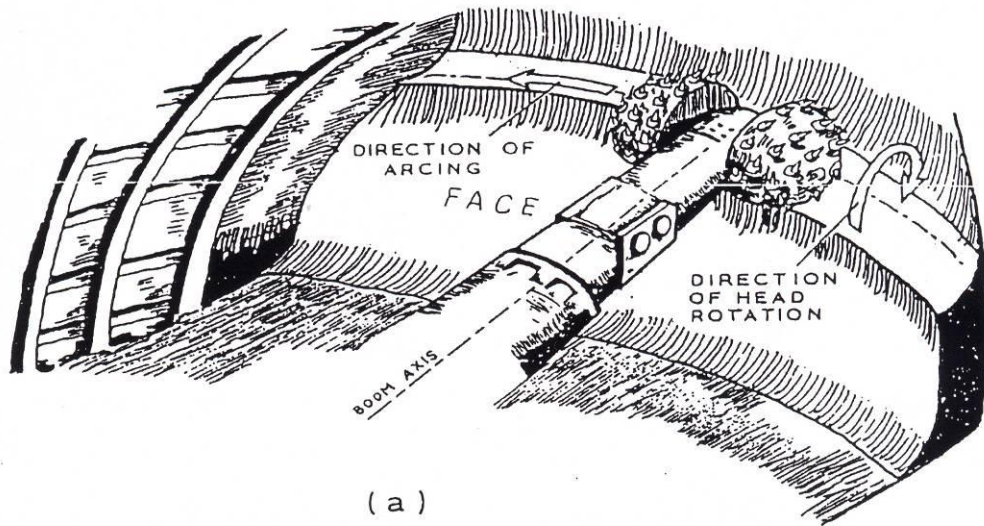


Figure 2.2. Ripping (a) and Milling (b) Type Cutting Heads (Hekimoğlu, 1984)

c) Cutting Picks

There are three styles of pick in general use: radial, forward attack and point attack (Figure 2.3). Radial picks have their shanks positioned normal to their cutting direction. The shanks of forward attack picks, on the other hand, are angled backwards from the cutting direction, usually at about 45°. Both of these picks use wedge tips. These picks are used for cutting coal and soft-medium hard rock. Point attack picks are essentially forward attack picks with conical tips. They usually have circular cross-section shanks and are free to rotate within their holders. They are generally used for cutting hard coal, medium, hard and abrasive rocks (Eyyuboğlu, 2000).



Figure 2.3. Radial, Forward-Attack and Point-Attack Picks

2.1.3.2. Loading Unit

The loading unit of a roadheader should have sufficient capacity to carry the amount of material cut by the cutting head. Roadheaders may have gathering arm, loading discs or encircling flight conveyor types of loading units.

2.1.3.3. Haulage Unit

Roadheaders move on crawler trucks. Provisions must be made to remove continuously the cut rock discharged by the boom miner. Numerous haulage systems are available, but the most successful have been bridge conveyors, shuttle cars, and other mobile equipment such as load-haul-dump vehicles, wheeled belt conveyors tower by the miner and discharging into the trucks, and belt loaders discharging into rail cars.

2.2. Roadheader Performance Prediction

The compressive strength of the rock to be excavated is often quoted as a measure of cuttability but compressive strength alone has been found to be a poor predictor of machine performance (Speight and Fowell, 1984). Factors that need to be considered when assessing roadheader performance and tool consumption rates are given in Table 2.2.

Table 2.3. Factors Influencing Roadheader Performance and Tool Consumption rates (Speight and Fowell, 1984)

Rock Material Properties	Strength, Toughness
Rock Degradation Properties	Hard Mineral Content, Grain size, Angularity, Cementation
Rock Mass Properties	Discontinuity frequency, Thickness and Position of Beds
Machine Characteristics	Slewing Forces, Cutting Torque, Stability, Cutting Speed, Head Geometry
Cutting Tool Properties	Type, Tip Geometry, Tungsten Carbide, Composition
Operational Characteristics	Made of Cutting Slewing Speed Advance/rev.
Tunnel Characteristics	Gradient, Size and Shape Presence of Water

The machine performance and rock cuttability can be estimated by various rock properties and methods.

2.2.1. Uniaxial Compressive Strength

Unconfined compressive strength is often used as the main predictor of cutting machine performance for rocks associated with coal seams or the weaker sedimentary rocks such as sandstone, siltstone and mudstone. On the other hand, when the range of application has to be extended into other rock materials, compressive strength alone is not always a good predictor of performance. Evaporate rocks, breccias and chalk containing flints are materials that do not follow the established relationships for compressive strength and excavation rate (Fowell et al., 1994). Figure 2.4 shows the relationship established between compressive strength and excavation rate.

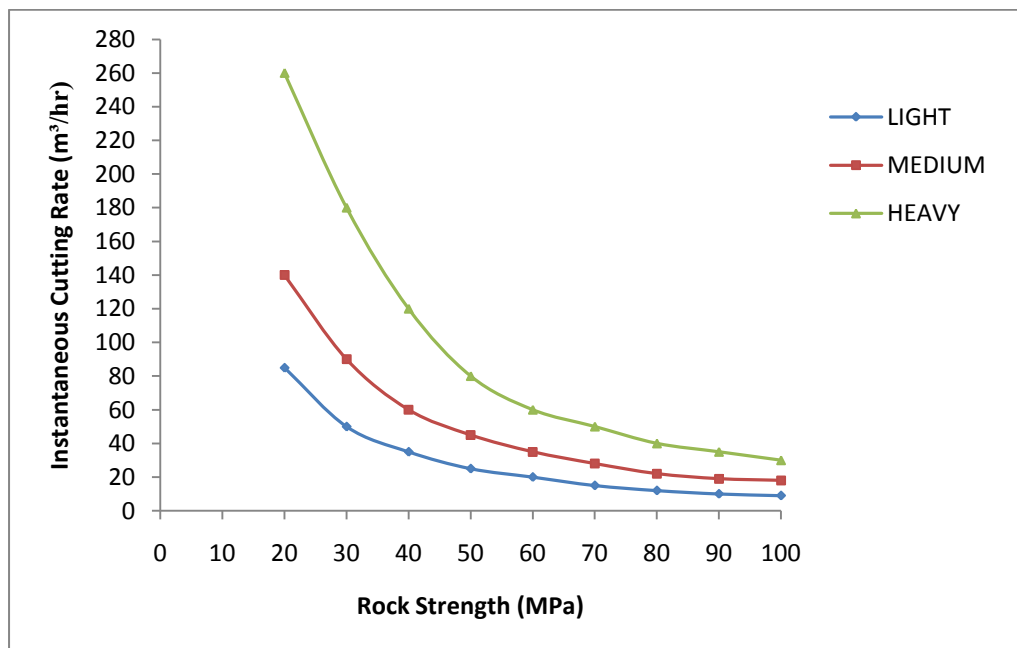


Figure 2.4. Typical ICR Curves for Axial Roadheaders (Fowell et.al., 1994)

Gehring (1989) studied the relationship between ICR and UCS for a milling type roadheader with 230 kW cutterhead power and an Alpine Miner AM 100 ripping type roadheader with 250 kW cutterhead power. Figure 2.5 shows the relationships obtained.

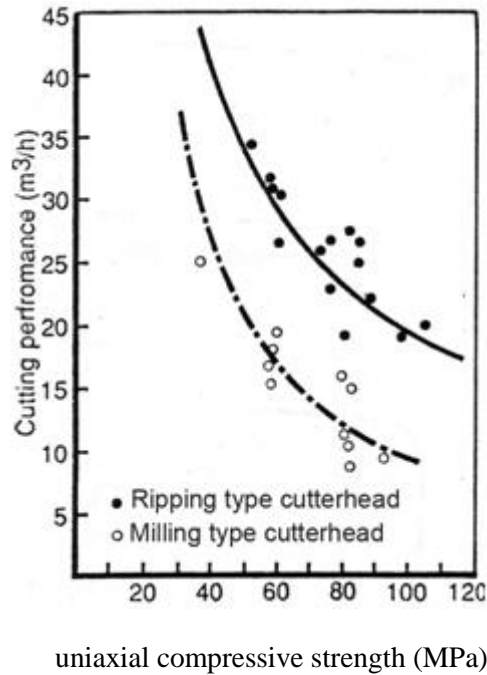


Figure 2.5. Comparison of Cutting Performance (Gehring, 1989)

Bilgin et. al (1996) studied the correlation between ICR, UCS and RQD. Figure 2.6 and Figure 2.7 show the relationship between ICR and UCS for rocks having RQD greater than 50 and less than 50, respectively. No correlation exists for rocks with RQD less than 50.

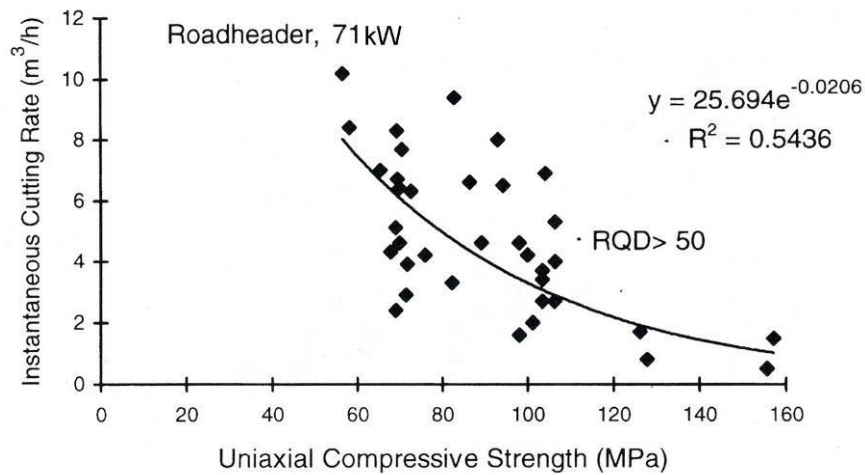


Figure 2.6. The Variation of Instantaneous Cutting Rate with Uniaxial Compressive Strength of Rock, RQD > 50 (Bilgin et. al, 1996)

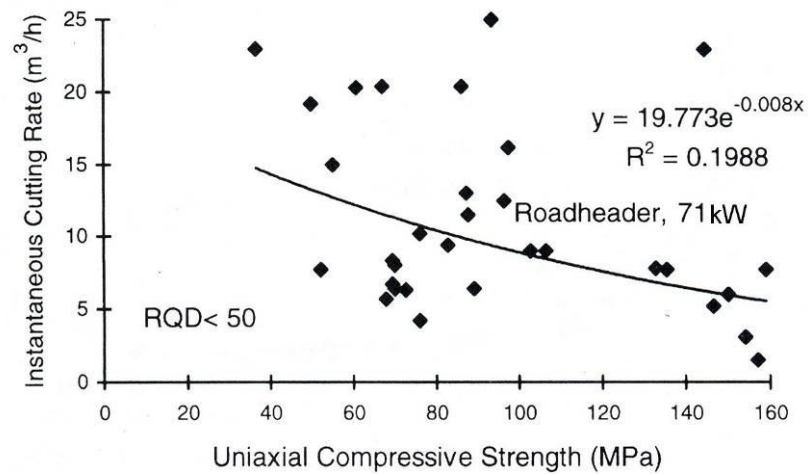


Figure 2.7. The Variation of Instantaneous Cutting Rate with Uniaxial Compressive Strength of Rock, RQD < 50 (Bilgin et. al, 1996)

Figure 2.8 shows the relationship between ICR and RQD. Results show better correlation as compared to UCS. Correlation has been improved by developing a prediction equation as:

$$ICR = 0.28P^{0.974} RMCI$$

where:

P = Motor power, HP

$RMCI$ = Rock mass cuttability index, MPA

$$= \sigma_c RQD/100^{2/3}$$

where:

σ_c = Uniaxial Compressive Strength, MPa

RQD = Rock quality designation, % (Bilgin et. al, 1996; Bilgin et. al, 1997; Eskikaya et. al, 1998)

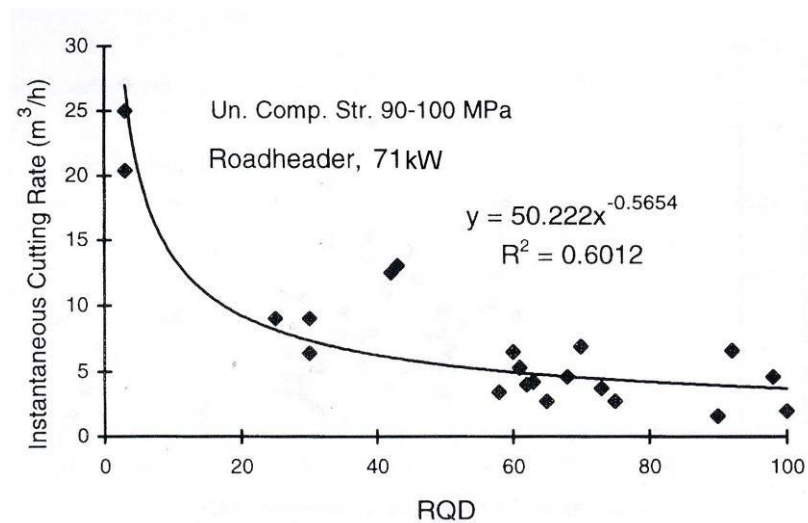


Figure 2.8. The Variation of Instantaneous Cutting Rate with RQD, $\sigma_c = 90-100$ MPa (Bilgin et. al, 1996)

Çopur et. al, (1998) studied the variation of cutting rate with UCS based on available field performance data. Figure 2.9 shows the relationship obtained using different types of roadheaders at the geological conditions encountered. The data shows significant scatter with very low coefficient of determination ($R^2 = 0.29$).

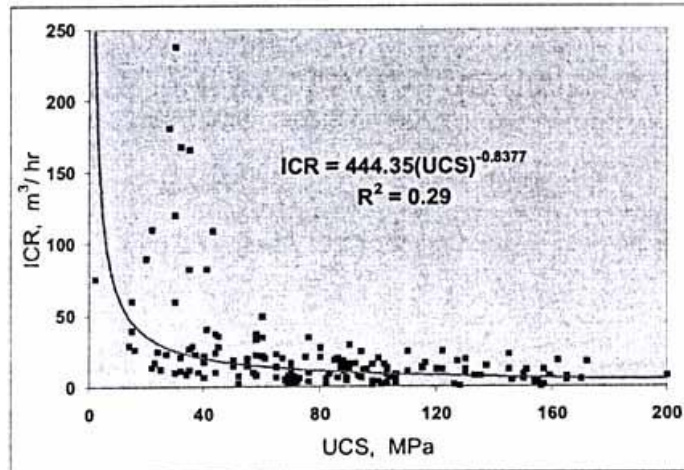


Figure 2.9. Plot of ICR (Instantaneous cutting rate) vs. UCS at Different Geological Conditions Encountered and All Types of Roadheaders (Çopur et. al, 1998)

Çopur et.al. (1998) obtained higher correlations by developing prediction equations which consider the roadheader weight and cutterhead power for transverse (ripping type) roadheaders. Figure 2.10 and Figure 2.11 show the relationships obtained for sedimentary rocks and evaporitic rocks respectively where;

$$RPI = P \times W / UCS$$

RPI = Roadheader penetration index

W = Roadheader weight (t)

P = Cutterhead power (kW)

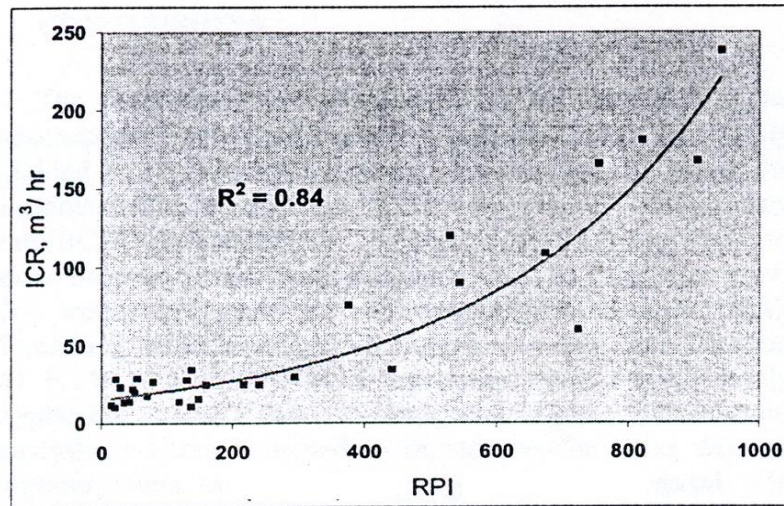


Figure 2.10. Plot of ICR vs. RPI for Sedimentary Rocks and Transverse Roadheaders (Çopur et. al, 1998)

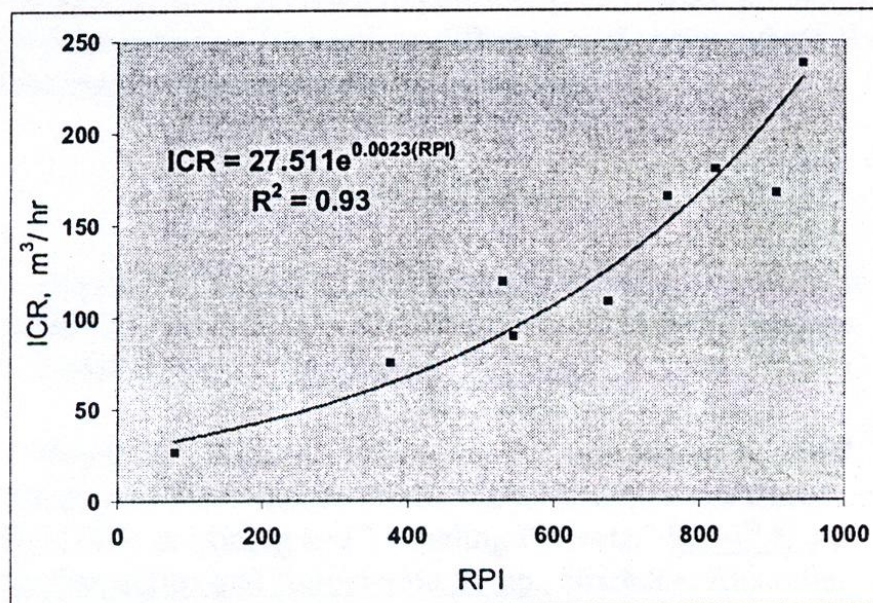


Figure 2.11. Plot of ICR vs. RPI for Evaporitic Rocks and Transverse Roadheaders (Çopur et. al, 1998)

Thuro & Plinninger (1999) determined the relationship between the cutting rate and the uniaxial compressive strength for 132 kW roadheader as shown in Figure 2.12. They have found that the correlation between UCS and cutting performance is not sufficient (Thuro and Plinninger, 1999).

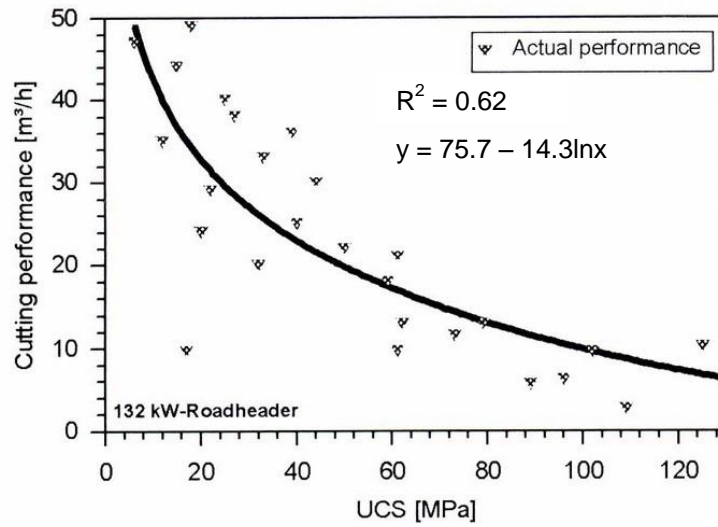


Figure 2.12. Cutting Performance Correlated with Compressive Strength of 26 Rock Samples (Thuro and Plinninger, 1999)

They obtained higher correlation by putting cutting performance against specific destruction work W_z (kJ/m^3) which has been introduced by Spaun and Thuro (1996). Figure 2.13 shows the correlation curve.

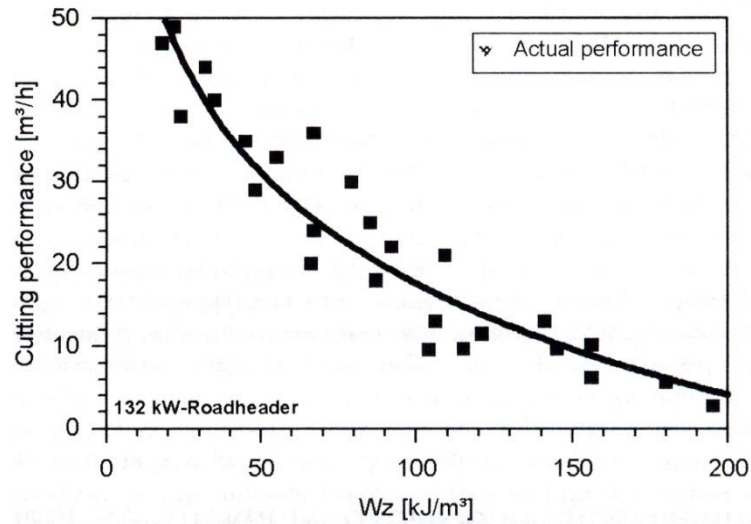


Figure 2.13. Cutting Performance Correlated with Destruction Work of 26 Rock Samples (Thuro and Plinninger, 1999)

As a result, although the uniaxial compressive strength of the rock to be excavated is often quoted as a measure of cuttability, the compressive strength alone is a poor predictor of machine performance if other effective factors such as machine weight, cutterhead power and other effective rock properties such as discontinuity spacing in the rock mass, brittleness of the material and abrasivity are not considered (McFeat-Smith, 1975; Fowell and Pycroft, 1980; Speight and Fowell, 1984; Thuro and Plinninger, 1999).

2.2.2. Tensile Strength and Shear Strength

Although models of rock failure under attack by drag tools using the shear strength of the rock have been proposed by Merchant (1945) and Nishimatsu (1972), the model used by Evans (1962) for coal, taking the tensile strength as the main criteria has found wider acceptance for predicting cutting forces in brittle rock materials.

Roxborough (1973) has shown that a modification to Evans theory can be acceptable to apply successfully to a number of rock materials to predict cutting forces. This approach does not yield the complete cuttability characteristics of a rock as it is based solely on the tensile strength property of the rock and cutting tool geometrical considerations.

2.2.3. Cone Indenter Hardness

The NCB cone indenter, which was developed by Mining Research and Development Establishment (MRDE) in U.K., is a portable instrument capable of giving a measure of rock strength without requiring the preparation of accurately shaped and finished specimens. The cutting action of drag-pick tools has been shown to be primarily an indentation action and rather good relationship exists between the cone indenter hardness and performance of selective roadheading machines employing drag (pick) type cutting tools (McFeat-Smith, 1975; MRDE, 1977). Table 2.3 gives the relationship between standard cone indenter hardness and the cutting performance.

Although the cone indenter gives some indication of cuttability, it is not applicable for all rocks since deviations have also been observed where rocks with low indenter numbers required high cutting energies (Fowell and Pycroft, 1980).

Table 2.4. Correlations Between Cone Indenter Number and Machine Performance (McFeat-Smith, 1975)

Standard Hardness	Cutting Performance	Cutting Pick Performance
6.0	Only selective cutting of these rocks is possible if in bands less than 0.30 m thick	Severe wear (Greater than 0.5 picks/m ³)
5.0	Roadheaders are not suited to these rocks. Some progress possible if softer bands present in face. Blasting will probably be required to assist excavation.	Rapid wear of picks. Shattering of pick inserts and shanks common.
4.0	Roadheader may cut satisfactorily if picks are changed regularly. High cutting energies (8-11 MJ/m ³) and vibrations will severely reduce life span of machine components.	Wear rates of 0.32 picks/m ³ or less likely. Cutting performance will be reduced if picks are not changed regularly. Shattered inserts not uncommon
3.0	Moderate drive rates. May be as low as 10 m ³ /h in hardest rocks.	Moderate wear rates (May be as low as 0.15 picks/m ³) Regular changing of slightly worn picks will assist cutting performance.
2.0	Satisfactory progress can be made. Cutting rates of 12.15 m ³ /h likely.	Low wear rates although regular inspection of picks is necessary.
1.0	Roadheaders excellently suited to these rocks. Good drive rates can be expected (Up to 20 m ³ /h).	Wear rates likely to be less than 0.08 picks/m ³ . Regular inspection of picks still advantageous

2.2.4. Shore Hardness

This method is suggested for the hardness determination of rock minerals using the shore scleroscope in laboratory or in situ (ISRM, 1981). Shore rock hardness may be obtained as an average of readings taken at random on individual mineral grains. Since the area of rock tested is very small a large number of tests are required to give good measure of the average hardness, individual tests are more directly influenced by the variation of mineralogical content of the rock.

The shore scleroscope has proved to be a valuable laboratory tool for the determination of rock hardness with good correlation with uniaxial compressive strength (Atkinson, et al., 1986).

But where samples have large number of hard crystals, the relationship is unreliable. Although the shore hardness indicates the cuttability to a certain extend, it may give unreliable results for some rocks. For example, although the shore hardness of the coal is generally high, it can be cut by the roadheaders easily (Bölükbaşı, 1986).

2.2.5. Schmidt Rebound Hardness

Schmidt hammer is suggested for the hardness determination of rocks in laboratory or in-situ. Schmidt hammer rebound values have been correlated with compressive strength by a number of workers (Atkinson et. al, 1986), but this method is of limited use on very soft or very hard rocks (ISRM, 1981).

Goktan and Gunes, 2005 determined Schmidt hammer rebound number by applying 15-20 continuous impacts at each test point and calculated the mean excluding suspected low values. Correlation of Schmidt rebound numbers determined as explained above against net cutting rates for a roadheader with cuttinghead power of 90 kW provided relatively high coefficient of determination ($R^2 = 0.73$) as shown in Figure 2.14.

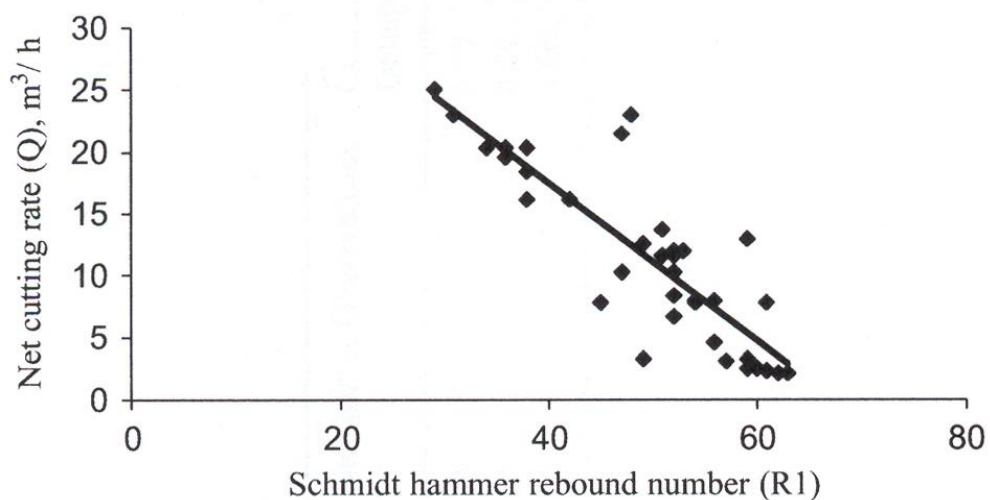


Figure 2.14. Relationship Between Schmidt Hammer Rebound Values and Net Cutting Rate (Gökten and Güneş, 2005)

Although a close correlation between Schmidt hammer rebound number and the advance rate of roadheaders was obtained for some rocks, rebound number was found to be insufficient to define the cuttability of rocks in general (Poole and Farmer, 1978).

2.2.6. Laboratory Cutting Specific Energy

Prediction of cuttability from a single rock property may be misleading and may give unreliable results. Instrumented standard cutting test was developed by the University of Newcastle upon Tyne and a good correlation has been found to exist between insitu machine performance and laboratory cutting specific energy (McFeat-Smith and Fowell, 1977; Fowell and Johnson, 1982).

Specific energy can be defined as the work done to excavate unit volume of rock and quoted in megajoules per cubic meter (MJ/m^3). It has been found that this laboratory measure of specific energy provides a good indication of likely machine performance. Figure 2.15 and Table 2.4 show the relationship obtained between the laboratory cutting specific energy (SE_L) and field instantaneous cutting rate (ICR) for Dosco Mk-2A and Dosco Mk-3 type roadheaders (McFeat-Smith and Fowell, 1977; Fowell and Pycroft, 1980). Although Mk-2A machine was considered as a medium-weight machine earlier, it is classified under the light-weight machines nowadays.

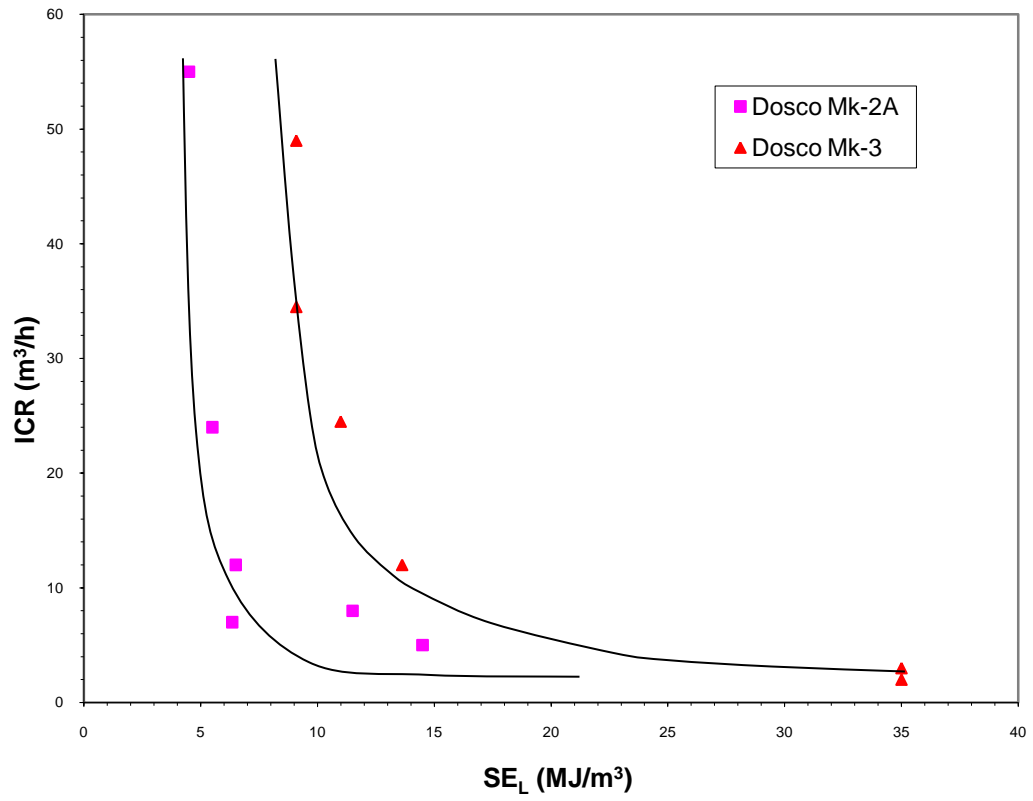


Figure 2.15. Prediction of Cutting Rate From Laboratory Specific Energy (Fowell and Johnson, 1982)

Table 2.5. Roadheader Performance Relative to Laboratory Specific Energy (Fowell and Pycroft, 1982)

Lab. spec. energy (MJ/m ³)	Cutting Performance (Dosco Mk-2A)	Lab. spec. energy (MJ/m ³)	Cutting Performance (Dosco Mk-3)
20	Machines can only cut these rocks at economic rates if they occur in thin bands (less than 0.3 m). Short term replacement of machine components may be required due to substantial cutting vibrations	32	Machines can cut only thin bands of these rocks and tool wear will be exceptionally high. Short-term damage to machine can be expected.
15	Poor cutting performance. Excavation may have to be assisted by blasting for rock at top end of scale. Shattered inserts should be expected. Regular replacement of slightly worn picks will improve energy requirements and reduce component wear. Point attack tools may be more beneficial.	25	Poor cutting performance particularly in massive rocks. Pick wear critical and cutting will improve by frequent inspection. Point attack picks essential.
12	Moderate-poor cutting performance. Shattered pick inserts can still be expected although less common. For abrasive rocks picks must be inspected frequently.	17	Moderate cutting performance to good at bottom of category. Picks should be inspected and changed regularly particularly when excavating abrasive rocks.
8	Moderate to good cutting performance with very low wear of machine components. Picks must be inspected and changed regularly particularly when excavating abrasive rocks.	8	Machine well suited to these rocks and rapid advance rates can be anticipated. Regular inspection and replacement of tools still advantageous.
5	Machine well suited to these rocks. Good advance rates can be anticipated. Regular inspection and replacement of worn picks still advantageous.		

Bölükbaşı (1989) carried out laboratory cutting tests and compared the predicted and actual machine performance for Dosco MK-2A machines at Çayırhan coal mine.

Keleş (2005) studied the relationships between the laboratory cutting specific energy and the insitu cutting rates for Dosco MK-2B medium-weight roadheader (38t) for the rocks encountered in Çayırhan and has found meaningful results.

Figure 2.16 compares the location of the performance prediction curve obtained for the medium-weight Dosco Mk-2B with those determined earlier for the light-weight (Dosco Mk-2A) and heavy-weight (Dosco Mk-3) roadheaders by McFeat-Smith and Fowell (1977); and Fowell and Johnson (1982).

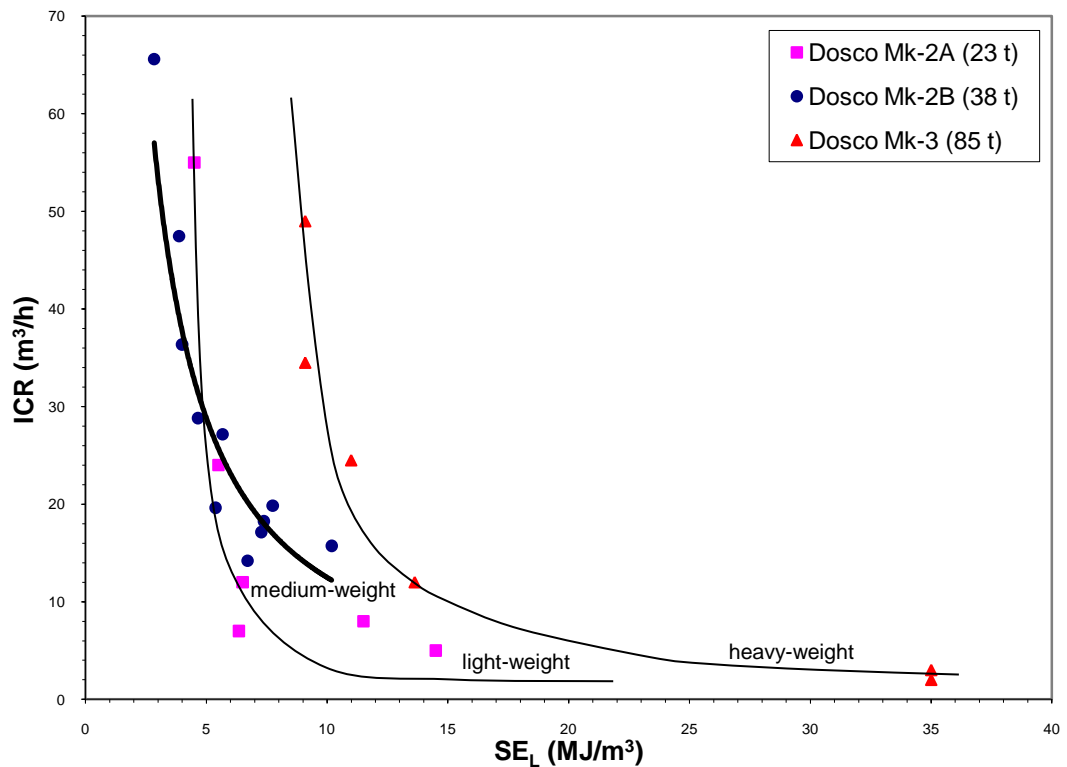


Figure 2.16. Comparison of the Performance Prediction Curve for the Medium-Weight Machines with Those of Light-Weight and Heavy Weight Machines (Keleş, 2005)

2.3. Wear Mechanisms in Rock Cutting

There are four mechanisms of tool degradation most likely to be observed when cutting rock:

i-Abrasive wear

ii-Micro chipping

iii-Gross Failure

iv-Thermal Cracking

It is important to recognize the main forms of wear in order to reduce their effect. Unfortunately it is found in practice that reducing one form of wear usually results in the occurrence of another, so a compromise must be sought. A common example of this is in optimization of the cobalt content in tungsten carbide alloys. Ideally the tool material should be as hard as possible to reduce the influence of abrasive wear. This is often achieved by reducing cobalt content and grain size. This however results in reduced toughness of the carbide and there is an increased likelihood of gross failure of the tool with the formation of large chips (Osburn, 1969; Hurt and Macandrew, 1985).

2.3.1. Abrasive Wear

Rock abrasiveness and the types of tool materials and manufacturing techniques are the main factors affecting abrasive wear.

2.3.2. Rock Abrasiveness

Abrasive wear is the most important of all mechanisms and it is a function of distance travelled in contact with the rock. Various factors affect the abrasiveness of rock, particularly important are:

i-Mineral Composition

ii-The hardness of mineral constituent

iii-Grain shape and size

iv-The type of matrix material

v-Physical properties of the rock, including strength, hardness and toughness.

Free and combined silica content is often regarded as a measure of the abrasiveness of a rock but other hard minerals also cause abrasiveness such as orthoclase, fluor spar, apatite and hornblends which range in hardness from 5 to 7.5 on the Mohs scale. In addition to determining the minerals present in a rock and their hardness, it is also necessary to determine the grain size, angularity and sphericity of the sharp minerals. The bonding strength of the matrix material will also directly affect cuttability and abrasive wear of cutting tools.

In rocks such as sandstones, the manner in which the quartz grains are integrated into the structure, and the strength of the matrix holding them in, are likely to be of prime importance in determining the mechanism of the wear. In practice, observations are such that the strongest sandstones are not necessarily the most abrasive. The stronger sandstones have a stronger matrix material, the quartz grains being much more rigidly cemented by silica than by calcite or iron oxide. When cutting the stronger sandstones with picks the whole rock chip is broken off before appreciable sliding over the surface of the tool has taken place. Where the tool is scraping against the rock, the grains of quartz by being held rigidly are more likely to be fractured off. The scratch marks on the tool, although deeper, are therefore possibly shorter and less damaging than cutting the softer rocks, where the individual grains of quartz are ripped out of the rock structure and ground along the surface of the tool before being able to escape.

Sandstones are bedded and so are generally fairly easy to cut, while granite, by virtue of its hardness and lack of bedding, is usually very difficult. Granite consists mainly of potash feldspar (approx.60%) and quartz (approx.20%) with the intergrown mineral crystals all about the same size. The potash feldspar often occurs as orthoclase (Mohs Hardness no.6 as opposed to quartz at hardness no.7), so that granite (in the general sense) may be rather less severe to cut than quartzites.

It can be observed that the inter-relations between rock competency, hardness and abrasivity are all of importance, however, even very weak rocks can cause excessive wear.

2.3.3. Tool Material and Manufacturing Techniques

The raw materials and manufacturing techniques that are used to produce tungsten carbide-cobalt alloys have a considerable influence on the ultimate life of the finished composite. As it is impossible to obtain the required product by melting due to decomposition of the monocarbide, WC, a powder metallurgy sintering technique is used. The main steps in the production of tungsten carbide-cobalt alloys are:

i-Tungsten ore concentrate (wolframite) is processed to ammonium paratungstate, tungstic acid, or tungstic oxide powder;

ii-This is reduced under hydrogen to tungsten metal powder;

iii-The tungsten is carburised by heating with carbon in non-oxidising conditions;

iv-The tungsten carbide powder is milled with cobalt powder to give the mixed powder;

v-The pressed compacts are sintered.

a) Effect of Carbide Additions on Properties

The two most common additions to tungsten carbide-cobalt alloys are titanium carbide and tantalum carbide.

A titanium carbide-tungsten carbide solid solution added to tungsten carbide-cobalt alloys increases the hardness while reducing the thermal conductivity. Although the hardness is improved by additions of titanium carbide the transverse rupture strength is decreased. An addition of tantalum carbide results in a higher transverse rupture strength at cutting temperatures, as the tantalum carbide forms a pure solid solution and inhibits the grain growth of the carbide phase (Montgomery, 1968a).

The alloys have been shown to have a beneficial effect on the resistance to edge wear in metal cutting (Suzuki and Hayashi, 1966).

The addition of titanium carbide to a tungsten carbide-cobalt alloy, it has been claimed (Jackson and Hartman, 1962), to increase the abrasive wear resistance as would be expected from the increased hot hardness of this alloy and the increased resistance to plastic deformation (Dawihl and Mal, 1965, Ekemar, Iggstrom and Heden, 1970), plastic flow occurring readily above 800°C.

b) The Effect of Tungsten Carbide Grain Size on Deformation

The smaller grains provide less opportunity for sufficient dislocations to pile up at grain boundaries and act as stress raisers to produce microcracks in adjacent grains (Osburn, 1968). It is possible that dislocation pile ups are not large enough to produce cracks in that particular grain. Although resistance to crack propagation has been increased, there is a greater probability of material failure as there is a reduction in the ability of the material to relieve stresses by plastic flow in the cobalt. The material will thus fail in brittle fashion at some higher stress level (Osburn, 1968).

Gurland (1954) has shown that a very wide distribution of carbide grain sizes exists with a preponderance of smaller sized grains. Osburn (1968) was of the opinion that blending of grain sizes would prove beneficial. A narrow particle size distribution has shown a marked improvement of transverse rupture strength for any given particle size (Exner and Gurland, 1970).

Latin concluded, from his studies of the cracking mode for carbide samples, that there was some indication of an increased resistance to cracking for the larger grain size (Latin, 1961).

Ivensen and others (Ivensen, Chistyakova and Eiduk, 1973) assumed that the excellent performance of coarse grained alloys in operations involving impact loading was attributable not only to their better deformability but also to the smaller strength loss suffered by them during deformation.

Generally the fracture path has been observed outside the tungsten carbide grains if these are small, less than 2 to 3 microns, but fracture has been observed to initiate in the larger carbide particles, of the order 5 microns (Parikh, 1957). No fractures have been observed to pass along the grain boundaries of the cobalt (Doeg, 1960).

For systems such as WC-Co, fracture generally occurs at the binder cobalt-carbide interface (Parikh, 1957) which is probably due to the fact that the cobalt-carbide interface has the lowest surface energy in the system.

While the addition of titanium carbide reduces the strength at room temperature, the addition of tantalum carbide has little or no adverse effect (Lardner, 1970). However, at elevated temperatures the addition of tantalum carbide improves the strength.

c) The Effect of Cobalt Content

The cobalt content is mostly used in the production of mining picks which is the variable to control the wear resistance of a cutting tool, due to its considerable effect on the hardness and fracture strength of tungsten carbide composites.

For tungsten carbide-cobalt alloys having a cobalt content greater than 10%, appreciable amounts of plastic deformation are shown before fracture. In general a cobalt content of greater than approximately 13% is needed for appreciable deformation, although the actual cobalt content will depend on the grain size (Hara and Yazu, 1968).

2.3.4. Micro Chipping

Micro chipping may result from two causes, impact or impact fatigue. Impact fatigue is the mechanism proposed by Montgomery (1968b) as the major wear mechanism operating during percussive drilling. Thus the occurrence of this type of wear is related to the number of stress reversals the tool experiences and is not so dependent to the maximum stress that the tip is exposed to.

Montgomery found that the chips vary in diameter from between 25 and 200Mm depending on the carbide composition and had a thickness of 10-14 Mm. The spalls start from crack in the worn surface and follow the WC/WC or WC/Co interfaces at a depth of a few grains.

Micro chipping can also result from the impact on the micro scale where with an increased rate of impact the surface of the carbide is not given the opportunity to deform and there is a tendency for micro chipping or flaking of the surface (Osburn, 1968).

2.3.5. Gross Failure

Gross failure may result from impact causing shattering of the carbide tip. On impacting against the rock, compressive stress waves are generated which on meeting an interface are only partially transmitted, the remainder being reflected as a highly destructive tensile stress wave, which is of high enough intensity, will cause tensile cracking of the insert. The complex geometry of the insert may cause reflection from several faces, the reflected stress waves may combine to produce failure of the insert. This type of failure may occur due to poor carbide i.e. low transverse and tensile strength, pores in the carbide acting to reflect stresses, or a thick braze. With a thin braze the material will not deform, allowing the waves to be transmitted to the insert carrier where they will be attenuated without damage other than possible fatigue failure (Osburn, 1968).

To some extent higher cobalt content carbides are used to overcome this type of failure, the cobalt acting as a crack stopper and absorbing the energy by plastic deformation, though it is also essential that the carbide is free from pores and the machine is operated in such a way that tool impact is reduced to a minimum. The introduction of iso-statically hot pressed carbide (Lardner, 1974) may prove of benefit in these situations.

2.3.6. Thermal Cracking

Carbide tip may be lost due to high temperature and consequent failure of the weld. Although tungsten carbide is considered to have good thermal fatigue and shock resistance (Osburn, 1968), there are many examples in practice where carbides have failed by thermal fatigue and shock. Thermal fatigue is most noticeable in non-abrasive rocks, by the formation of a snake-skin crazing on the surface of the carbide.

The application of water to cutting tools is an area requiring further research. Generally the application of water is beneficial, provided adequate quantities are applied to cool the tool and promote efficient debris clearance.

From preliminary Lathe studies (Maher,1973) it would appear that if insufficient water is used, a slurry is formed which acts as a grinding medium accelerating the wear process.

Operating conditions should avoid situations where the tools are alternatively cooled with cold water, this leads to thermal cracking.

2.4. Effect of Pick Blunting on Cutting Performance

Picks and cutting tools play an important part in the winning of coal and driving roadways with cutting machines. The need to design efficient cutting tools is self evident, but like all tools which are used in continuous chipping and breaking down of hard materials, they are constantly subjected to wear and blunting. For this reason, it is important to know what effect blunting has for, if it is large, good performance characteristics associated with a particular design could easily be lost if the tool blunts easily. Sharp picks are inevitably blunted to a greater or lesser extent by use, even where hard materials such as tungsten carbide are employed at the tip, and material is in effect worn with blunted tools. It is highly important to see to what extent the elimination of a sharp edge will result in an increase of the forces acting and in a decrease in cutting performance.

Some studies of the influence of pick wear on cutting performance have been made by Dalziel and Davies (1964) but the experiments are not sufficiently advanced to enable generally applicable conclusions to be reported.

Dalziel and Davies (1964) carried out cutting experiments with asymmetric wedge tool. Five degrees of blunting were tested with flats of width 20, 48, 96 and 122 by 10^{-3} inches. The sharp and final condition of the tool is shown in figure 2.17.

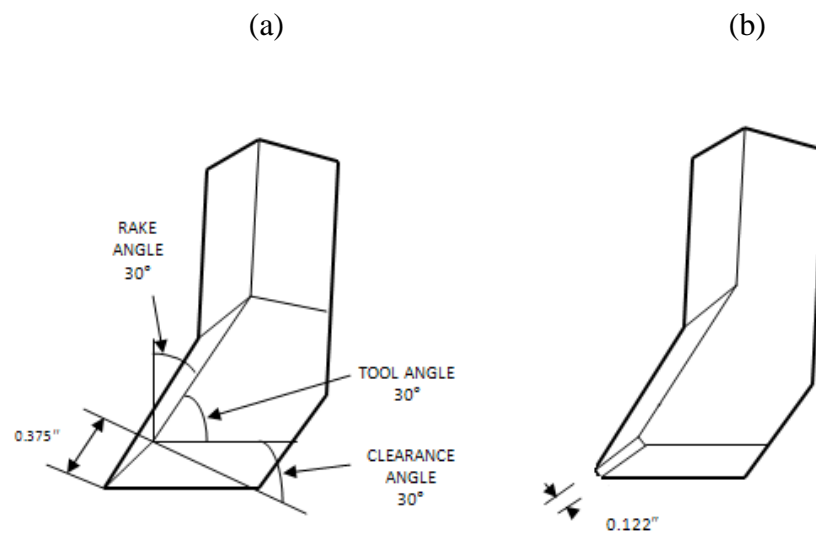


Figure 2.17. Sharp (a) and Blunt (b) Cutting Tools (Dalziel and Davies, 1964)

The forces acting on a blunt tool were measured while cutting linear grooves in flat coal surfaces at a constant depth of cut of 0.25 inch. Two components of force were measured, the cutting force acting on the tool parallel to the direction of cut and the normal force acting perpendicular to the coal surface. The peak cutting and normal forces associated with chip formation were evaluated and resolved in a direction perpendicular to the wear flat to obtain a new parameter which was designated as fracture force. Dalziel and Davies (1964) found that the fracture force appears to be related to the width of the blunt flat by a half-power law and the increase reaches to about 7 times with the highest wear flat as compared to sharp tool.

Evans and Pomeroy (1966) carried out coal cutting tests to study the cutting forces on picks blunted by grinding known lengths of flat parallel to the tool path and perpendicular to the rake face (Figure 2.18). Table 2.5 shows the results obtained.

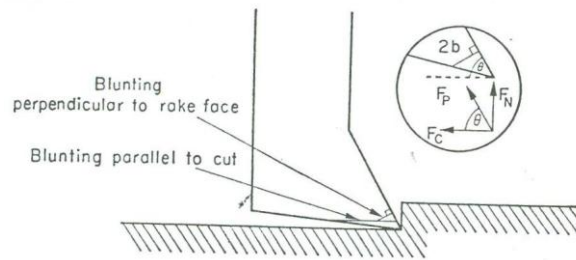


Figure 2.18. Systematic Blunting of Wedges Used to Groove Coal (Evans and Pomeroy, 1966)

Table 2.6. The Effect of Systematic Blunting on the Forces Required to Cut Grooves in Cwmtillery, Graw Coal (Evans and Pomeroy, 1966)

Tool Condition	Cutting Force (lbf)	Normal Force (lbf)
Sharp	38 ± 3	7 ± 1
1/16 in.flat perpendicular to rake face	88 ± 6	66 ± 6
1/8 in. flat parallel to tool path	35 ± 1	6 ± 1
1/16 in. flat perpendicular to rake face and 1/16 in.flat parallel to tool path	81 ± 5	58 ± 4

Results with wedge type drag tools showed that blunting perpendicular to the rake face has a much larger effect on cutting force than blunting parallel to the tool path.

Evans and Pomeroy (1966) carried out experiments to study the effect of variation in the widths of the wear flats either perpendicular to the rake face or parallel to the direction of cutting. Variation in the length parallel to the direction of cutting did not produce any consistent effect with blunting perpendicular to the rake face a definite relationship has been established. The width of the wear flat perpendicular to the rake face was varied from 2×10^{-3} to 122×10^{-3} inch. From the mean cutting force (F_c) and normal forces (F_n), the forces acting perpendicular to the wear flat (F_p) were calculated and the following relationship was obtained for wedge type tools;

$$F_p = 1540 b^{0.52} \text{ lbf} \quad (2.1)$$

Where b is the semi-width of the wear flat in inches (Evans and Pomeroy, 1966).

The relationship between force parameters and the wear flat was studied by Johnson and Morgans (1969), and the relationship has been shown to be a power law.

Bölükbaşı (1973) studied the effects of blunting of blades of a model coal plough, on haulage force and specific energy in cutting and loading. Four degrees of blunting, perpendicular to rake face were tested with flats of width 0.25, 0.50, 1.00 and 1.50 mm. The mean haulage force was increased from 1.89 kN to 2.75 kN and the specific energy was increased from 1.34 kJ/kg to 1.77 kJ/kg when the sharp blades were replaced by blunt ones having a land of width 1.50 mm.

Kenny and Johnson (1976) studied the effect of pick wear on cutting performance for Bunter sandstone using picks with positive rake angle. Figures 2.19 and 2.20 show the relationships between the wear flat, specific energy and mean cutting force.

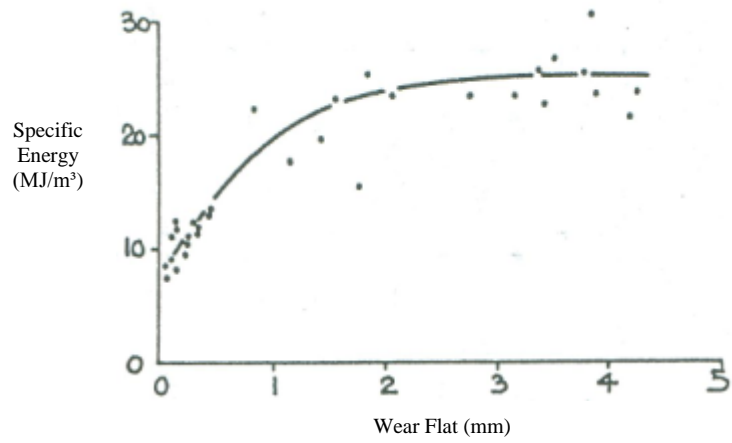


Figure 2.19. Relationship Between Specific Energy and Wear Flat (Kenny and Johnson, 1976)

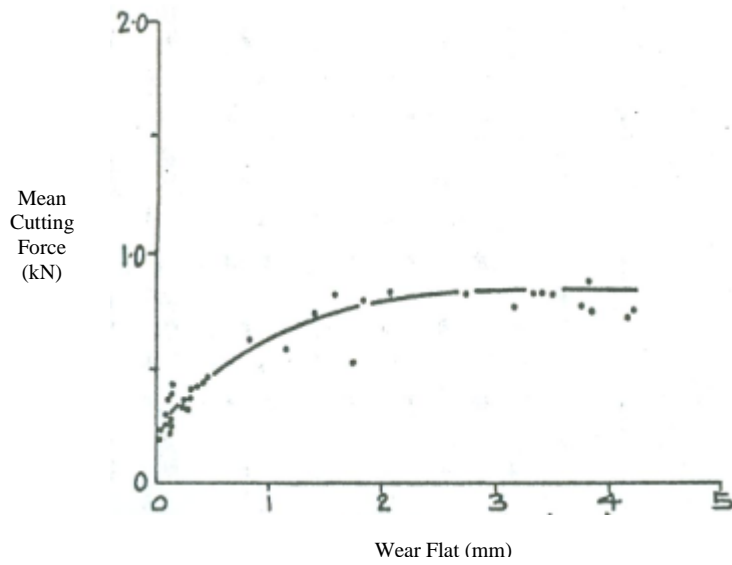


Figure 2.20. Relationship Between Mean Cutting Force and Wear Flat (Kenny and Johnson, 1976)

CHAPTER 3

EXPERIMENTAL PROCEDURE

Rock property tests and laboratory cutting tests were carried out on rock samples obtained from various coal fields such as Çayırhan, Tınaz, Seyitömer and Elbistan.

3.1. Rock Property Tests

3.1.1. Uniaxial Compressive and Tensile Strength Tests

Uniaxial compressive and tensile strength (Brazilian) tests were carried out according to ISRM Suggested Methods (ISRM,2007).

3.1.2. Cone Indenter Test

Cone indenter tests were carried out using the NCB Cone Indenter.

3.1.2.1. Apparatus

Figure 3.1 shows the NCB Cone Indenter designed to determine the hardness of rock by measuring its resistance to indentation by a hardened tungsten carbide cone.

The instrument comprises a portal steel frame 175 mm long in which a steel strip is clamped along a longitudinal axis. In the middle of one longitudinal side of the frame a dial gauge is inserted in such a way that its probe is in contact with one side of the steel strip. In the middle of the opposite longitudinal side of the frame is fitted a micrometer with a hollow spindle into which is inserted a tungsten carbide cylinder with a conical tip having a 40° cone angle. The flat base of the cylinder is in contact with a steel ball so that the cylinder is free to rotate in its mounting. The micrometer is used to measure the amount of indentation and the gauge indicates the distance the spring is deflected.



Figure 3.1. NCB Cone Indenter

3.1.2.2. Procedure

Testing procedure is described in the apparatus manual (MRDE, 1977). The main steps are;

- Test specimens with approximate dimensions of 12 mm x 12 mm x 6 mm should be prepared with sound and clean test surface.
- Dial gauge is set to 0.0 and micrometer reading is taken (M_0).
- The micrometer is to be turned until the dial gauge shows 0.635 (D_1) and the micrometer is read again (M_1).

3.1.2.3. Calculation

The penetration of the cone into the specimen is calculated from the formula:

$$P = (M_1 - M_0) - D_1 \quad (3.1)$$

The standard cone indenter number is calculated from the formula:

$$I_s = 0.635/P \quad (3.2)$$

3.1.3. Shore Hardness Test

Shore hardness is suggested for the hardness determination of rocks, using the shore scleroscope in the laboratory or in-situ (ISRM, 2007). Figure 3.2 shows the shore scleroscope used in the tests.



Figure 3.2. Model C-2 Type Shore Scleroscope

The shore scleroscope consists of a diamond or tungsten carbide tipped mass which is fitted into a vertical guide tube and set at a predetermined height. Practically, the mass is raised by suction about 300 mm. The specimen is mounted on the anvil situated below the tube and the mass is allowed to fall freely onto the surface of the specimen by squeezing the rubber bulb of the equipment. After striking the surface the mass rebounds and the height of rebound which is indicated on a graduated tube, is a measure of the samples resilience. The test requires smooth flat surfaces and the specimen should have a minimum test surface of 10 cm² and a minimum thickness of 1 cm. At least 20 hardness determinations should be made (ISRM, 2007).

3.1.4. Schmidt Rebound Hardness Test

Schmidt rebound hardness values of the rock samples were determined using L-type Schmidt hammer shown in Figure 3.3.



Figure 3.3. L-Type Schmidt Hammer

The plunger of the hammer is placed against the specimen and is depressed into the hammer by pushing the hammer against the specimen vertically. Energy is stored in a spring which automatically rebounds at a prescribed energy level and impacts a mass against the plunger. The height of rebound of the mass is measured on a scale and is taken as the measure of hardness. If instrument is not vertically downward pointed, gravitational effect due to inclination of hammer must be accounted and the results should be corrected for inclination. At least 20 individual tests shall be conducted on any rock sample (ISRM, 2007).

3.1.5. Petrographic Analyses

Thin-section analyses were carried out at the Geological Engineering Department of the METU to determine the petrographic descriptions of the samples. Thin-sections were also analyzed to determine the mean mineral grain size of the rock samples.

3.1.6. Density Determination

Densities of the rock specimens were determined by weighing right cylindrical rock samples with known volumes.

3.2. Laboratory Cutting Tests

The standard cutting test has been developed by Roxborough and Phillips (1974) to simulate the cutting action of a drag-pick tool and to measure the corresponding cutting properties of rock materials. The cuts are made at a depth of 5 mm with a standardized geometry and composition tungsten carbide chisel-shaped tool mounted on an instrumented cutting rig. Cuts can be made either on around the surface of a 76 mm diameter rock core or on the smoothed surface of a rock block. The strain gauge output from the dynamometer is recorded as analogue ultra violet traces which are analysed together with other recorded information such as weight of debris and length of cut.

3.2.1. The Rock Cutting Set-up

Cutting tests were carried out using the rock cutting setup at the Mining Engineering Department of the Middle East Technical University. Figure 3.4 shows the setup which consists mainly of a shaping machine, a dynamometer and a recording unit.



Figure 3.4. Rock Cutting Setup

3.2.1.1. Shaping Machine

Cutting is performed using a modified shaping machine having a stroke of 625 mm and a power of 4 kW. The rig can be raised, lowered or traversed relative to the cutting tool and can accommodate a block of rock having a length of 50 cm, a width of 35 cm and a height of 30 cm. The cross-head of the shaper has been modified to accept a triaxial force dynamometer and a tool holder.

3.2.1.2. Triaxial Dynamometer

The shaping machine is fitted with a 150 kN triaxial dynamometer which resolves the force acting on the tool during cutting into three mutually perpendicular components; the in-line cutting force, the normal force tending to push the tool out of the rock and the lateral force tending to move the tool sideways. For cuttability studies and the specific energy determination only the cutting forces are directly recorded and also continuously integrated on to an ultraviolet multi-channel recorder with the help of an integrator.

3.2.1.3. Recording Unit

Recording unit consists of a SE 995 6-channel alternating current bridge conditioning unit (excitation output of 5 volts), a SE 6151 conditioning amplifier, a SE 6150 12 channel ultra-violet oscillograph and an integrator.

Electrical signals coming from the dynamometer are amplified and the direct cutting and mean forces are recorded on the UV paper. Figure 3.5 shows a typical UV recording.

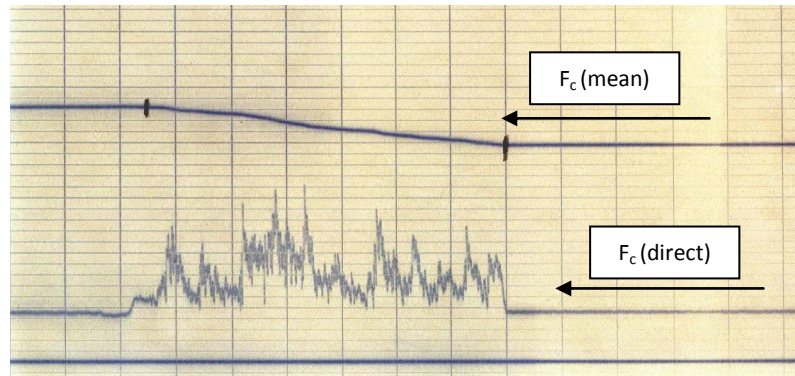


Figure 3.5. Typical Records of Direct and Mean Cutting Forces on an Ultraviolet Paper

3.2.1.4. Calibration

The dynamometer and the recording unit need to be calibrated to analyse the U.V. records to determine cutting forces. Pressure gauge of a hydraulic jack was first calibrated under the testing machine. Force is applied horizontally to the tip of the cutting bit in opposite direction of cutting at increasing values and the recording unit has been calibrated to read up to 5 kN. Calibration constant has been determined as kN/mm of deviation from zero position.

3.2.1.5. Standard Conditions for a Cutting Test and the Degrees of Blunting

Cutting tests with sharp and blunt picks were carried out at the following standard cutting conditions (Fowell and Johnson, 1982; McFeat-Smith and Fowell, 1977).

Depth of cut : 5 mm

Cutting speed : 150 mm / s

Type of cutting pick

Rake angle : -5°

Back clearance angle : 5°

Cutting width : 12.7 mm

Composition : Tungsten carbide
with 10% cobalt

The experiment steps are:

- The rock is cut at standard conditions,
- The recording paper is analyzed and mean cutting force (F_c) is calculated in kN,
- The length cut (L) is measured in meters,
- The amount of rock cut is weighed and volume of the rock cut is calculated by using its density. Then laboratory cutting specific energy is calculated by the following formula:

$$SE = \frac{F_c(kN) \times 10^3 \times L(m)}{\frac{10^6}{V(m^3)}} = MJ / m^3 \quad (3.3)$$

Figure 3.6 (a) shows a standard sharp pick used in the experiments. Since the standard pick has negative rake, standard picks were blunted by grinding with 40° wear angle to obtain wear flats of width 1 mm, 2 mm, 3 mm and 4 mm. Figure 3.6 (b) shows a pick blunted to 4 mm wear flat.

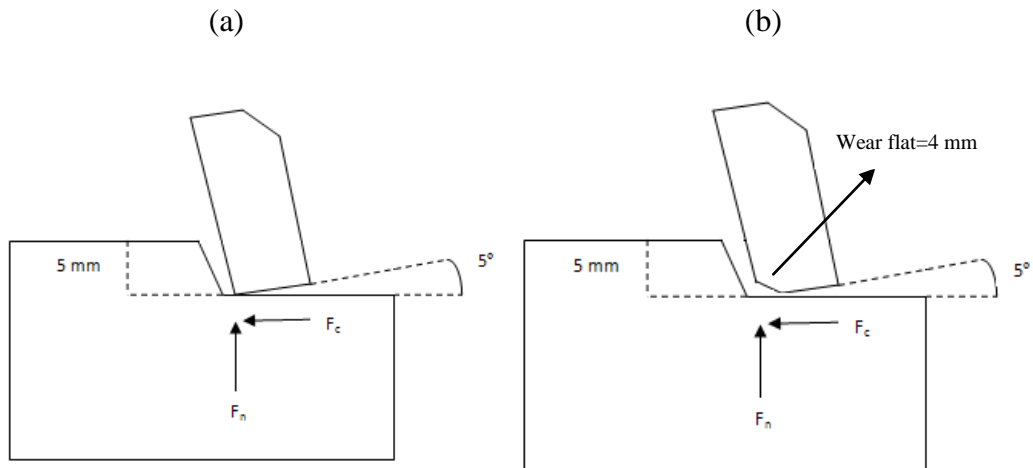


Figure 3.6. Sharp (a) and Blunted (b) Standard Cutting Picks

Figure 3.7 shows the blunting of a pick by using a diamond grinding disc and Figure 3.8 shows the sharp and 1 mm, 2 mm, 3 mm and 4 mm blunted picks.

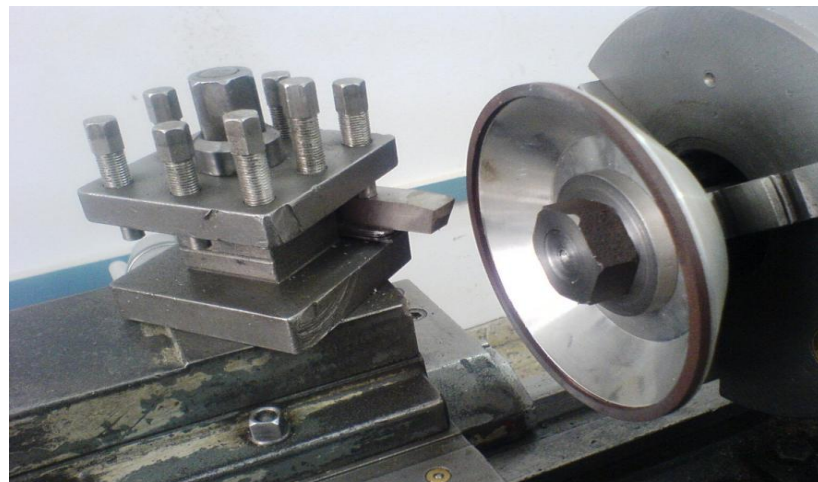


Figure 3.7. Blunting of a Standard Pick by Using Diamond Grinding Disc

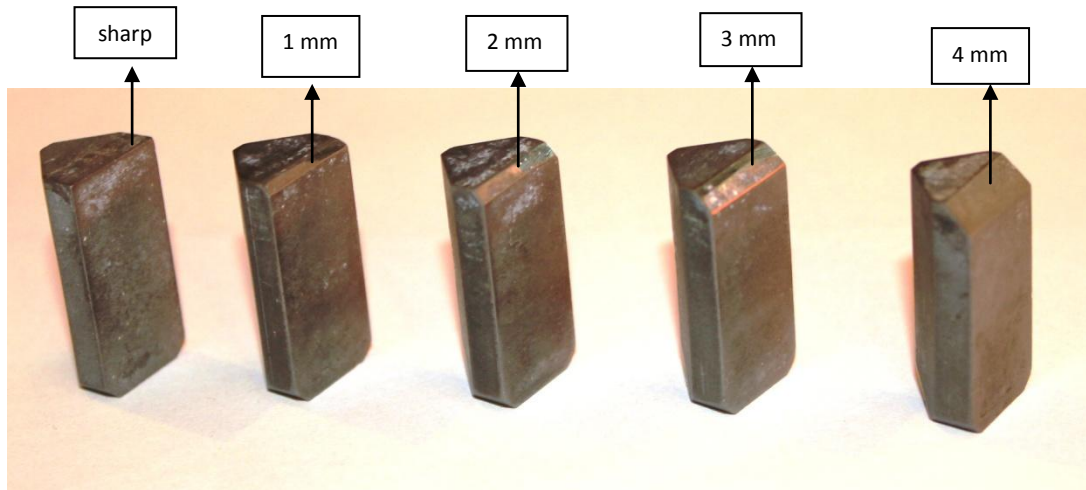


Figure 3.8. Sharp and Blunted Picks Used in the Tests

3.3. Size Distribution and Coarseness Index

Size distribution and coarseness index gives a comparative measure of size and distribution of the debris produced. The debris obtained after each cut was sized from 22.23 mm, 19.05 mm, 12.70 mm, 8 mm, 4.76 mm and 2.0 mm sieve sizes and the cumulative weight percentage of each size fraction into which the debris has been graded was determined. The sum of the cumulative weight percentages gives the coarseness index ($C.I_n$) whose value depends on the size and number of sieves used. Table 3.1 shows the sieve sizes employed and the calculation of coarseness index.

Table 3.1. Calculation of Coarseness Index

Size Fraction	Weight (gr)	Weight (%)	Cumulative Weight (%)
+22.23 mm	0	0	0
-22.23 mm +19.05 mm	-	-	-
-19.05 mm +12.7 mm	-	-	-
-12.7 mm +8 mm	-	-	-
-8 mm +4.76 mm	-	-	-
-4.76 mm +2.0 mm	-	-	-
-2.0 mm	-	-	100
Total	-	100	$C.I_n =$

CHAPTER 4

EXPERIMENTAL RESULTS AND DISCUSSIONS

Rock property and laboratory cutting tests were carried out on various rock samples having different strengths. Thin-section analyses were carried out at the Geological Engineering Department of METU.

4.1. Rock Property Test Results

Table 4.1 shows the rock property test results. Tests were not carried out on higher strength rocks due to the limited capacity of the rock cutting setup and the possibility of having a cutting tool or dynamometer failure. Table 4.2 shows the results of thin-section analyses on rock samples.

Table 4.1. Rock Property Test Results

Type of Rock	Uniaxial Compressive Strength (MPa)	Brazilian Tensile Strength (MPa)	Cone Indenter No. (Is)	Shore Hardness	Schmidth Hammer Hardness	Density (gr/cm ³)
Limestone 1	6.08	0.78	0.89	3.10	16.18	1.86
Limestone 2	28.69	5.52	1.66	15.30	35.40	2.22
Limestone 3	5.75	0.59	0.30	7.10	23.40	1.42
Limestone 4	18.38	2.39	1.21	14.20	29.70	1.69
Clayey limestone	5.77	1.32	0.60	21.60	25.04	1.02
Mudstone 1	28.30	3.38	1.52	30.30	37.20	2.15
Mudstone 2	28.19	4.63	1.63	22.70	25.86	2.17
Mudstone 3	31.75	1.93	1.27	13.20	32.60	2.01
Mudstone 4	64.15	10.17	2.07	29.10	45.80	1.91
Mudstone Siltstone	26.00	5.05	1.19	13.40	21.66	1.79
Marl 1	19.00	2.40	1.15	16.83	18.00	1.70
Marl 2	6.31	1.64	0.67	7.50	18.24	1.24
Altered tuff	25.06	4.00	1.33	17.50	32.00	1.95
Lithic tuff 1	28.04	1.97	1.24	25.30	44.00	1.70
Lithic tuff 2	11.45	2.03	0.78	16.60	29.20	1.53
Claystone	13.00	1.61	0.50	6.80	20.80	1.42
Siltstone 1	29.03	7.56	2.09	36.50	39.40	2.11
Siltstone 2	36.13	8.73	3.63	22.00	45.20	2.20
Andesite	34.34	5.92	2.19	46.50	45.20	2.07
Travertine	47.84	5.89	2.79	25.10	43.60	2.46
Ranges from Min. to Max.	5.75-64.15	0.59-10.17	0.30-3.63	3.10-46.50	16.18-45.80	1.02-2.46

4.2. Thin Section Results

Table 4.2 shows petrographic characteristics of the rock samples and Table 4.3 shows the mineral grain sizes determined by analyzing thin sections.

Table 4.2. Petrographic Characteristics

Sample	Characteristic	Quartz Content (%)	Cementation
Limestone 1	beige fine grained	1	well crystal compacted, well cemented
Limestone 2	brown colored, very fine grained	1-2	well cemented
Limestone 3	brownish beige very fine grained	0	well cemented
Limestone 4	beige colored, very fine grained and laminated	0	well compacted, well cemented
Mudstone 1	very fine grained and laminated	25-30	well cemented
Mudstone 2	red colored, fine grained	10	well cemented
Mudstone 3	light green colored	20	well cemented
Mudstone 4	greenish brown banded and laminated	35	Well compacted, well cemented
Mudstone Siltstone	brownish colored bands irregular lenses of mudstone alternating with darker colored and fine grained siltstone	4-5	well compacted, well cemented
Clayey Limestone	light brown colored laminated, very fine grained calcites and clay minerals	1	well compacted, well cemented
Marl 1	light colored, very fine grained	2	Well cemented, well compacted
Marl 2	beige colored, very fine grained calcite and clay minerals	1-2	Well cemented, well compacted
Altered Tuff	yellowish brown colored, fine grained	85	not containing cementation
Lithic Tuff 1	light violet colored volcanic rock with phenocrysts and rock fragments	10	compacted, not containing cementation
Lithic Tuff 2	very fine grained matrix, well rounded to angular fragments of volcanic rocks	4	not containing cementation
Claystone	beige colored, fine grained	20-25	Cemented, compacted
Siltstone 1	beige colored, fine grained	20	Well cemented, well compacted
Siltstone 2	brownish colored, very fine grained	1	Well cemented, well compacted
Andesite	pink colored, fine grained porphyritic texture	0	Not containing cementation
Travertine	light colored, medium grained calcite	1	Well crystal compacted

Table 4.3. Mineral Grain Sizes

Sample	Grain Size Lowest (μm)	Grain Size Highest (μm)	Grain Size Weighed Average (μm)
Limestone 1	90.00	160.00	126.00
Limestone 2	20.00	20.00	20.00
Limestone 3	30.00	30.00	30.00
Limestone 4	20.00	100.00	55.00
Clayey Limestone	20.00	20.00	20.00
Mudstone 1	20.00	20.00	20.00
Mudstone 2	50.00	270.00	125.00
Mudstone 3	80.00	120.00	98.00
Mudstone 4	40.00	270.00	92.00
Mudstone-siltstone	20.00	20.00	20.00
Marl 1	20.00	60.00	44.00
Marl 2	40.00	40.00	40.00
Altered Tuff	90.00	700.00	272.00
Lithic Tuff 1	80.00	1500.00	419.00
Lithic Tuff 2	90.00	900.00	362.00
Claystone	25.00	25.00	25.00
Siltstone 1	40.00	40.00	40.00
Siltstone 2	50.00	700.00	135.00
Andesite	180.00	1500.00	477.00
Travertine	40.00	40.00	40.00

4.3. Cutting Test Results

Table 4.4 shows cutting test results on rock samples with cutting picks having varying wear flats. The results show that as compared to sharp picks, cutting force increases 2-3 times and the cutting specific energy increases 4-5 times when the wear flat is increased to 4 mm. Tests with 4 mm pick could not be applied for siltstone 2 and travertine not to cause any damage to the cutting set-up due to very high cutting forces encountered.

Table 4.4. Cutting Test Results

Type of Rock	Width of Wear Flat (mm)	Mean Cutting Force (kN)	Laboratory Cutting Specific Energy (MJ/m ³)
Limestone 1	Sharp	0.56	6.74
	1	0.57	7.64
	2	0.71	9.85
	3	0.79	12.29
	4	0.94	15.37
Limestone 2	Sharp	1.26	8.68
	1	1.61	13.83
	2	2.05	21.37
	3	3.57	42.63
	4	4.82	57.55
Limestone 3	Sharp	0.19	1.93
	1	0.21	2.22
	2	0.26	2.67
	3	0.28	2.84
	4	0.36	4.35
Limestone 4	Sharp	0.64	4.24
	1	0.80	5.93
	2	1.03	7.23
	3	1.42	11.48
	4	1.58	14.55
Clayey Limestone	Sharp	0.32	2.36
	1	0.38	2.58
	2	0.45	3.33
	3	0.55	4.20
	4	0.61	5.12
Mudstone 1	Sharp	1.56	17.96
	1	1.92	24.53
	2	2.37	26.91
	3	2.92	40.05
	4	3.94	54.07
Mudstone 2	Sharp	1.41	12.03
	1	1.63	18.92
	2	2.07	23.73
	3	2.68	31.94
	4	3.62	43.12
Mudstone 3	Sharp	0.88	7.99
	1	1.25	14.56
	2	1.44	14.98
	3	2.05	22.71
	4	2.52	37.01
Mudstone 4	Sharp	2.18	19.86
	1	3.18	33.39
	2	3.22	33.28
	3	4.86	55.03
	4	4.94	79.64
Mudstone-Siltstone	Sharp	0.84	8.92
	1	1.01	9.58
	2	1.04	10.24
	3	1.29	10.62
	4	1.60	15.77

Table 4.4. Cutting Test Results (continued)

Type of Rock	Width of Wear Flat (mm)	Mean Cutting Force (kN)	Laboratory Cutting Specific Energy (MJ/m ³)
Marl 1	Sharp	0.34	2.07
	1	0.34	2.17
	2	0.44	3.90
	3	0.56	4.21
	4	0.71	4.30
Marl 2	Sharp	0.36	2.18
	1	0.42	2.79
	2	0.58	3.86
	3	0.72	4.90
	4	0.74	5.90
Altered Tuff	Sharp	1.15	10.90
	1	1.54	16.62
	2	1.89	21.08
	3	2.47	28.97
	4	2.89	36.85
Lithic Tuff 1	Sharp	0.99	7.47
	1	1.20	12.40
	2	1.45	16.91
	3	2.29	27.05
	4	2.74	31.91
Lithic Tuff 2	Sharp	0.74	6.52
	1	0.80	10.02
	2	0.92	11.74
	3	1.22	15.45
	4	1.64	19.61
Claystone	Sharp	0.21	1.44
	1	0.20	1.71
	2	0.21	1.79
	3	0.25	1.92
	4	0.28	2.15
Siltstone 1	Sharp	1.46	9.96
	1	2.01	15.67
	2	2.40	19.19
	3	2.58	22.08
	4	3.36	33.34
Siltstone 2	Sharp	2.20	27.68
	1	3.80	39.58
	2	5.11	48.92
	3	6.57	87.39
	4	Not tried for safety	
Andesite	Sharp	2.47	23.34
	1	3.45	42.34
	2	4.17	50.25
	3	6.03	64.21
	4	6.31	86.90
Travertine	Sharp	3.26	28.28
	1	4.84	43.79
	2	5.89	61.78
	3	7.51	84.45
	4	Not tried for safety	

4.4. Relationships Between Laboratory Cutting Specific Energy, Mean Cutting Force and Wear Flats With Uniaxial Compressive Strengths

Figure 4.1 shows the relationships between uniaxial compressive strength and laboratory cutting specific energy at different wear flats. Figures show that rather good correlation exists between the laboratory cutting specific energy and the increase in uniaxial compressive strength. Although increase in wear flat causes slight increase in specific energy for low strength rocks, it increases rapidly with increasing wear flat and uniaxial compressive strength, reaching 4-5 times as compared to sharp picks for high strength rocks.

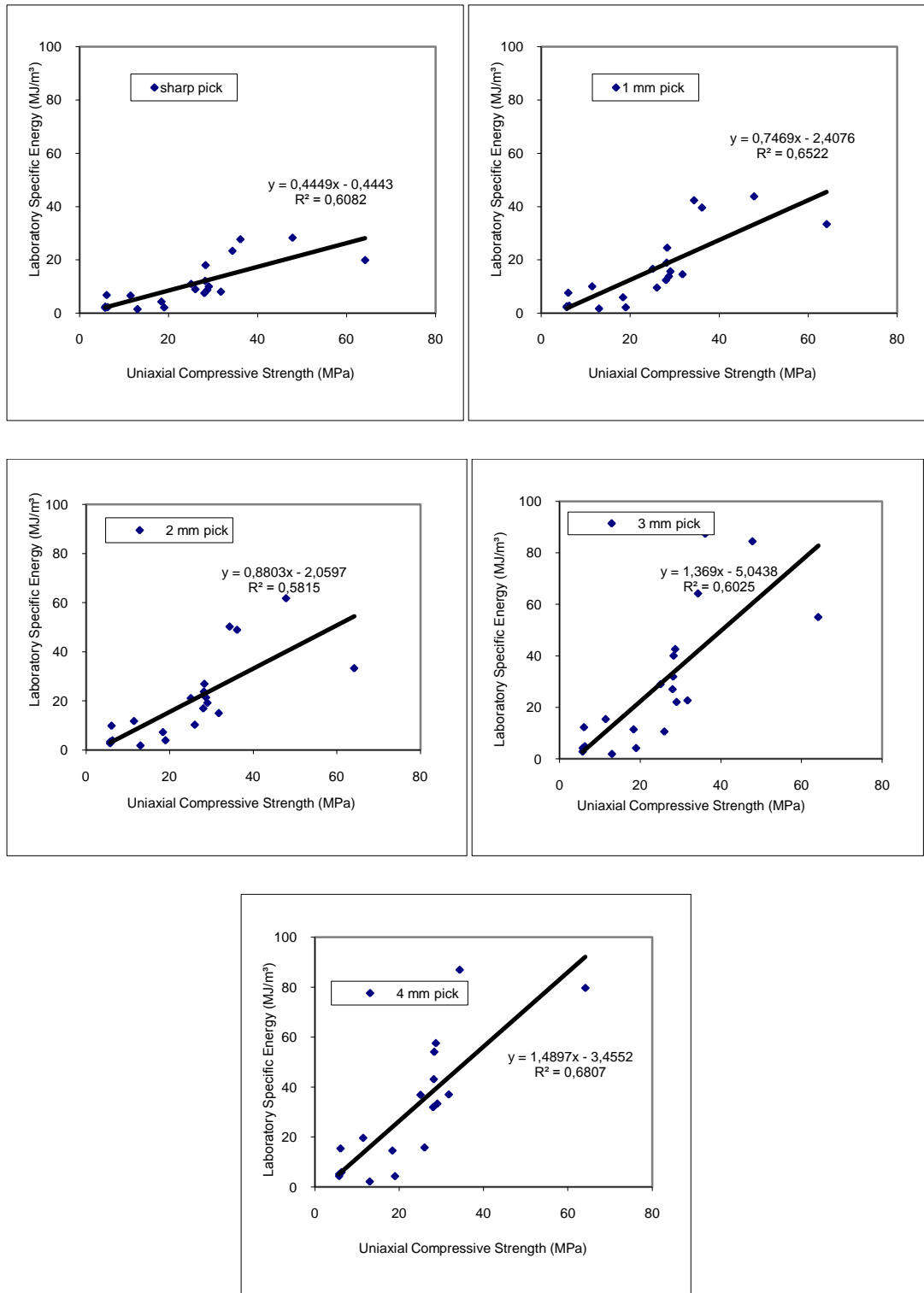


Figure 4.1. Relationships Between Uniaxial Compressive Strength and Laboratory Cutting Specific Energy at Different Wear Flats

Figure 4.2 shows the establishment of the critical wear flats at varying compressive strengths if the limiting cutting specific energy above which poor cutting performance will be obtained is considered to be 25 MJ/m³ (see Table 2.4). As it can be seen from the figure, although the cutting specific energy remains below 25 MJ/m³ even with 4 mm wear flat for rocks having UCS (uniaxial compressive strength) less than about 20 MPa, the critical limit is exceeded even with 1 mm wear flat pick when the uniaxial compressive strength exceeds about 35 MPa.

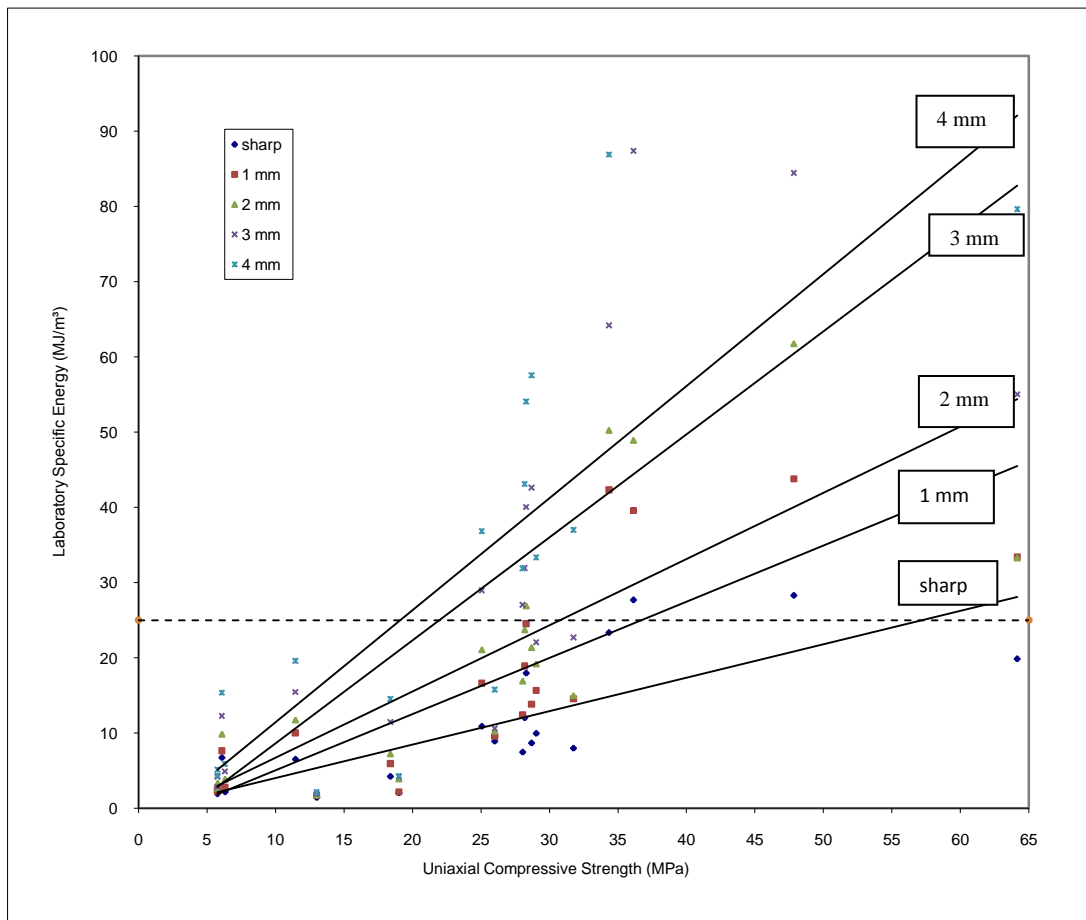


Figure 4.2. Critical Wear Flats for Varying Uniaxial Compressive Strengths

Figure 4.3 shows the relationships between the mean cutting force and the uniaxial compressive strength at different wear flats. The relationships are similar to laboratory cutting specific energies. Mean cutting force for higher compressive strengths increases 2-3 times with 3-4 mm wear flats as compared to sharp picks.

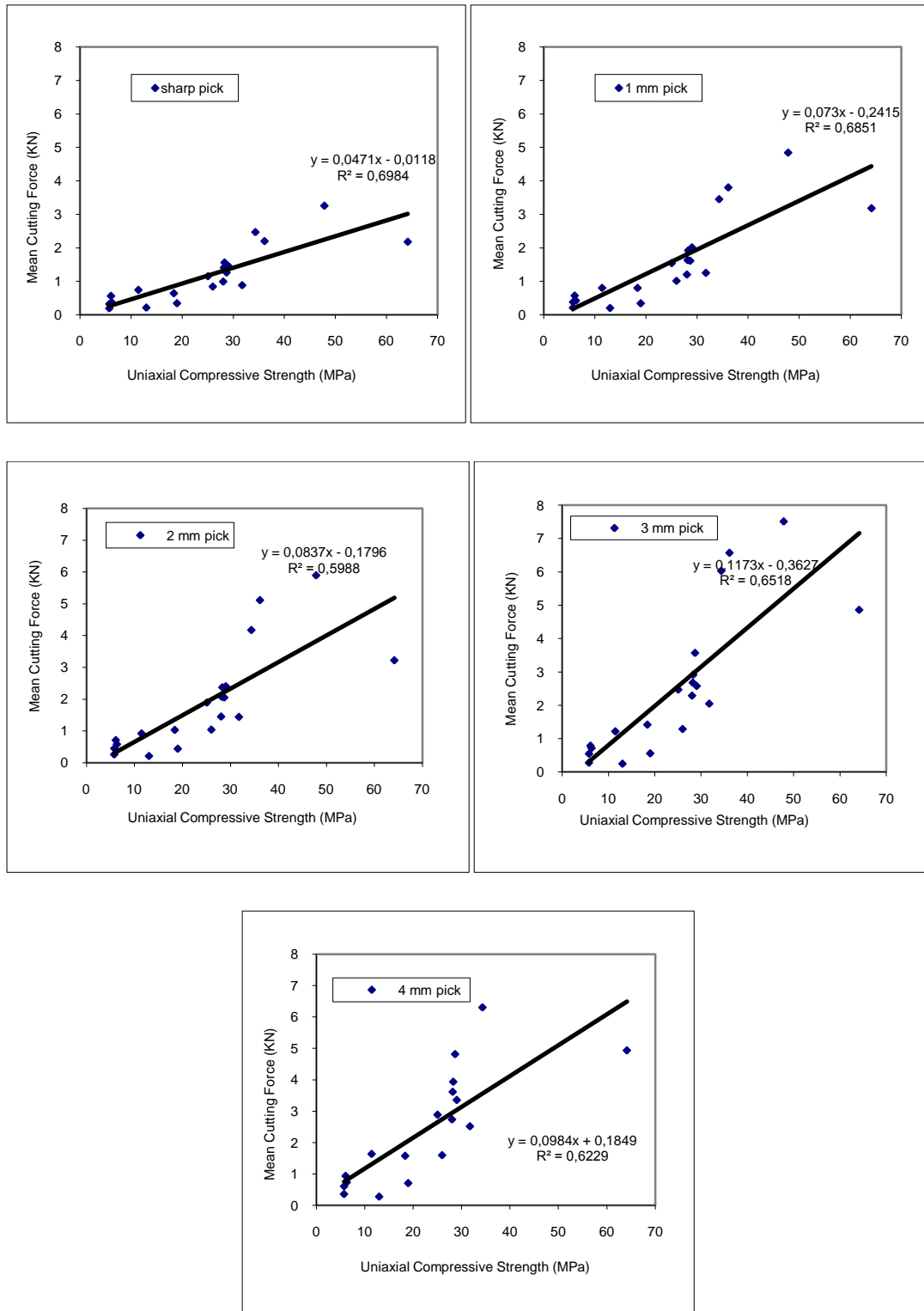


Figure 4.3. Relationships Between Uniaxial Compressive Strength and Mean Cutting Force at Different Wear Flats

4.5. Relationships Between Laboratory Cutting Specific Energy, Mean Cutting Force and Wear Flats With Tensile Strengths

Figure 4.4 shows the relationships between Brazilian Tensile Strength and laboratory cutting specific energy at different wear flats. Figures show that rather low correlation exists between the specific energy and the increase in tensile strength. Although the increase in wear flat causes slight increase in specific energy for low tensile strengths, it increases rapidly as the tensile strength and wear flat increase, reaching about 4 times as compared to sharp picks for higher tensile strengths.

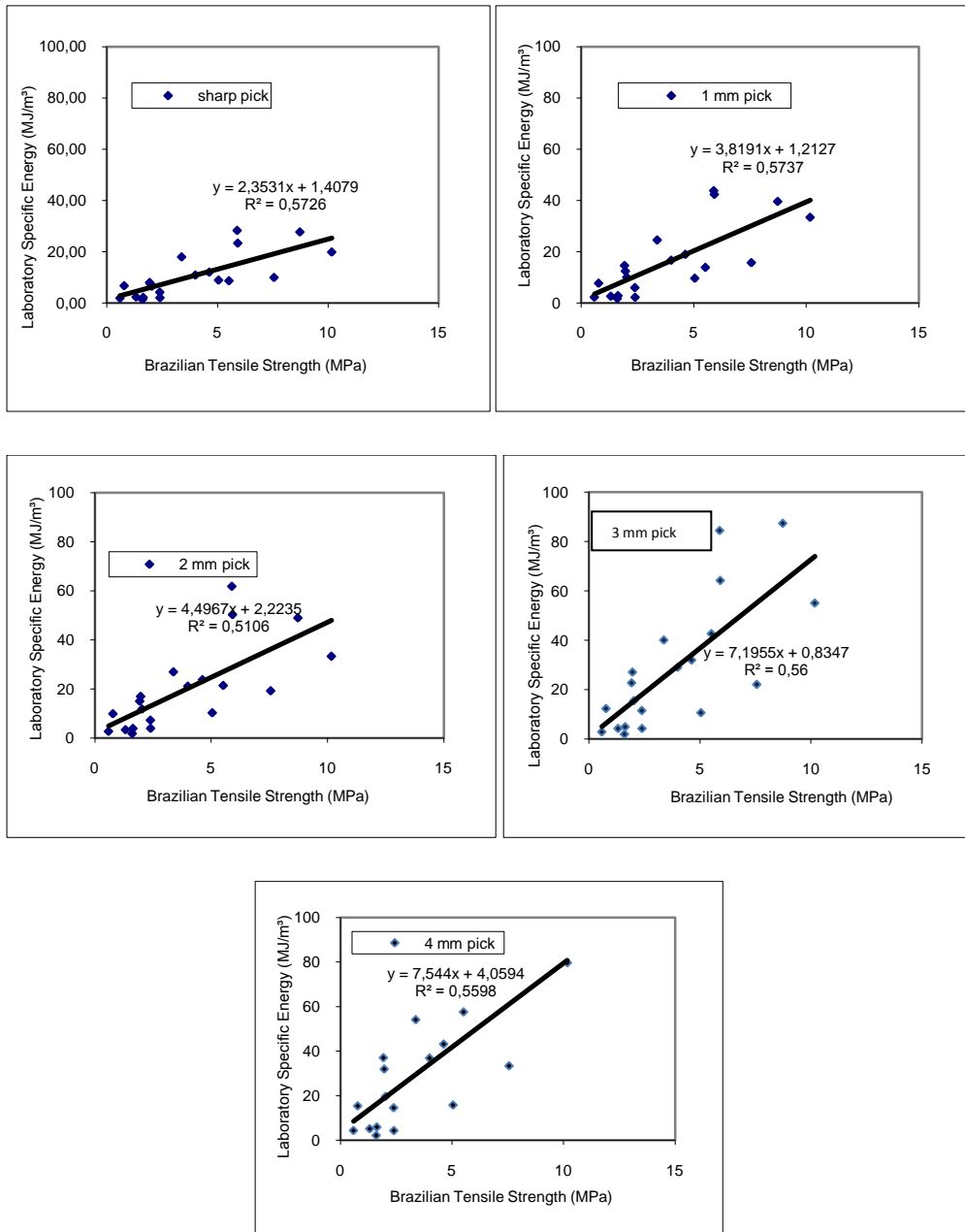


Figure 4.4. Relationships Between Brazilian Tensile Strength and Laboratory Specific Cutting Energy at Different Wear Flats

Figure 4.5 shows the establishment of the critical wear flats at varying tensile strengths if the limiting cutting specific energy above which poor cutting performance will be obtained is considered to be 25 MJ/m³. As it can be seen from the figure, although the cutting specific energy remains below 25 MJ/m³ even with 4 mm wear flat for rocks having BTS (brazilian tensile strength) less than about 3 MPa, the critical limit is exceeded even with 1 mm wear flat picks when the BTS exceeds about 6 MPa.

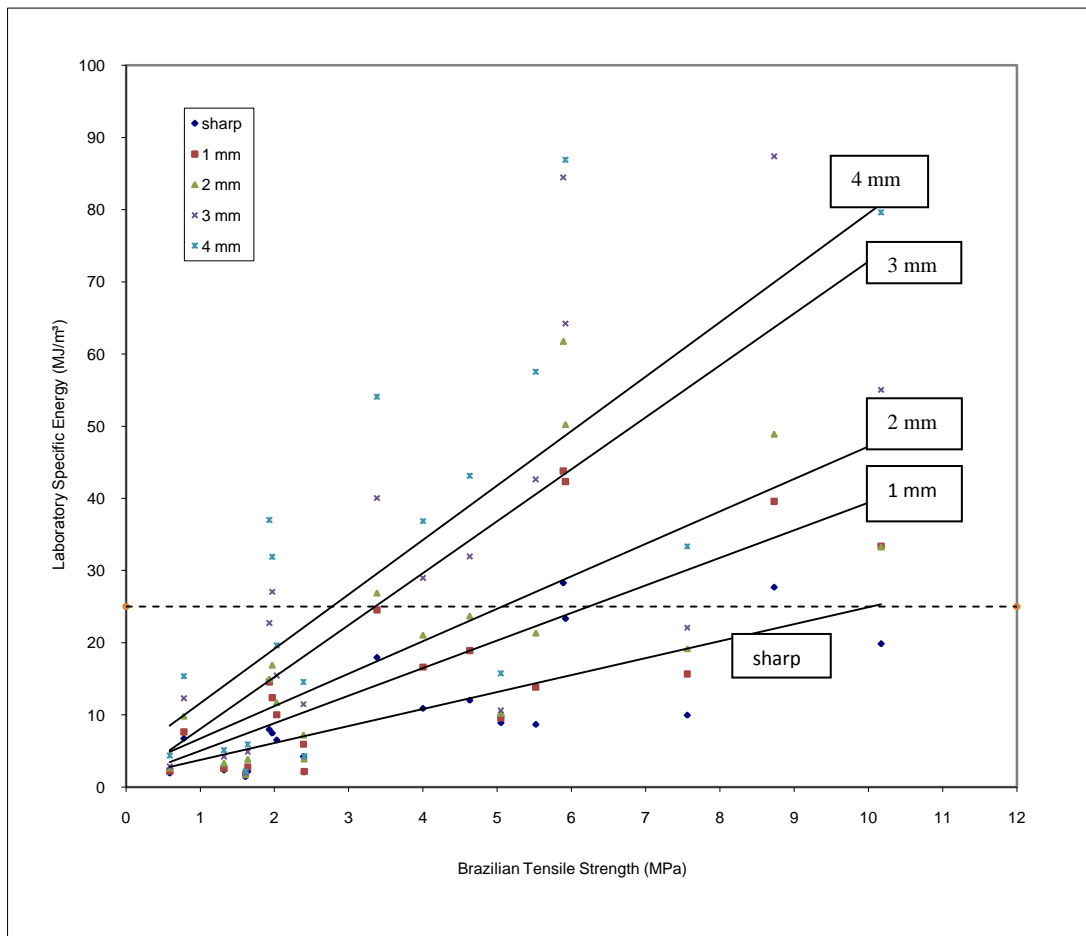


Figure 4.5. Critical Wear Flats for Varying Brazilian Tensile Strengths

Figure 4.6 shows the relationships between the mean cutting force and the Brazilian Tensile Strength at different wear flats. The relationships are similar to laboratory cutting specific energies. Mean cutting force for higher tensile strengths increases 2-3 times with 3-4 mm wear flats as compared to sharp picks.

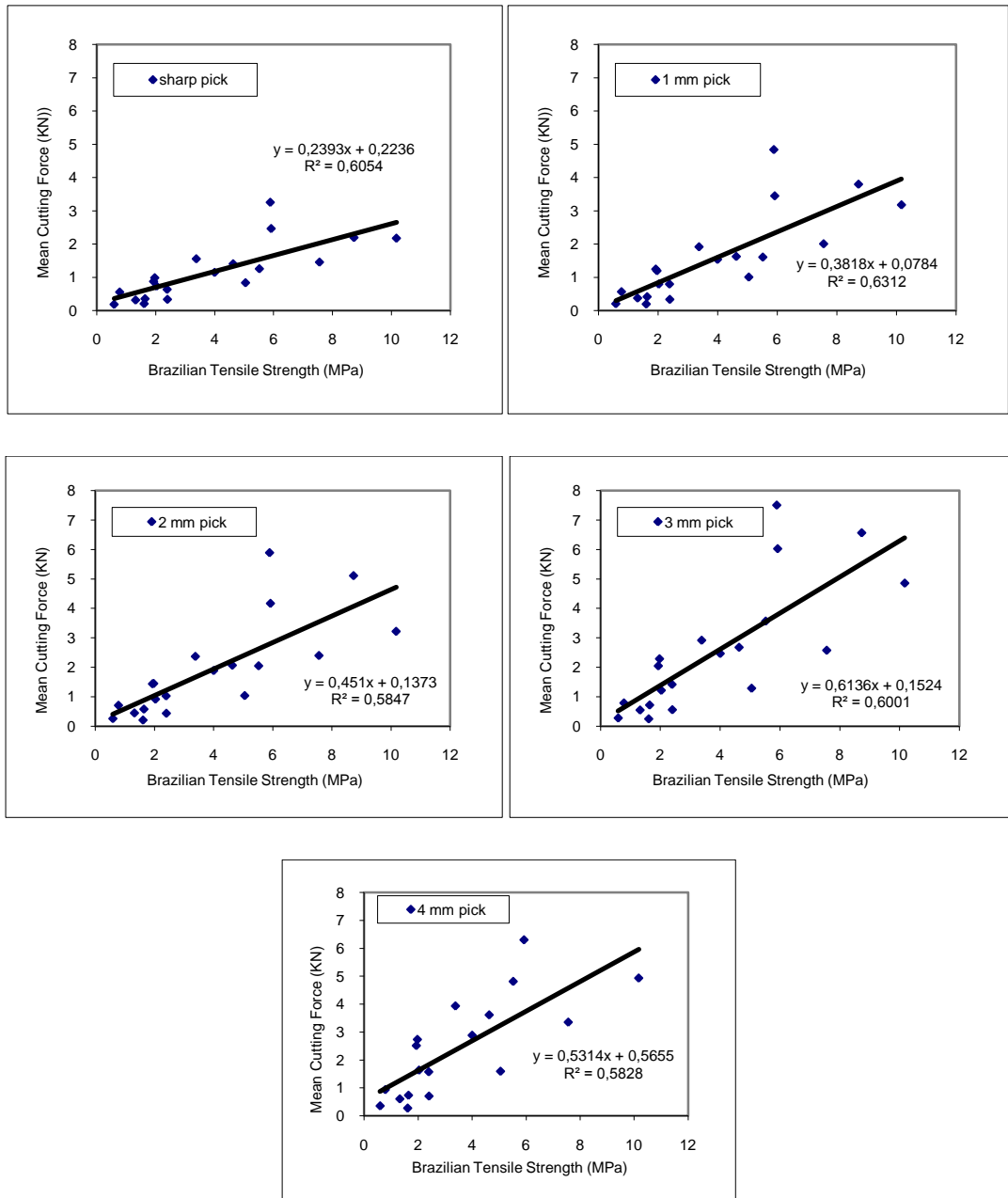


Figure 4.6. Relationships Between Brazilian Tensile Strength and Mean Cutting Force at Different Wear Flats

4.6. Relationships Between Laboratory Cutting Specific Energy, Mean Cutting Force and Wear Flats with Cone Indenter Hardness

Figure 4.7 shows the relationships between the laboratory cutting specific energy and standard cone indenter hardness at different wear flats. Figures show that the relationship is linear and rather high correlation exists between the specific energy and the standard cone indenter values. The rate of increase in specific energy gets higher with increasing wear flats, being about 3-4 times larger with 4 mm wear flat as compared to sharp picks at a cone indenter hardness of about 2.

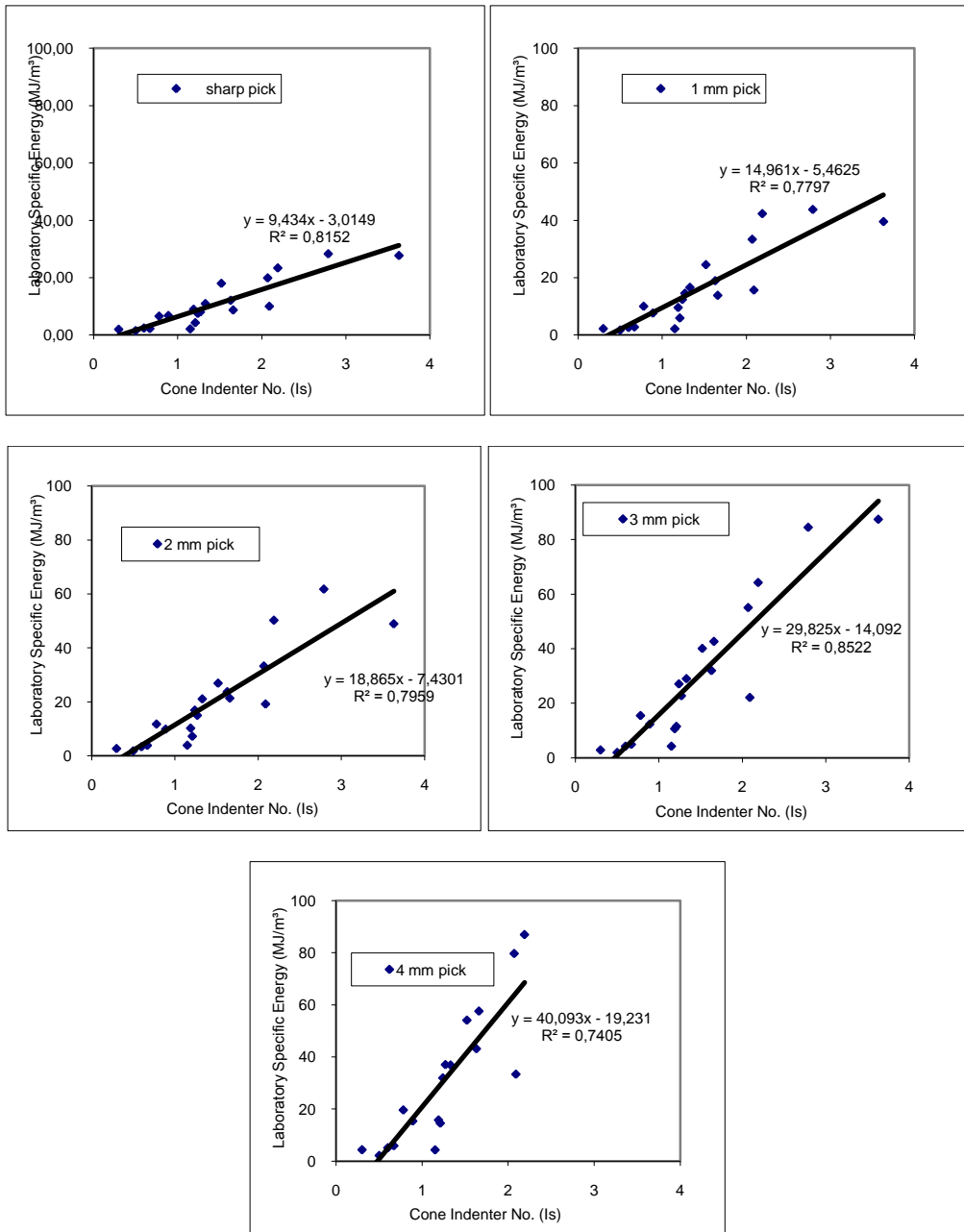


Figure 4.7. Relationships Between Cone Indenter Number and Laboratory Specific Cutting Energy at Different Wear Flats

Figure 4.8 shows the establishment of the critical wear flats at varying cone indenter numbers if the limiting cutting specific energy above which poor cutting performance will be obtained is considered to be 25 MJ/m³. As it can be seen from the figure, although the cutting specific energy remains below 25 MJ/m³ even with 4 mm wear flat for rocks having cone indenter number of less than 1.2, the critical limit is exceeded even with 1 mm wear flat pick when the cone indenter number is above 2.

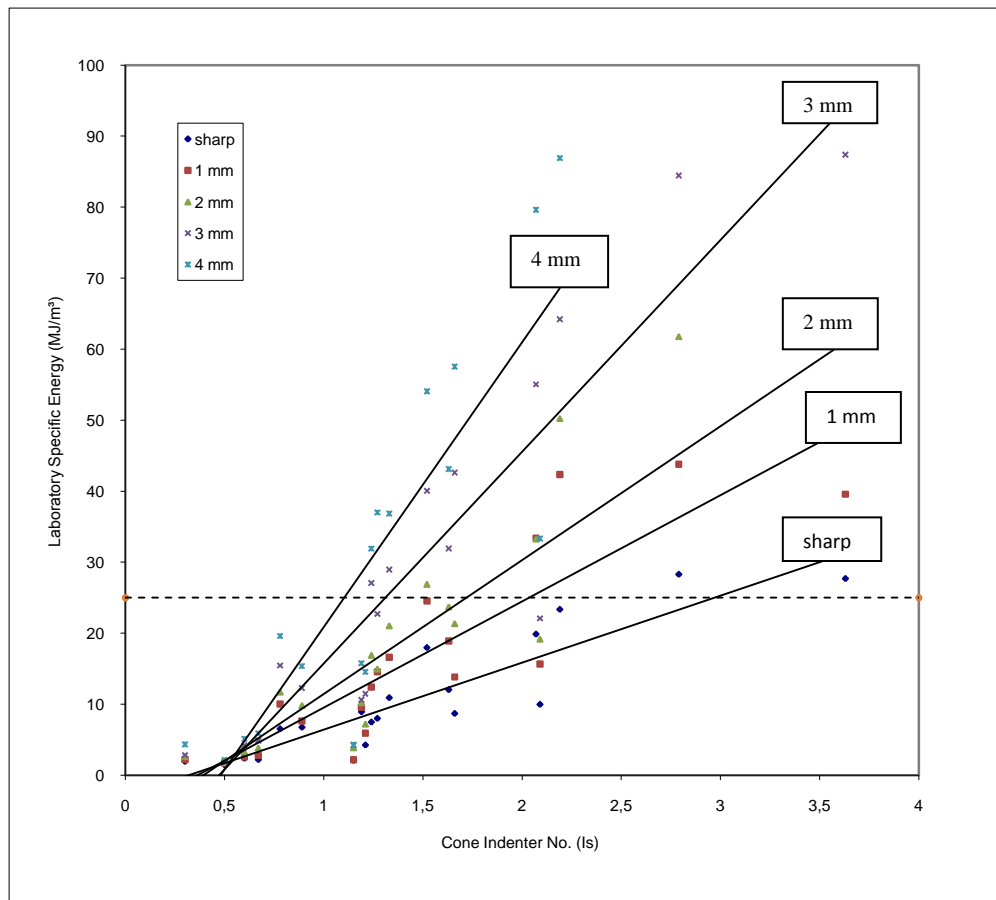


Figure 4.8. Critical Wear Flats for Varying Standard Cone Indenter Numbers

Figure 4.9 shows the relationships between the cone indenter number and the mean cutting force at different wear flats. The relationships are similar to cutting specific energies. Mean cutting force increases 2-3 times with 3-4 mm wear flats as compared to sharp picks for rocks with higher cone indenter numbers.

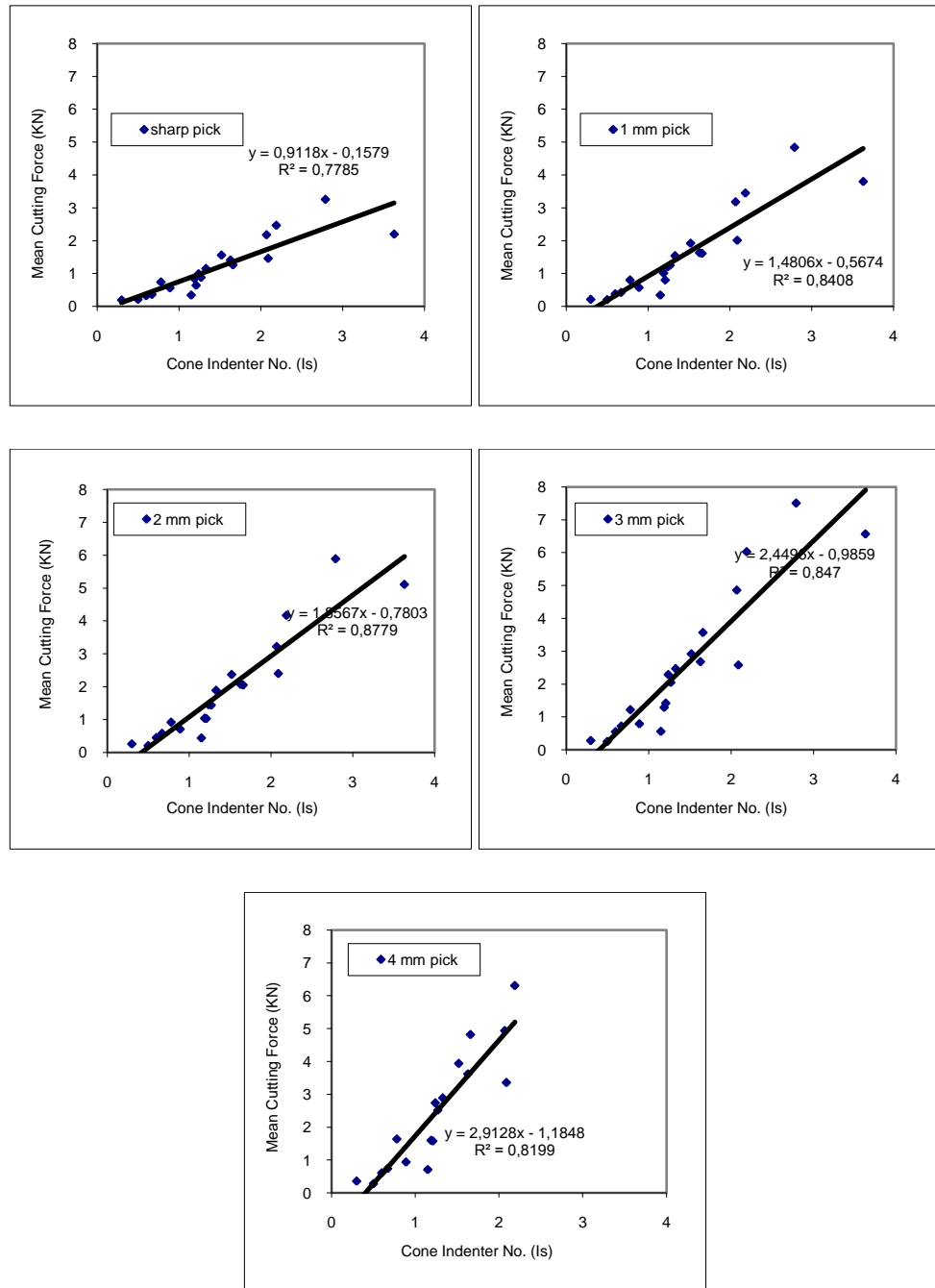


Figure 4.9. Relationships Between Cone Indenter Number and Mean Cutting Force at Different Wear Flats

4.7. Relationships Between Laboratory Cutting Specific Energy, Mean Cutting Force and Wear Flats With Shore Hardness

Figure 4.10 shows the relationship between the laboratory cutting specific energy and shore hardness at different wear flats. Figures show that low correlation exists between specific energy and the shore hardness. Although the increase in wear flat causes slight increase in specific energy for low shore hardness values, it increases rapidly as the shore hardness and wear flat increase, reaching about 4 times as compared to sharp picks for higher shore hardness values.

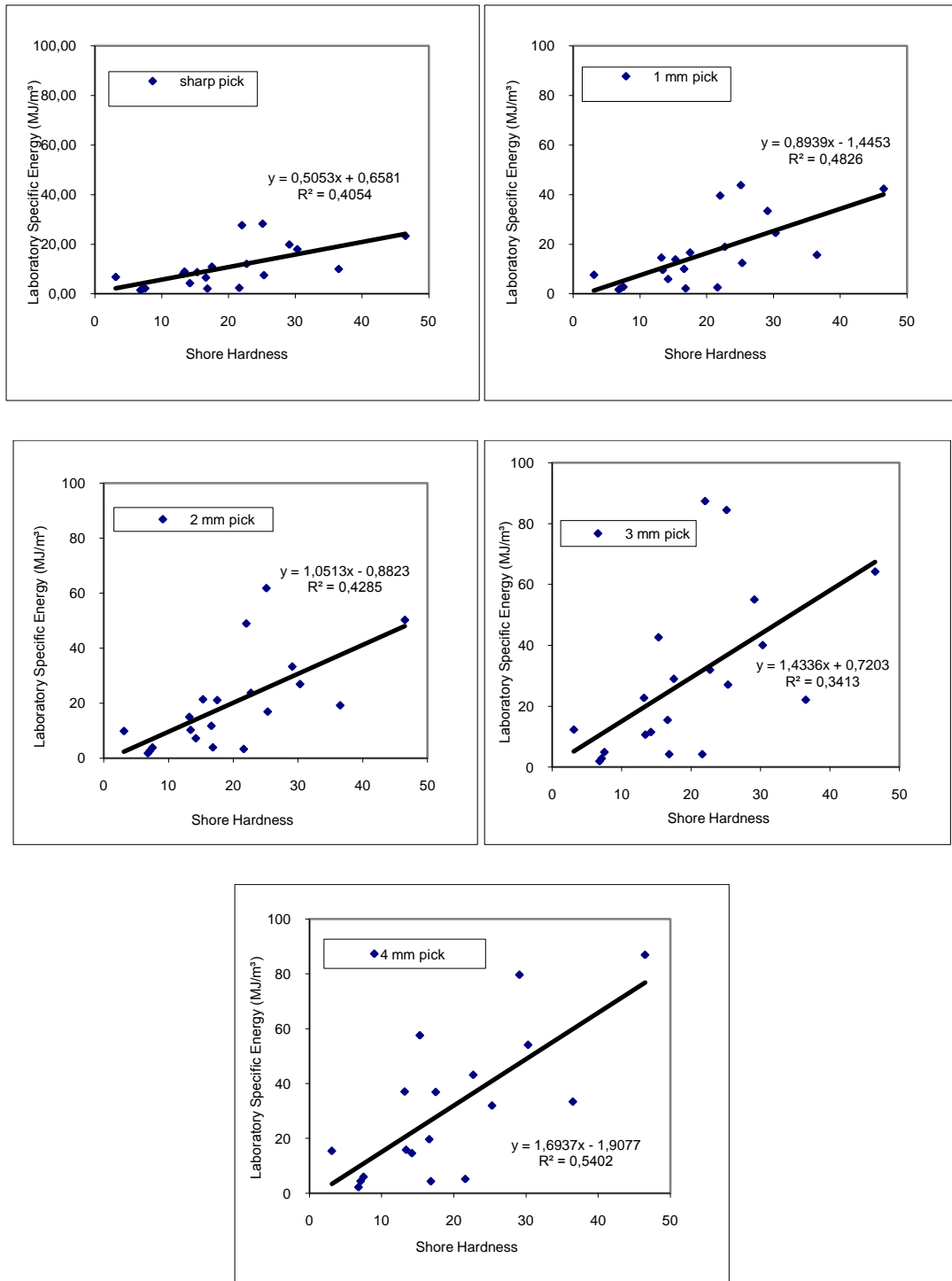


Figure 4.10. Relationships Between Shore Hardness and Laboratory Specific Cutting Energy at Different Wear Flats

Figure 4.11 shows the establishment of the critical wear flats at varying shore hardness values if the limiting cutting specific energy above which poor cutting performance will be obtained is considered to be 25 MJ/m³. As it can be seen from the figure, although the cutting specific energy remains below 25 MJ/m³ even with 4 mm wear flat for rocks having shore hardness of less than 15, the critical limit is exceeded even with 1 mm wear flat pick when the shore hardness is above 30.

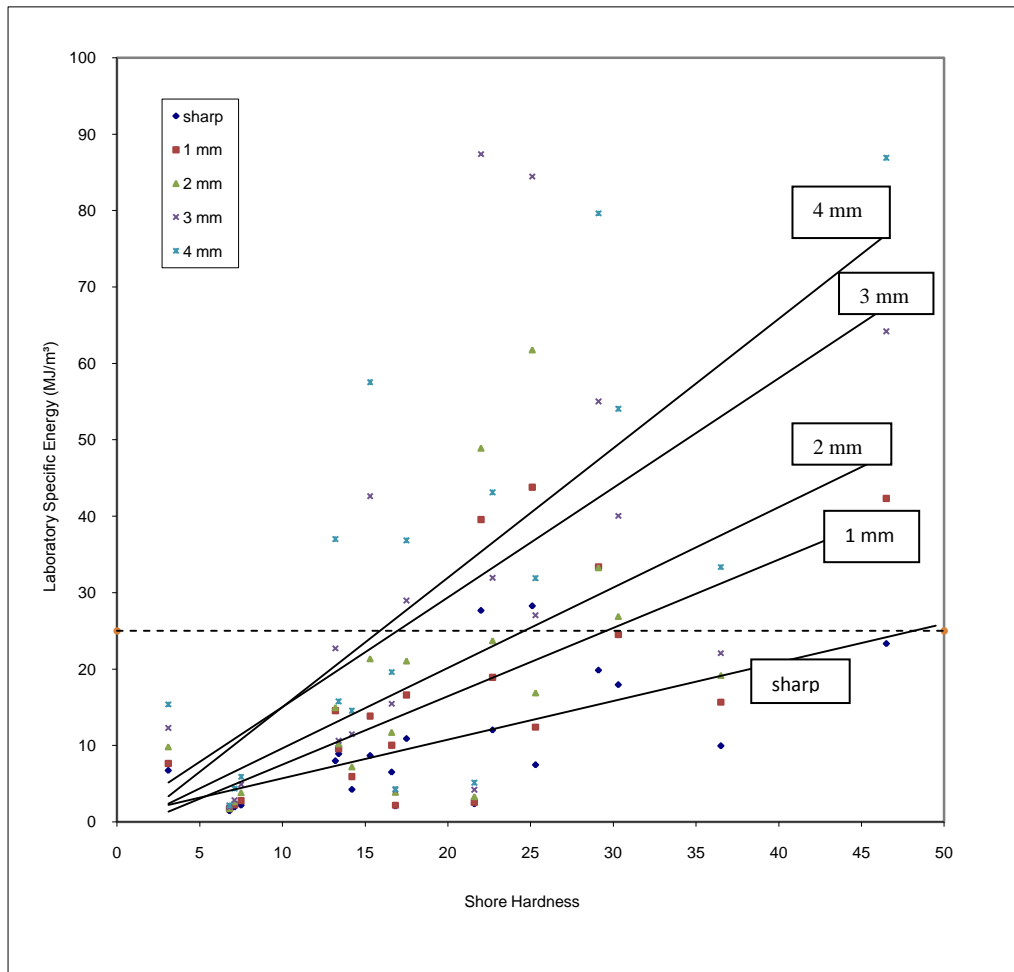


Figure 4.11. Critical Wear Flats for Varying Shore Hardness Values

Figure 4.12 shows the relationships between the shore hardness and the mean cutting force at different wear flats. The relationships are similar to cutting specific energies. Mean cutting force increases 2-3 times with 3-4 mm wear flats as compared to sharp picks.

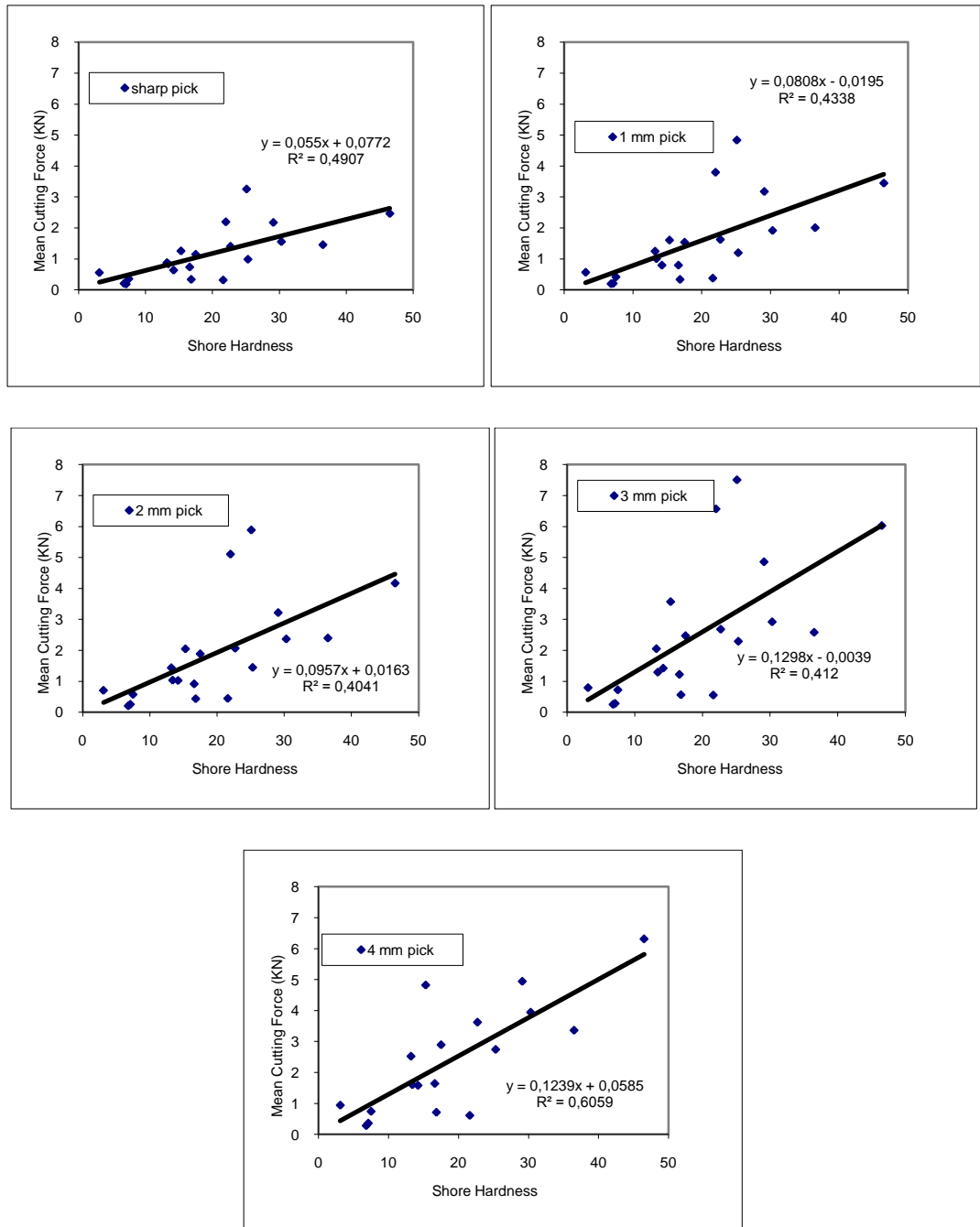


Figure 4.12. Relationships Between Shore Hardness and Mean Cutting Force at Different Wear Flats

4.8. Relationships Between Laboratory Cutting Specific Energy, Mean Cutting Force and Wear Flats With Schmidt Hammer Hardness

Figure 4.13 shows the relationship between the laboratory cutting specific energy and schmidth hardness values at different wear flats. Figures show that rather good correlation exists between specific energy and the schmidth hammer hardness. Although the increase in wear flat causes slight increase in specific energy for low shore hardness values, it increases rapidly as the schmidth hammer hardness and wear flat increase, reaching about 3-4 times as compared to sharp picks for higher schmidth hammer values.

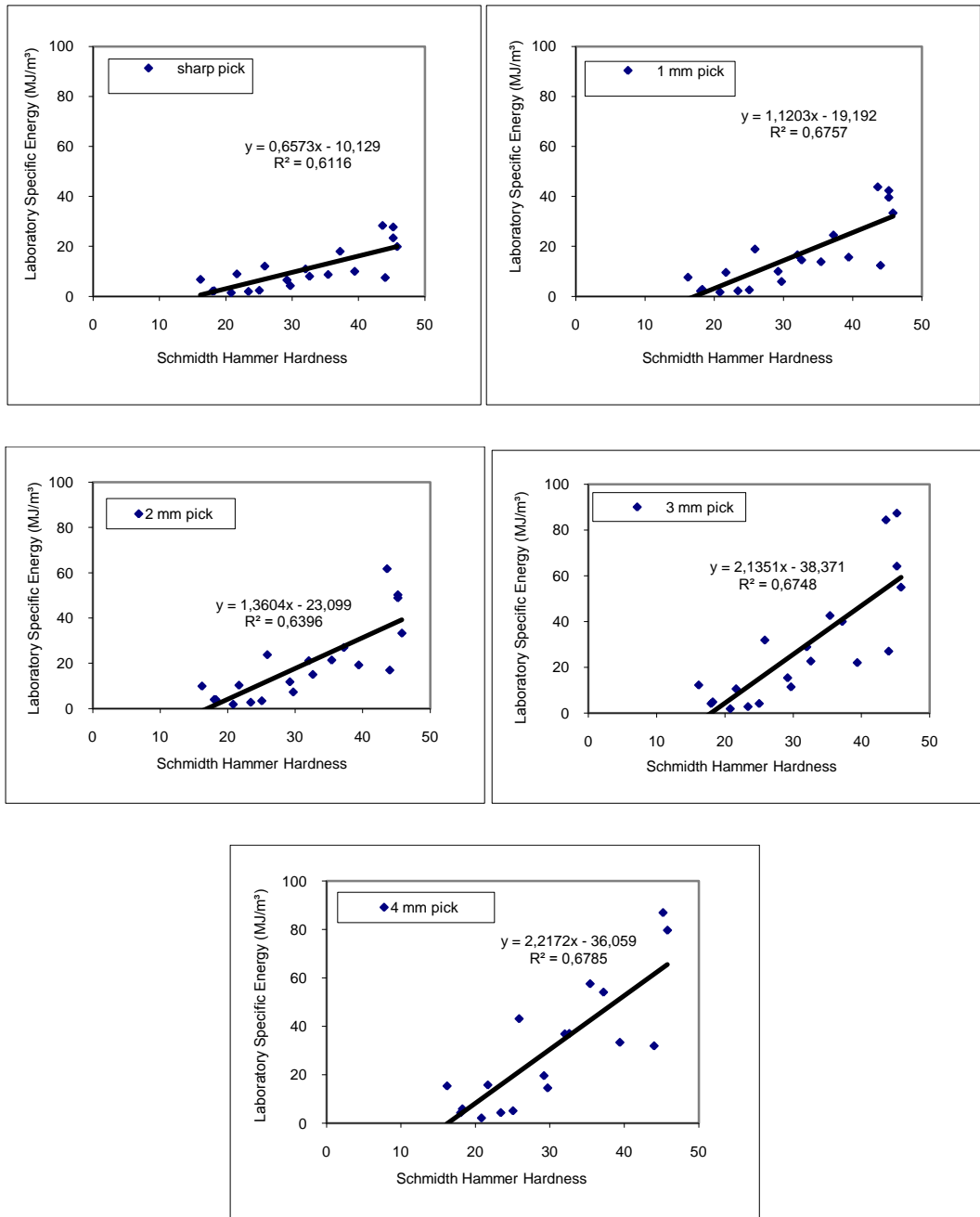


Figure 4.13. Relationships Between Schmith Hammer Hardness and Laboratory Specific Cutting Energy at Different Wear Flats

Figure 4.14 shows the establishment of the critical wear flats at varying schmidth hammer hardness values if the limiting cutting specific energy above which poor cutting performance will be obtained is considered to be 25 MJ/m³. As it can be seen from the figure, although the cutting specific energy remains below 25 MJ/m³ even with 4 mm wear flat for rocks having schmidth hammer values of less than about 25-30, the critical limit is exceeded even with 1 mm wear flat pick when the schmidth hammer hardness exceeds about 40.

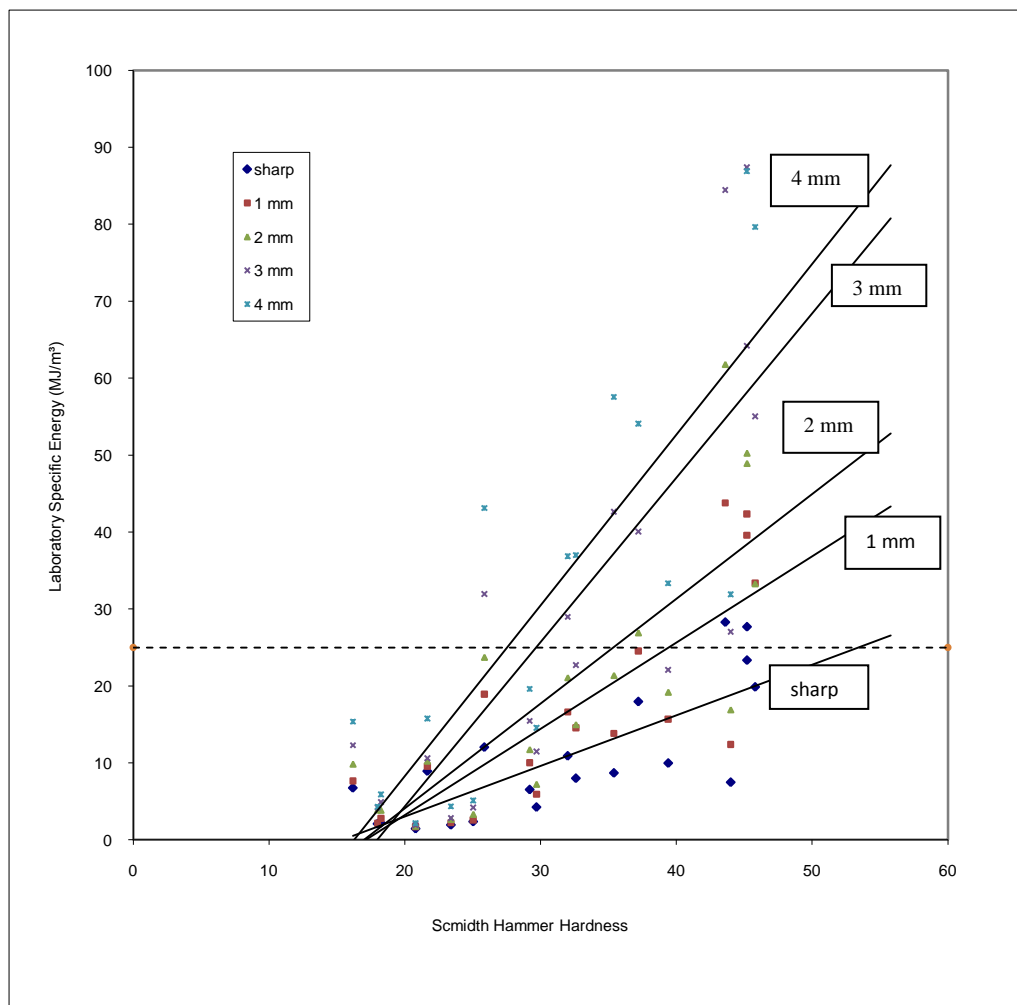


Figure 4.14. Critical Wear Flats for Varying Schmidth Hammer Hardness

Figure 4.15 shows the relationships between the schmidth hammer hardness and the mean cutting force at different wear flats. The relationships are similar to cutting specific energies. Mean cutting force increases 2-3 times with 3-4 mm wear flats as compared to sharp picks.

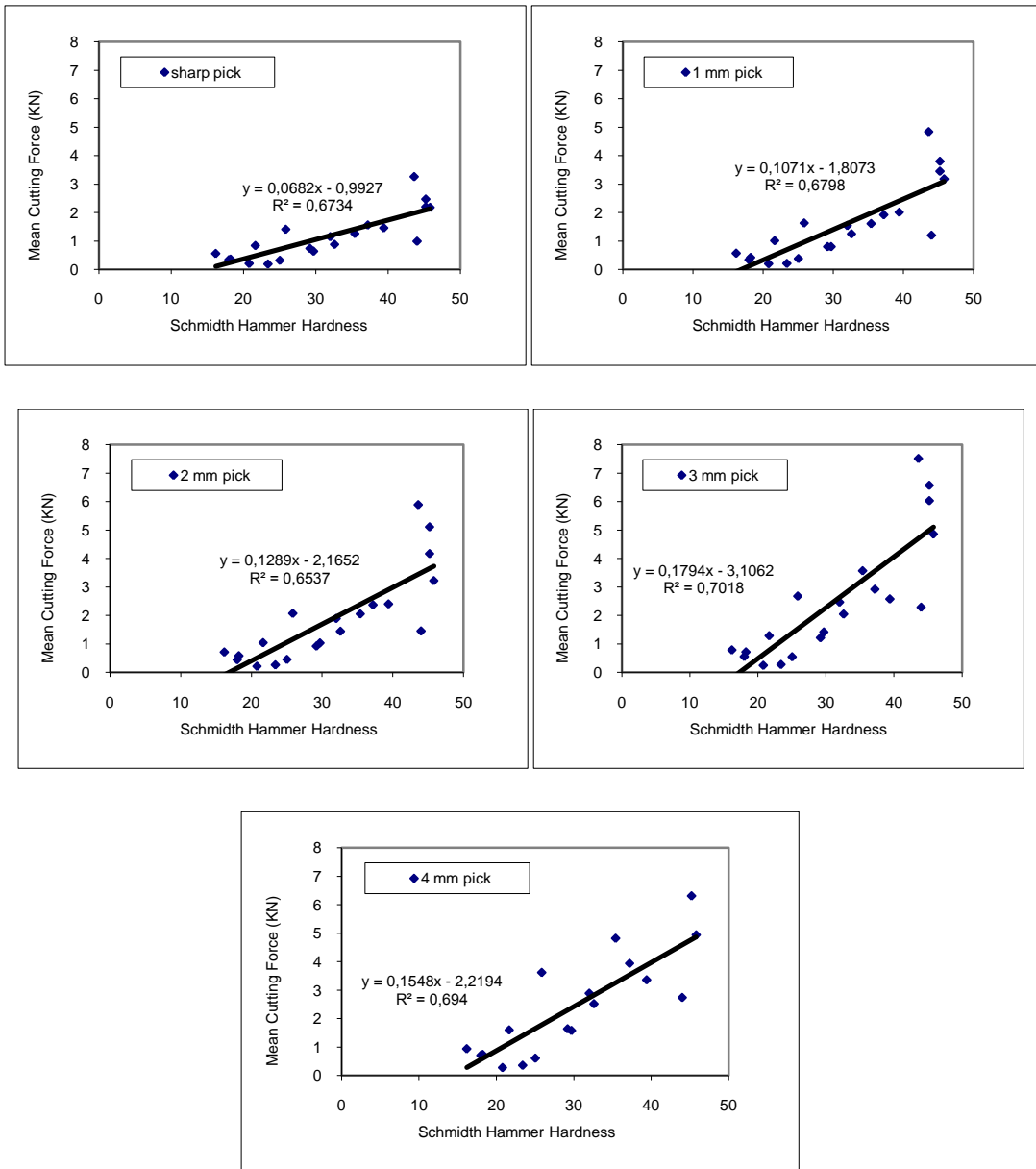


Figure 4.15. Relationships Between Schmidt Hammer Hardness and Mean Cutting Force at Different Wear Flats

4.9. Relationships Between Laboratory Cutting Specific Energy, Mean Cutting Force and Wear Flats With Density

Figure 4.16 shows the relationships between the laboratory cutting specific energy and density at different wear flats. Figures show that the relationship is linear and rather low correlation exists between the specific energy and the density. The rate of increase in specific energy gets higher with increasing wear flats, being about 3-4 times larger with 4 mm wear flat as compared to sharp picks at a density of about 2,2 gr/cm³.

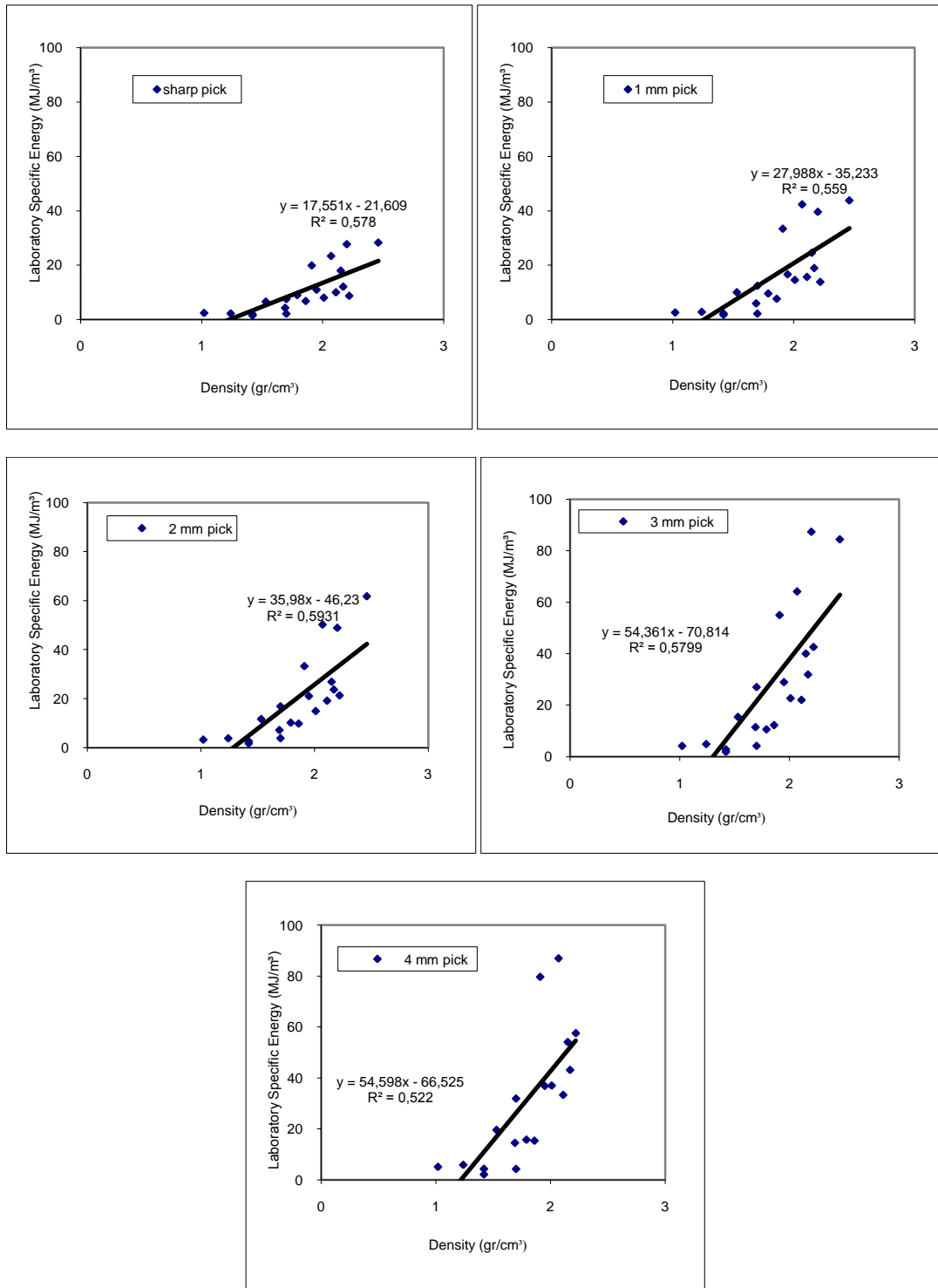


Figure 4.16. Relationships Between Density and Laboratory Specific Cutting Energy at Different Wear Flats

Figure 4.17 shows the establishment of the critical wear flats at varying densities if the limiting cutting specific energy above which poor cutting performance will be obtained is considered to be 25 MJ/m^3 . As it can be seen from the figure, although the cutting specific energy remains below 25 MJ/m^3 even with 4 mm wear flat for rocks having a density less than $1,7 \text{ gr/cm}^3$, the critical limit is exceeded even with 1 mm wear flat pick when the density is above $2,2 \text{ gr/cm}^3$.

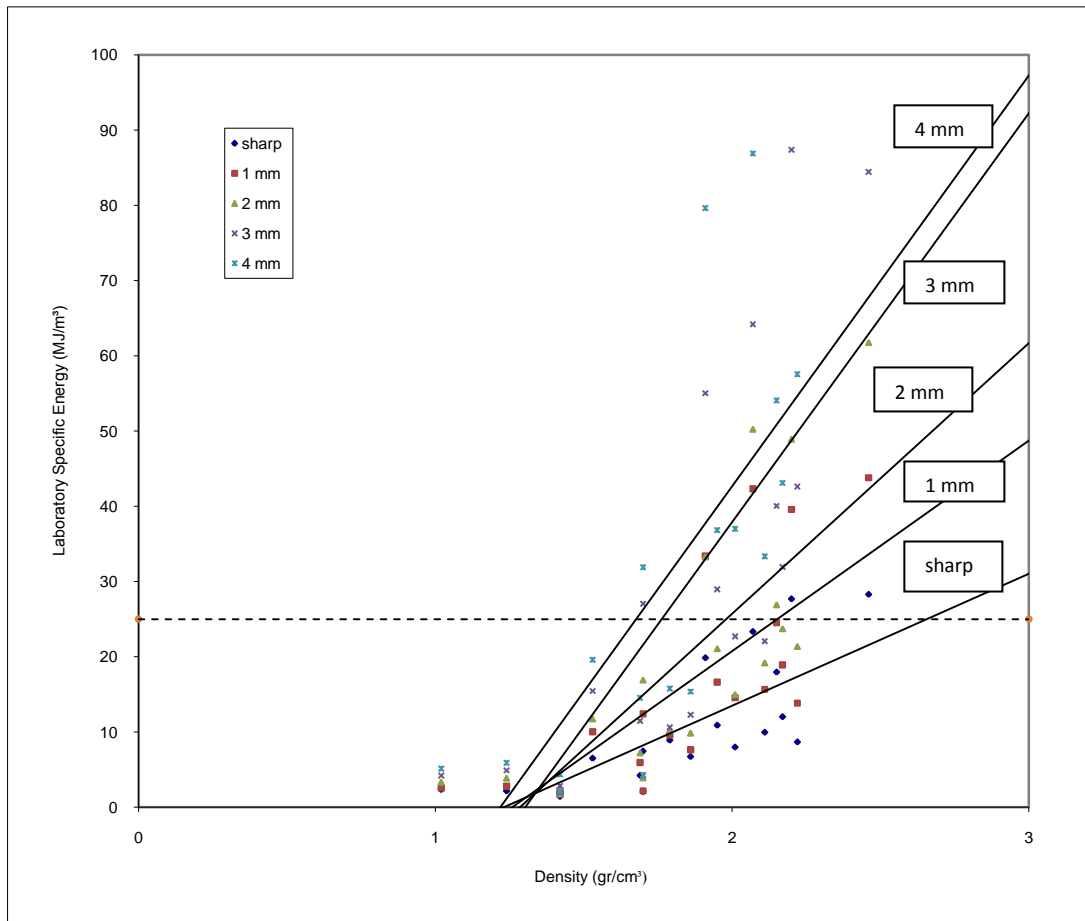


Figure 4.17. Critical Wear Flats for Varying Density

Figure 4.18 shows the relationships between the density and the mean cutting force at different wear flats. The relationships are similar to cutting specific energies. Mean cutting force increases about 2 times with 4 mm wear flat as compared to sharp picks for the rocks with higher densities.

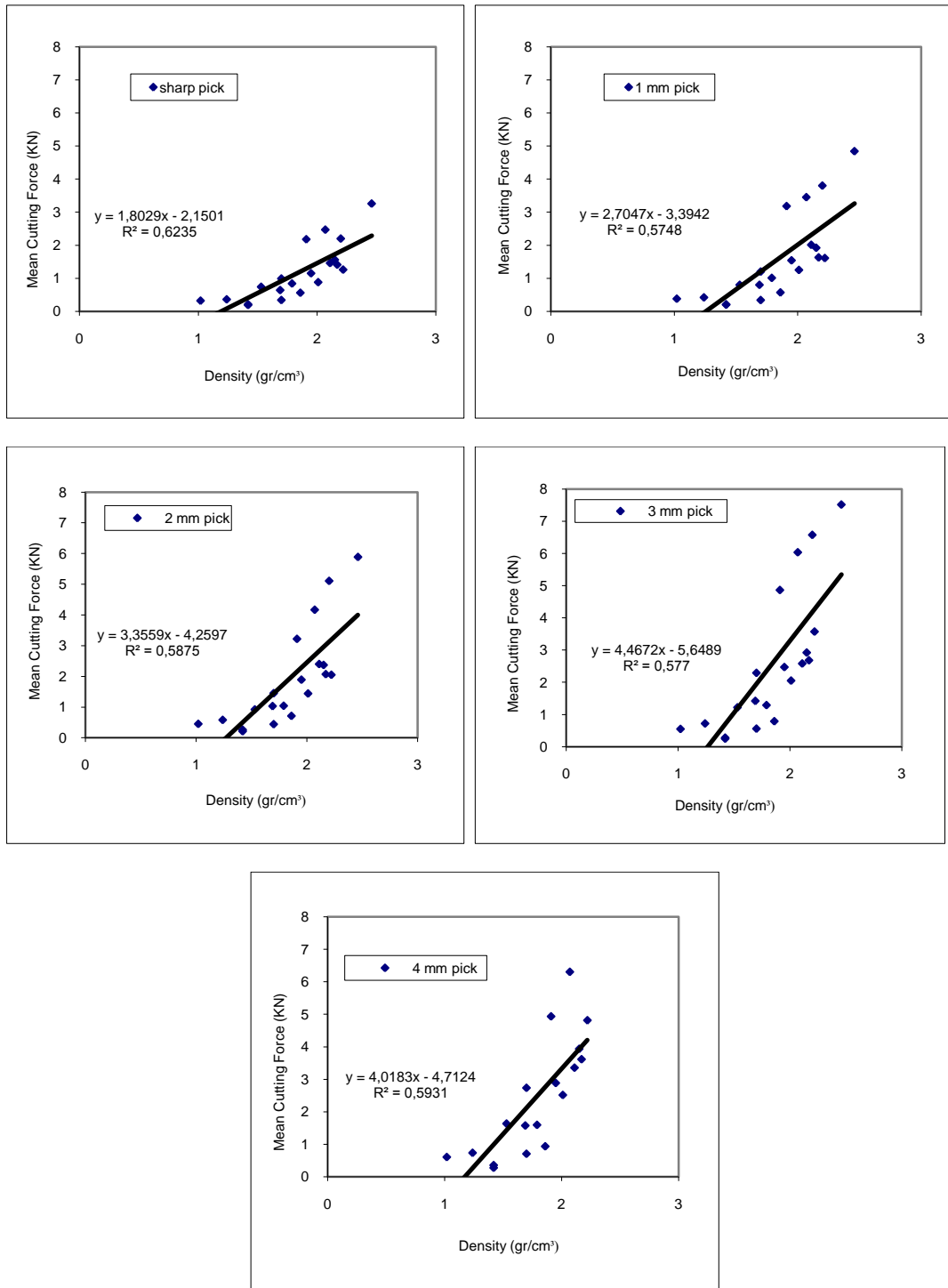


Figure 4.18. Relationships Between Density and Mean Cutting Force at Different Wear Flats

4.10. Effect of Mineral Grain Size on Cutting Specific Energy

Figure 4.19 shows the relationships between the laboratory cutting specific energy and the mean grain size and Figure 4.20 shows the relationships between the mean cutting force and the mean grain size.

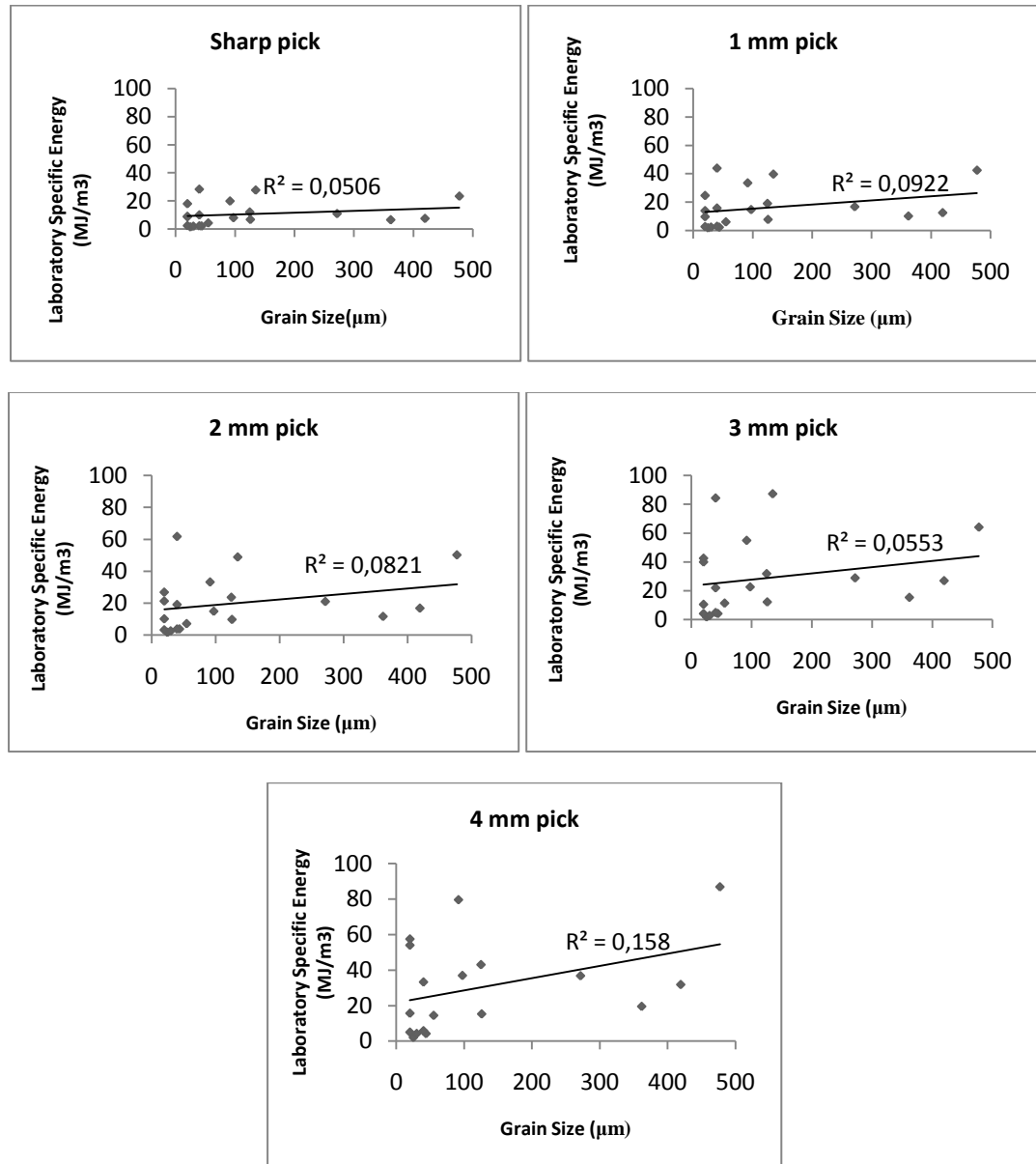


Figure 4.19. Relationships Between the Mineral Grain Size and the Laboratory Cutting Specific Energy at Various Wear Flats

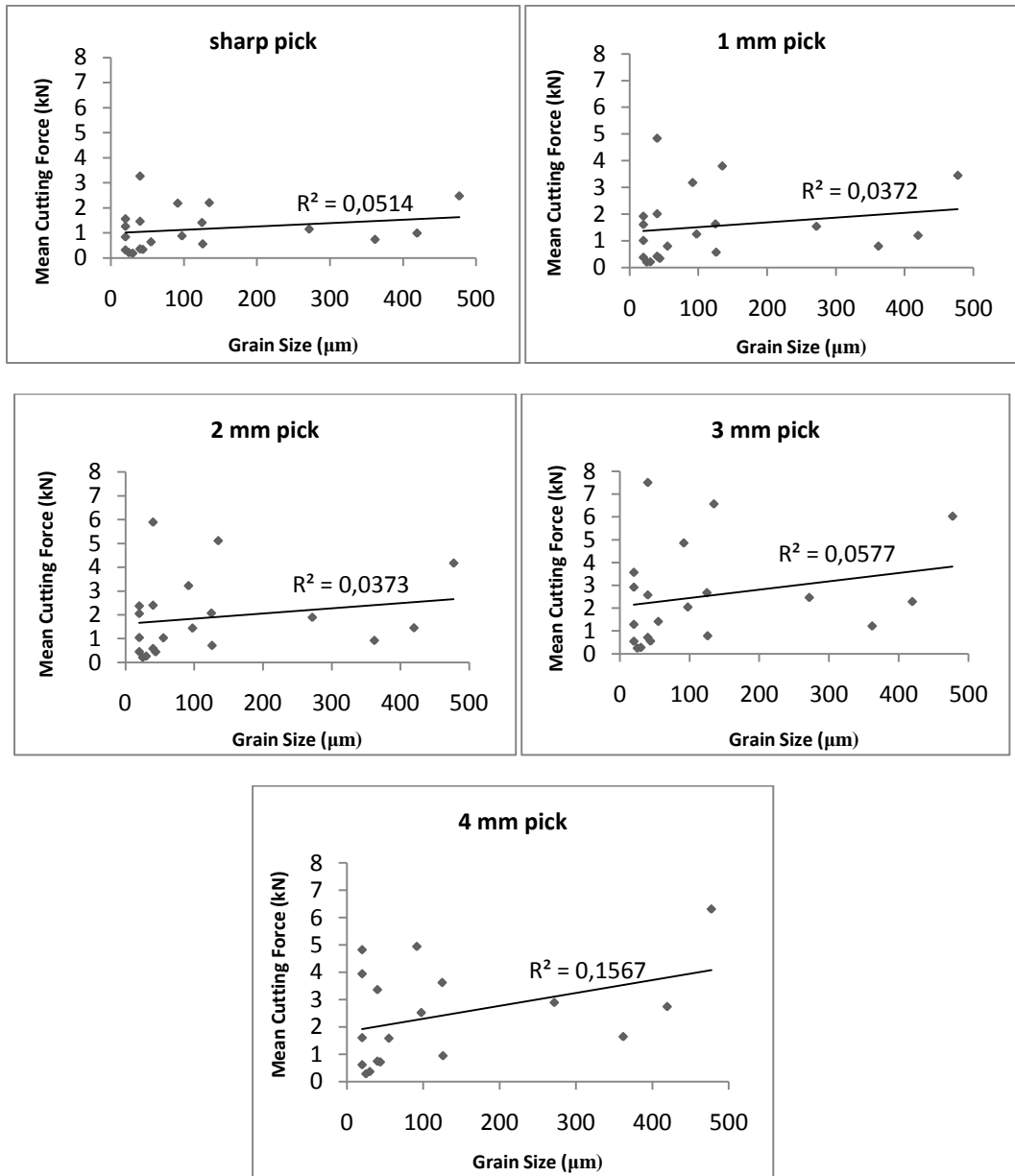


Figure 4.20. Relationships Between the Mineral Grain Size and the Mean Cutting Force at Various Wear Flats

As it can be seen from the figure, there is no correlation between the grain size, cutting specific energy and the cutting force for sharp and blunted cutting picks.

4.11. Effect of Breakout Angle

Area cut during a test was calculated using the weight of chips obtained during the cutting processes, length of cut and the density. Breakout angles were determined considering the width of the standard pick (12,7 mm) and the standard depth of cut (5 mm). Table 4.5 shows the breakout angles with sharp picks.

Table 4.5. Breakout Angles With Sharp Picks

Sample	Density (gr/cm ³)	Cutting Area (cm ²)	Breakout Angle (θ, Degree)	Uniaxial Compressive Strength (Mpa)	Laboratory Cutting Specific Energy (MJ/m ³)
Limestone 1	1.86	0.83	42	6.08	6.74
Limestone 2	2.22	1.47	72	28.69	8.68
Limestone 3	1.42	1.07	57	5.75	1.93
Limestone 4	1.69	1.53	74	18.38	4.24
Clayey Limestone	1.02	1.39	70	5.77	2.36
Mudstone 1	2.15	0.87	43	28.30	17.96
Mudstone 2	2.17	1.16	63	28.19	12.03
Mudstone 3	2.01	1.11	62	31.75	7.99
Mudstone 4	1.91	1.17	61	64.15	19.86
Mudstone-Siltstone	1.79	1.00	46	26.00	8.92
Marl 1	1.70	1.04	47	19.00	2.07
Marl 2	1.24	1.68	76	6.31	2.18
Altered Tuff	1.95	1.06	59	25.06	10.90
Lithic Tuff 1	1.70	1.38	67	28.04	7.47
Lithic Tuff 2	1.53	1.13	61	11.45	6.52
Claystone	1.42	1.46	73	13.00	1.44
Siltstone 1	2.00	1.56	74	29.03	9.96
Siltstone 2	2.30	0.91	47	36.13	27.68
Andesite	2.07	1.08	58	34.34	23.34
Travertine	2.46	1.16	64	47.84	28.28

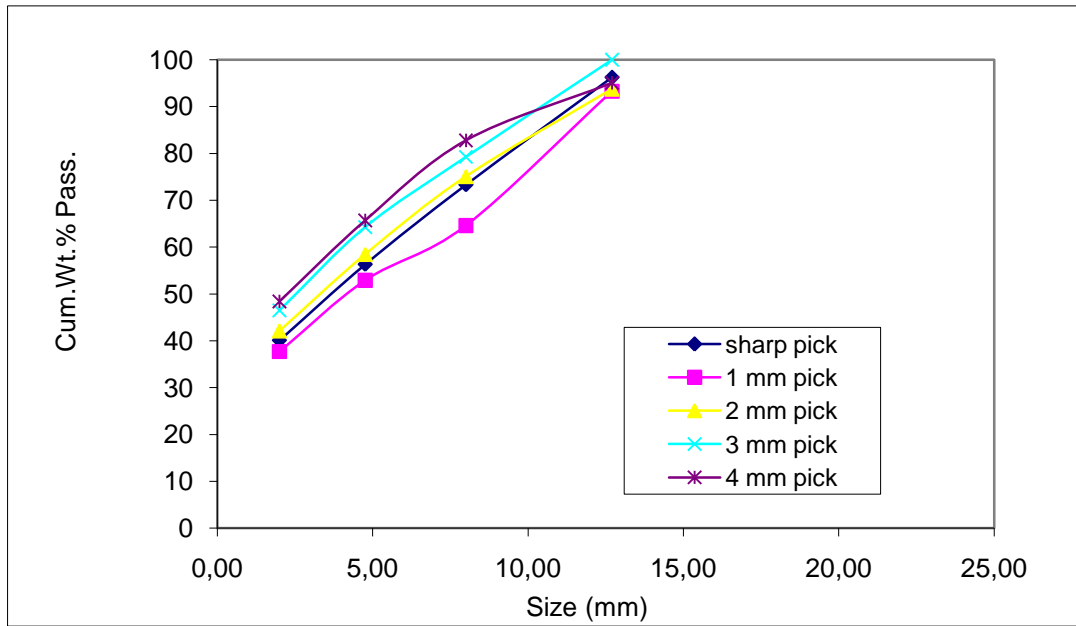
As expected, the effect of higher breakout angle is generally reflected as reduction in the cutting specific energy. A typical result can be observed for limestone 1 and limestone 2. Although rock hardness values for limestone 2 are considerably higher as compared to limestone 1, cutting specific energy for limestone 2 is not as high as expected. This can be explained by higher breakout angle (72°) of limestone 2 as compared to limestone 1 (42°). Cutting force for limestone 2 on the other hand, is much higher as compared to limestone 1 as expected.

4.12. Effect of Wear Flat on Size Distribution and Coarseness Index

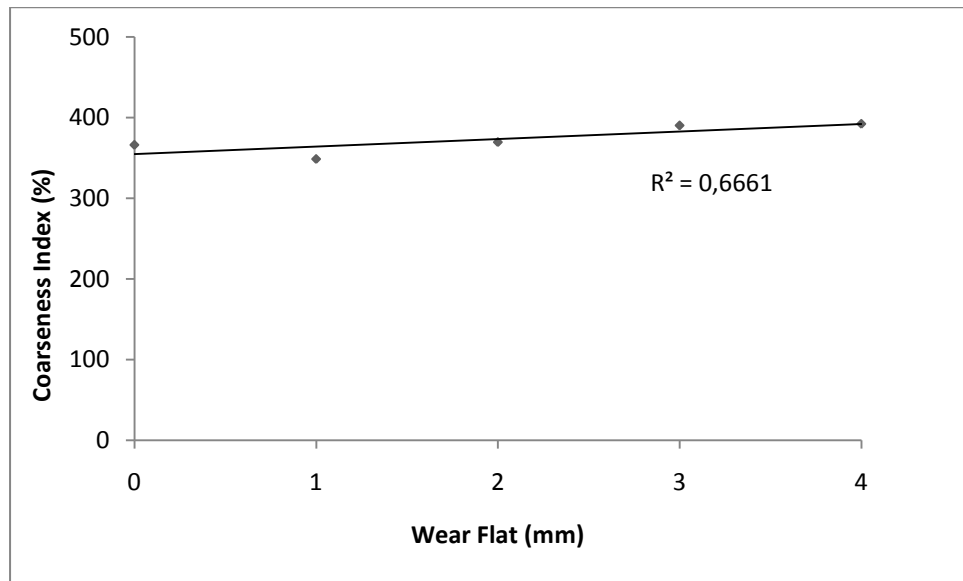
Figures 4.21, 4.22, 4.23, 4.24, 4.25, 4.26, 4.27, 4.28, 4.29, 4.30, 4.31, 4.32, 4.33, 4.34, 4.35, 4.36, 4.37, 4.38, 4.39 and 4.40 show the size distribution and coarseness index results obtained for different rock types at different wear flats.

Size distribution curves show no conclusive results about the effect of blunting on product degradation rate. Coarseness Index values on the other hand, give better idea about the degradation effect.

Coarseness Index curves show that although increase in wear flat causes a slight increase in the rate of degradation for some rock types, this effect is not consistent since similar increase has not been observed for all rock types.

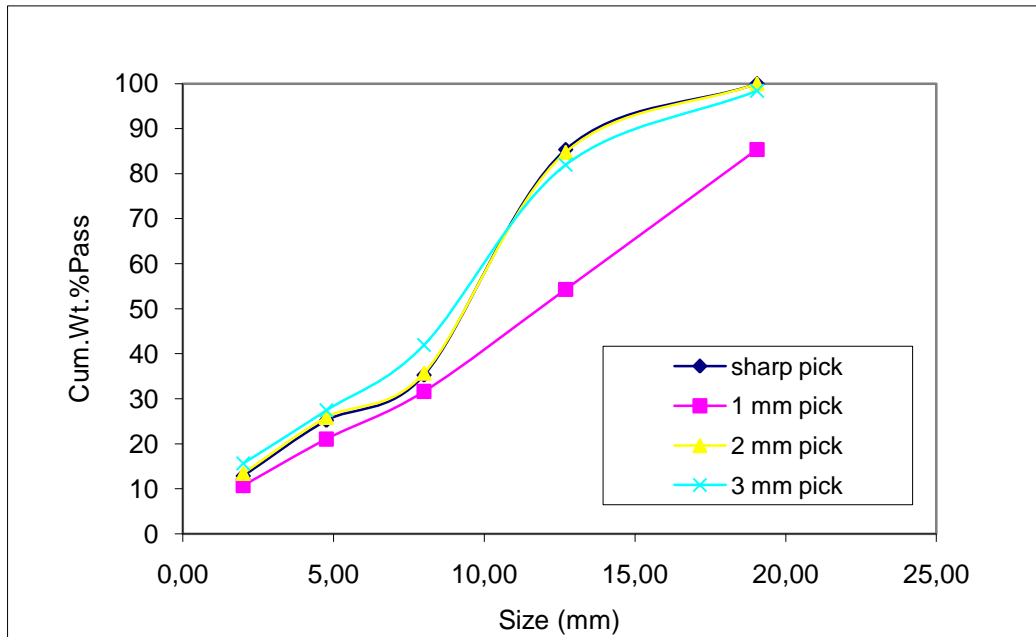


(a)

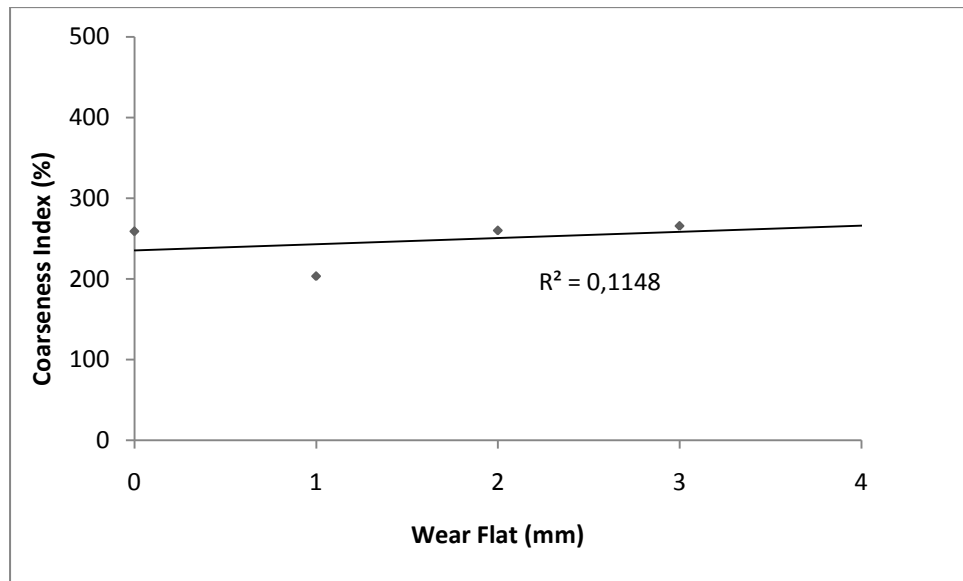


(b)

Figure 4.21. Effect of Wear Flat on Size Distribution (a) and Coarseness Index (b) for Limestone 1

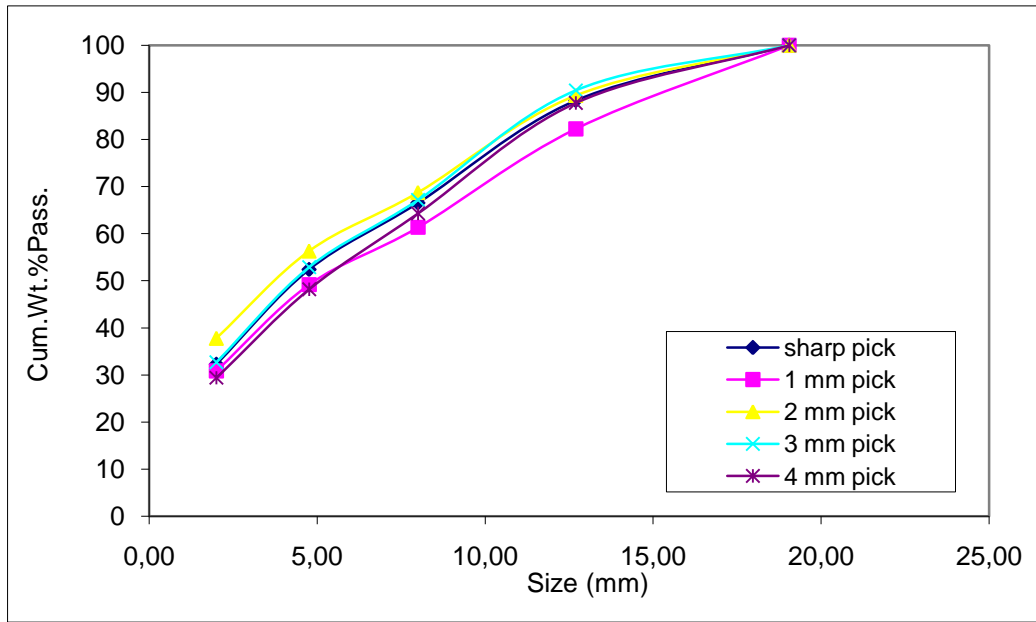


(a)

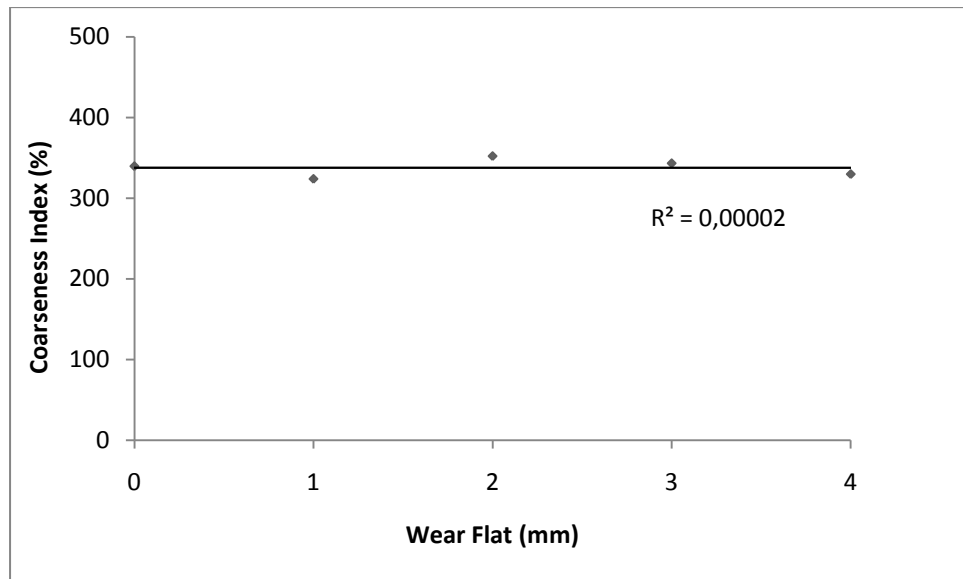


(b)

Figure 4.22. Effect of Wear Flat on Size Distribution (a) and Coarseness Index (b) for Limestone 2

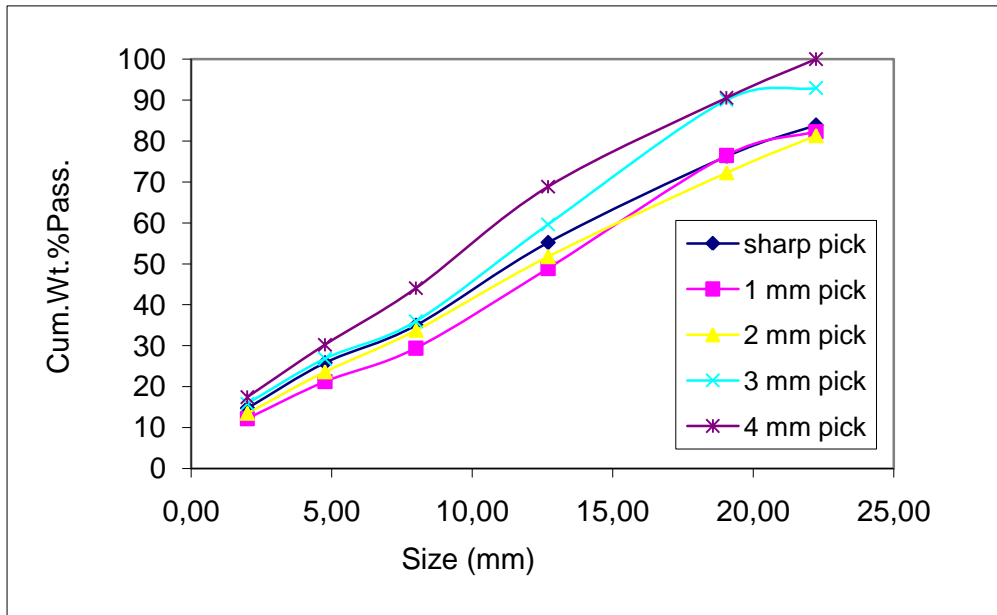


(a)

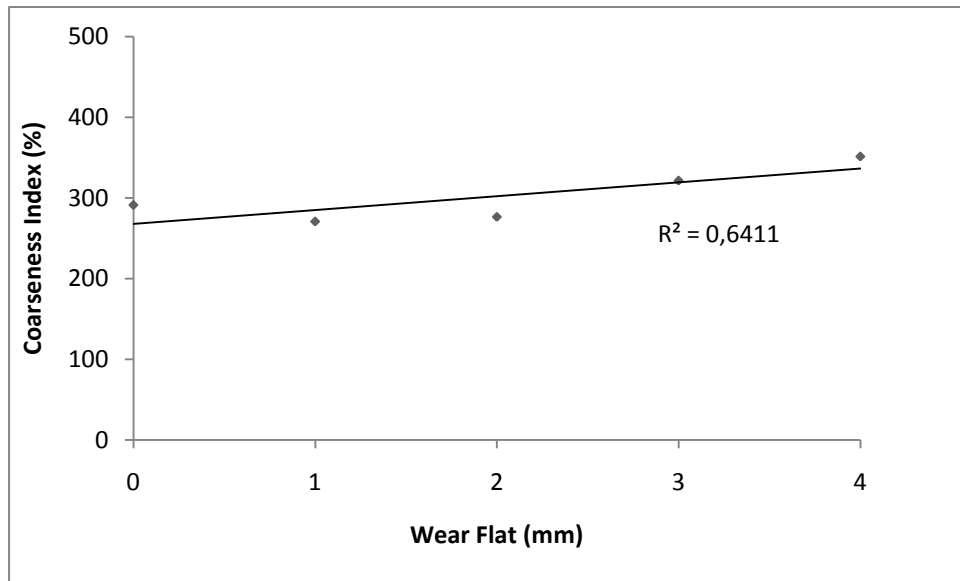


(b)

Figure 4.23. Effect of Wear Flat on Size Distribution (a) and Coarseness Index (b) for Limestone 3

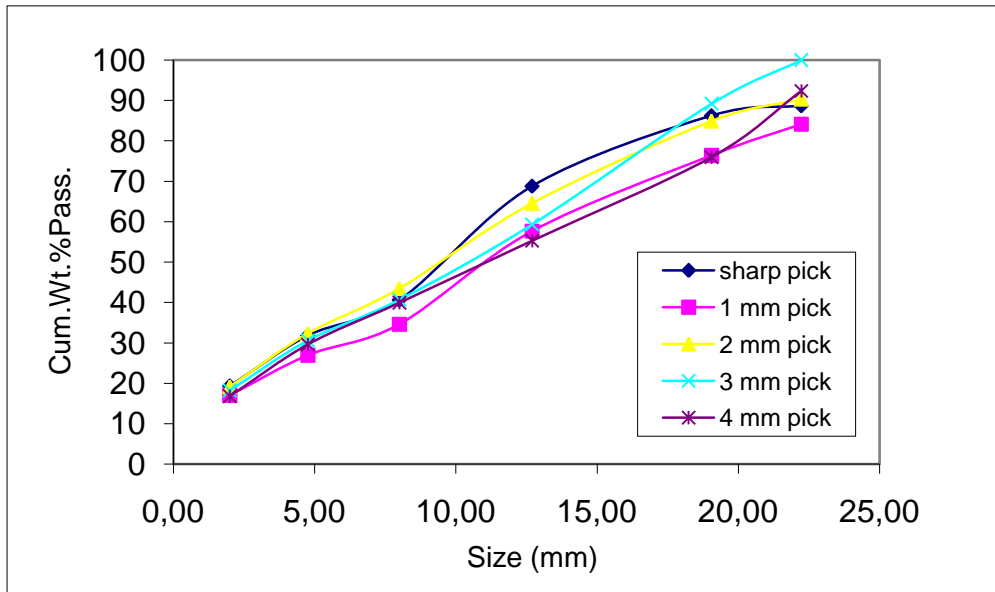


(a)

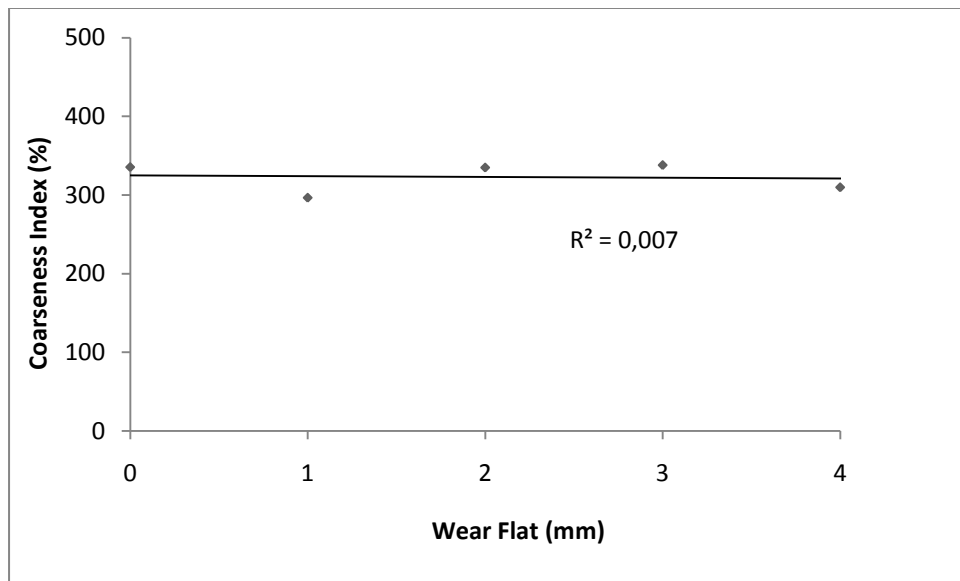


(b)

Figure 4.24. Effect of Wear Flat on Size Distribution (a) and Coarseness Index (b) for Limestone 4

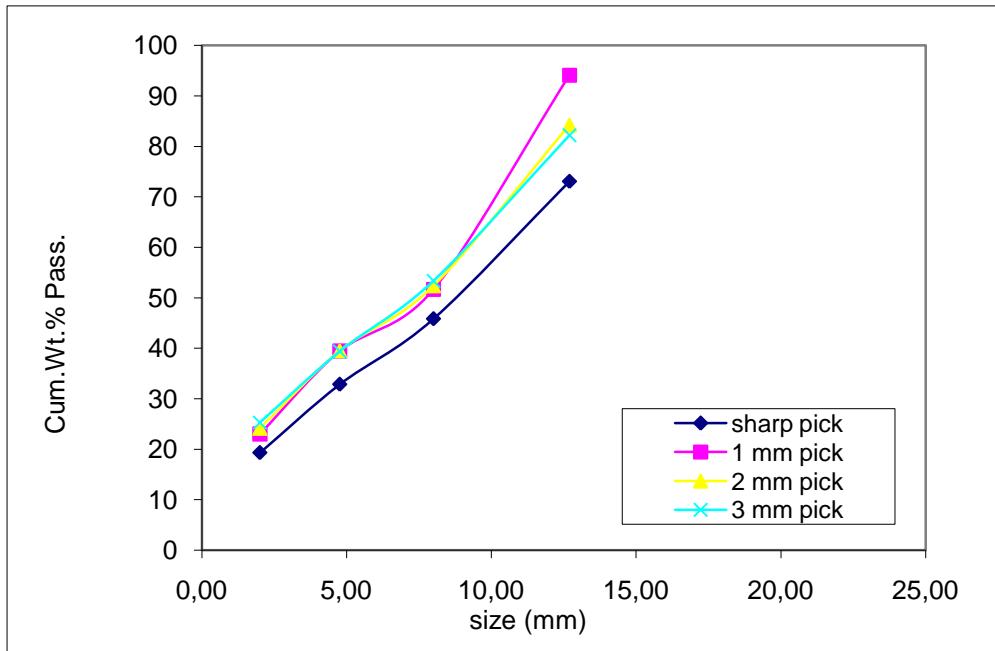


(a)

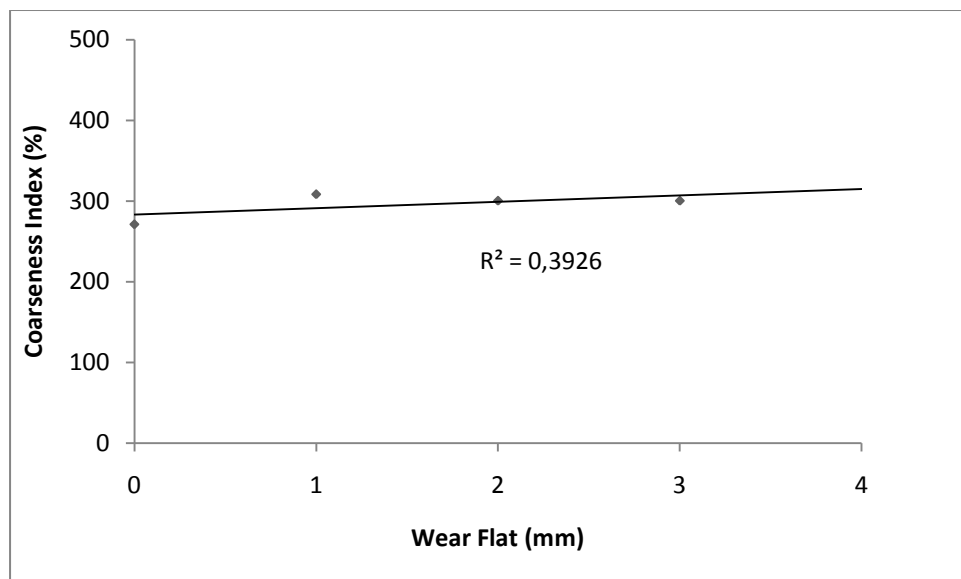


(b)

Figure 4.25. Effect of Wear Flat on Size Distribution (a) and Coarseness Index (b) for Clayey-Limestone

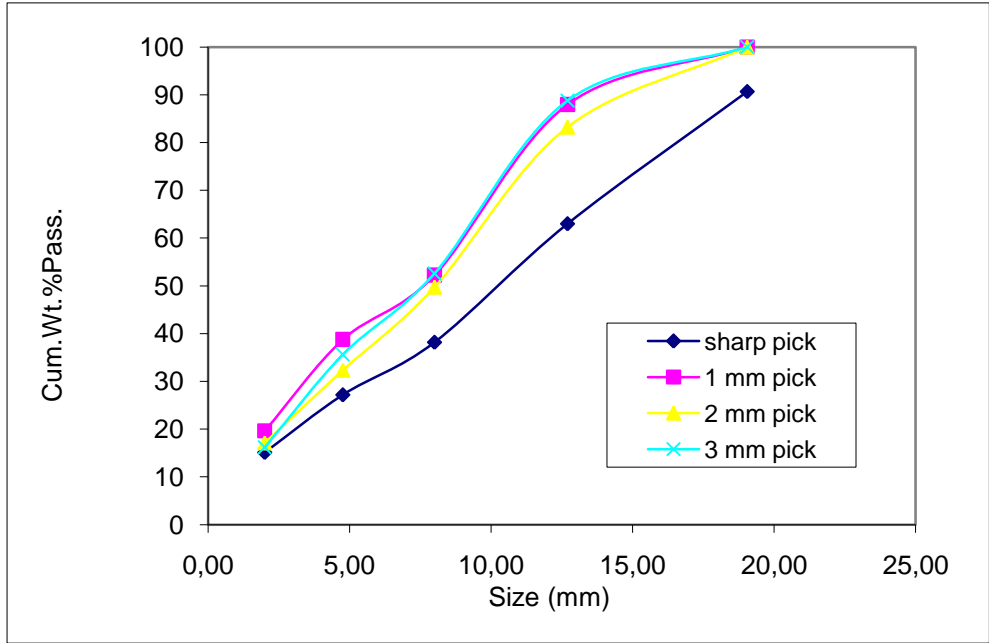


(a)

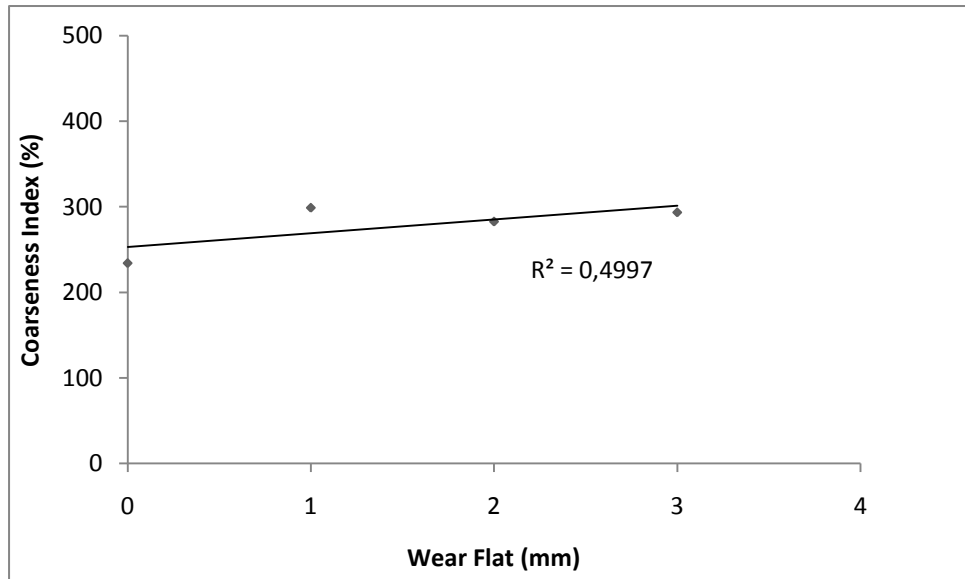


(b)

Figure 4.26. Effect of Wear Flat on Size Distribution (a) and Coarseness Index (b) for Mudstone 1

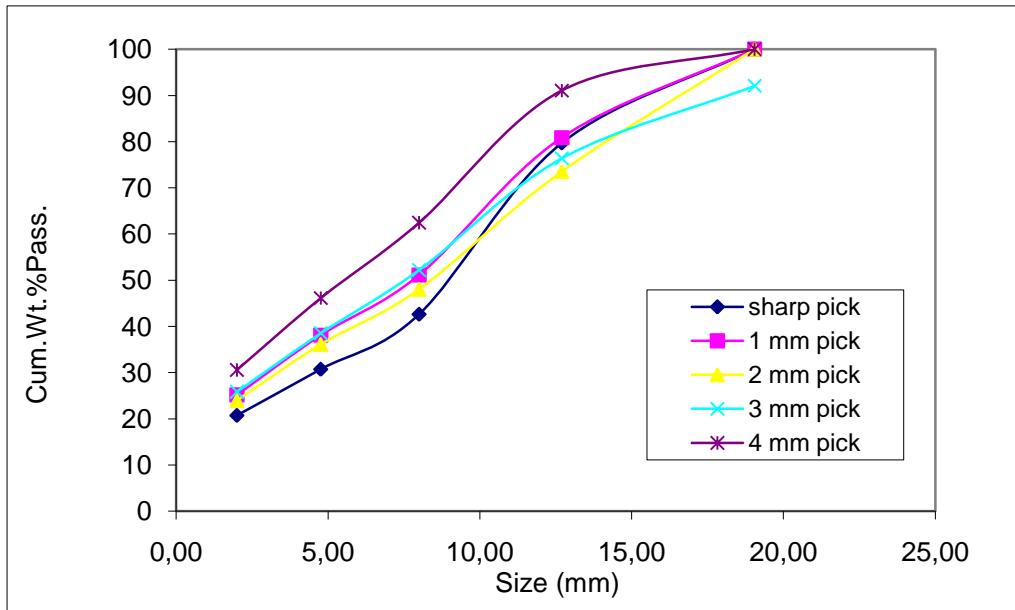


(a)

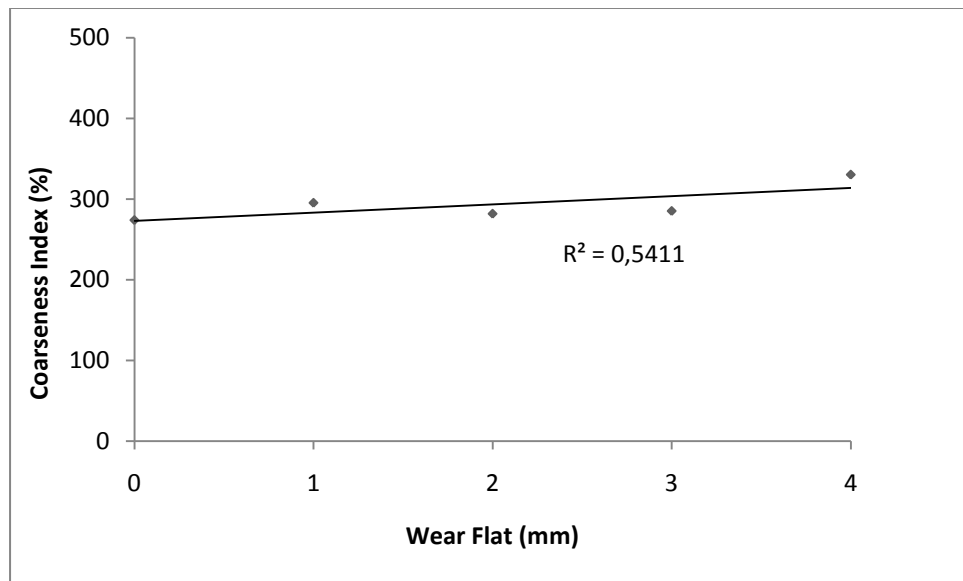


(b)

Figure 4.27. Effect of Wear Flat on Size Distribution (a) and Coarseness Index (b) for Mudstone 2

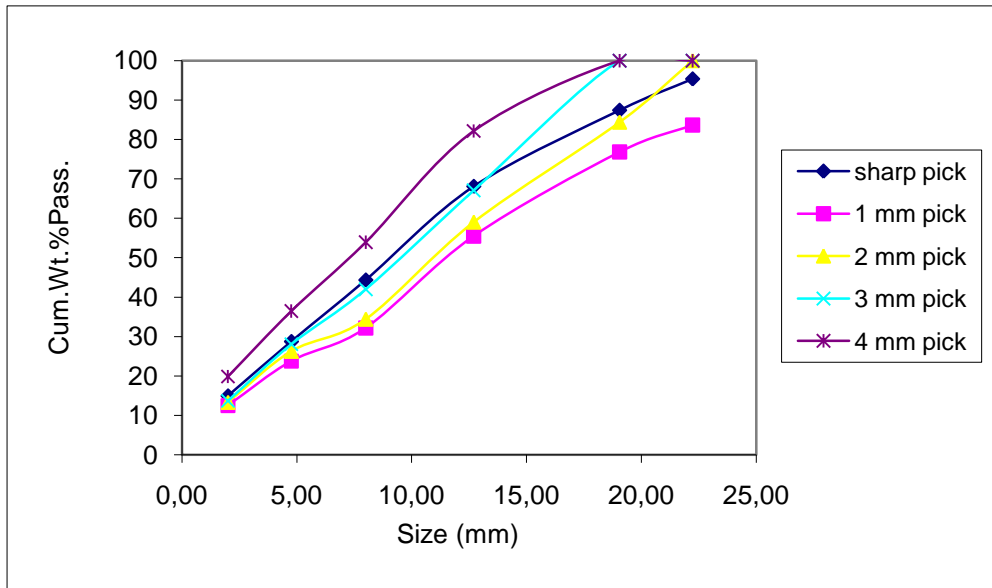


(a)

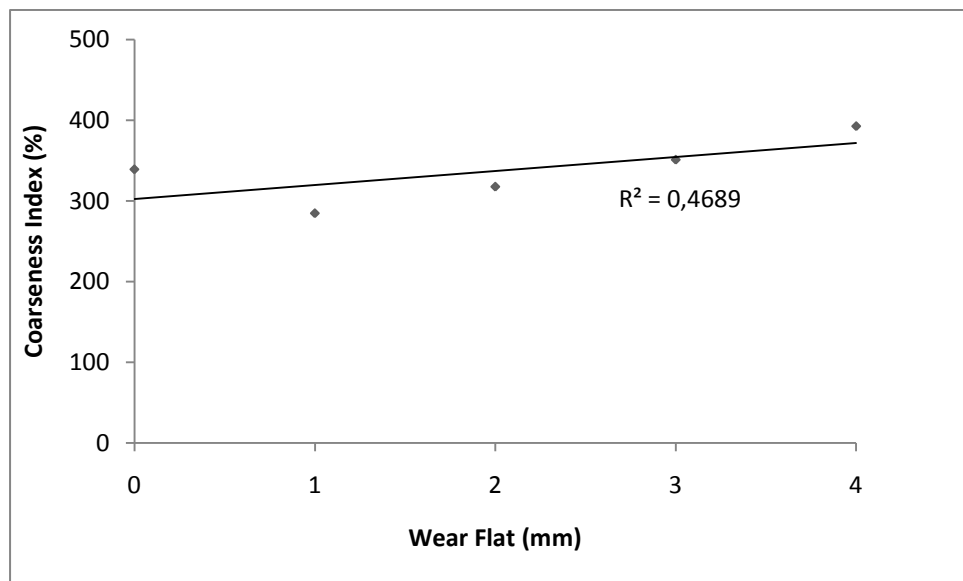


(b)

Figure 4.28. Effect of Wear Flat on Size Distribution (a) and Coarseness Index (b) for Mudstone 3

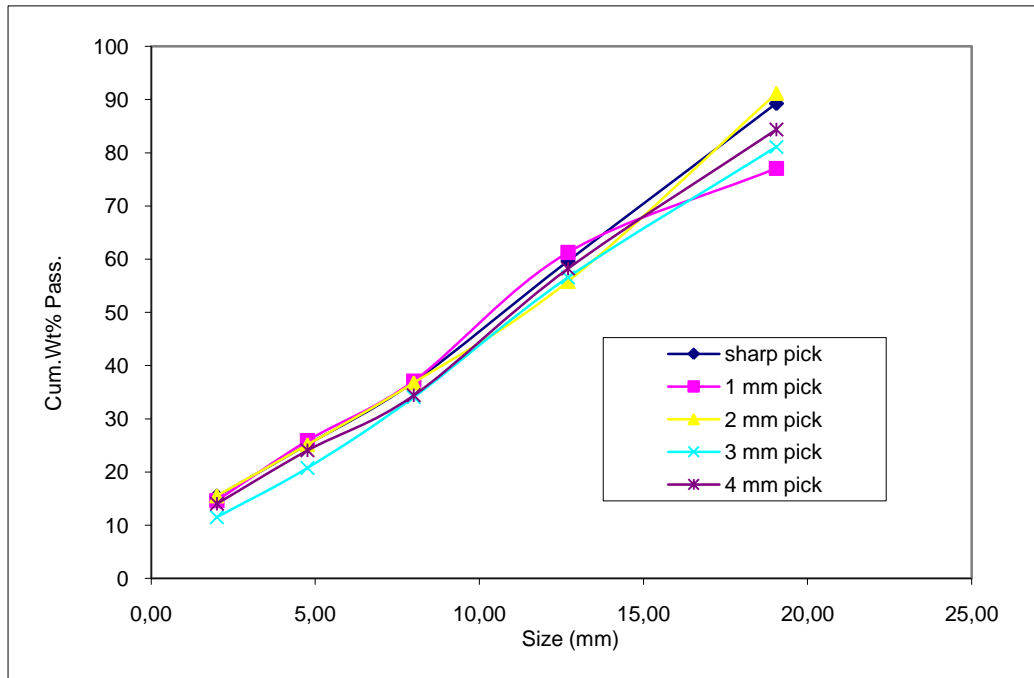


(a)

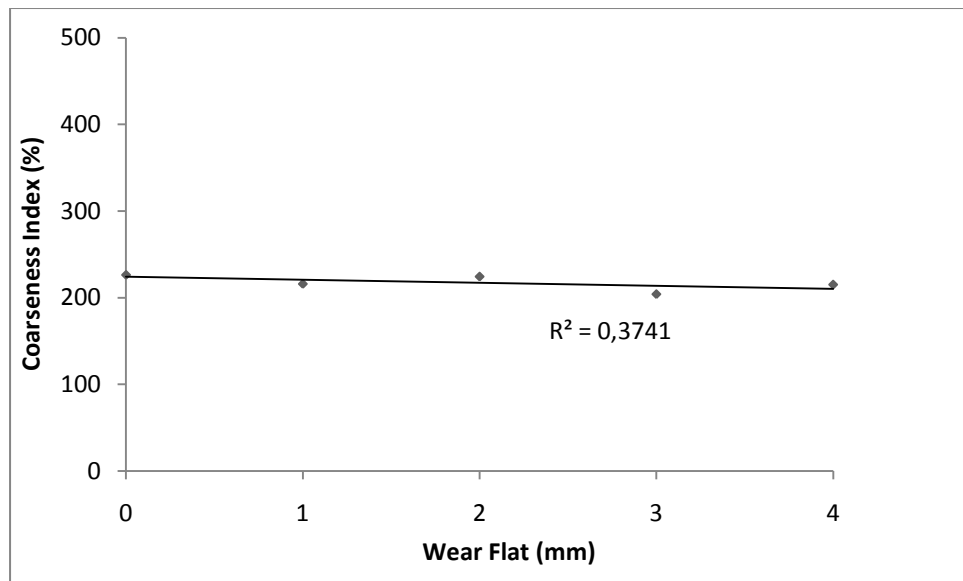


(b)

Figure 4.29. Effect of Wear Flat on Size Distribution (a) and Coarseness Index (b) for Mudstone 4

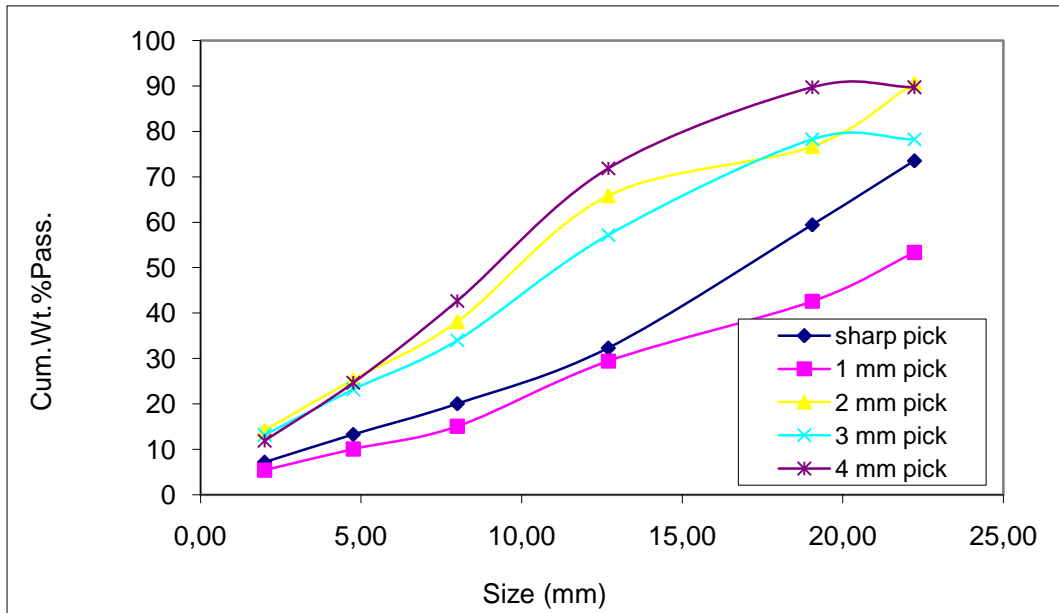


(a)

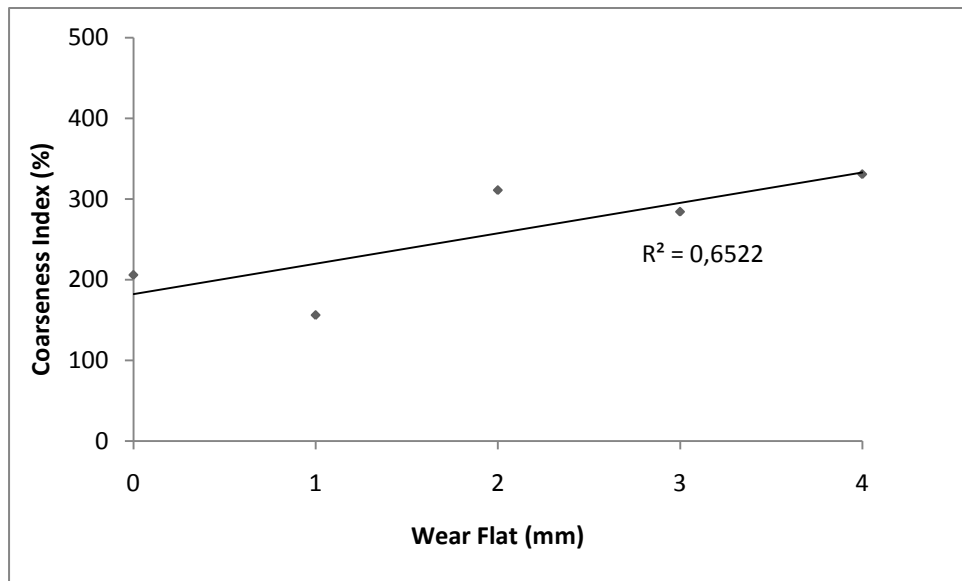


(b)

Figure 4.30. Effect of Wear Flat on Size Distribution (a) and Coarseness Index (b) for Mudstone-Siltstone

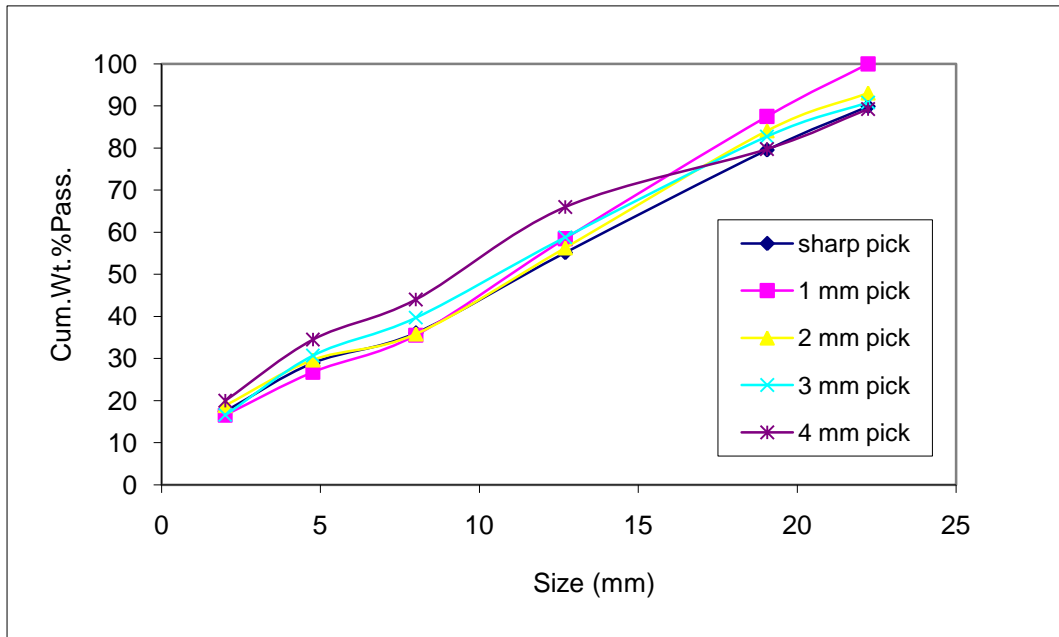


(a)

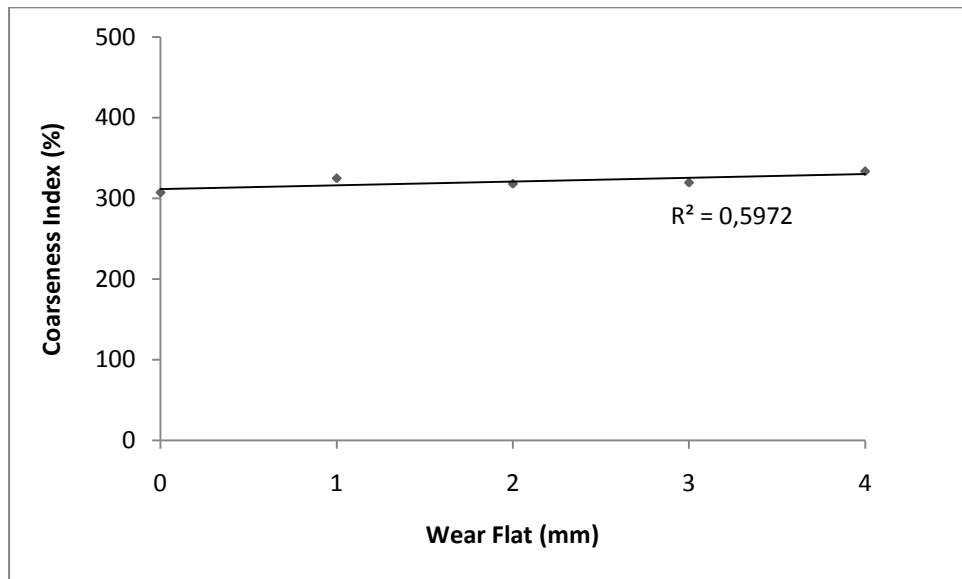


(b)

Figure 4.31. Effect of Wear Flat on Size Distribution (a) and Coarseness Index (b) for Marl 1

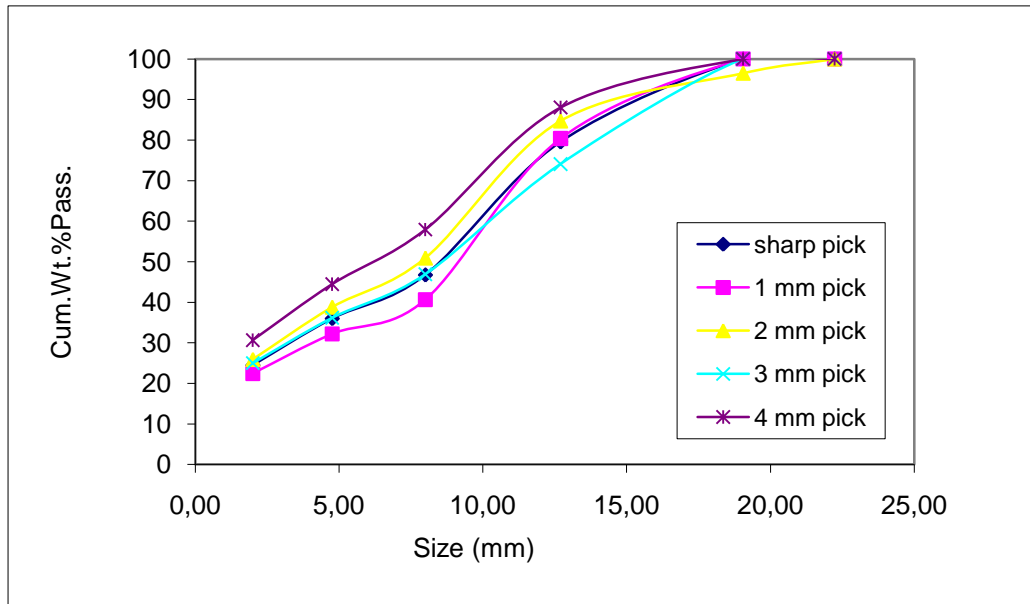


(a)

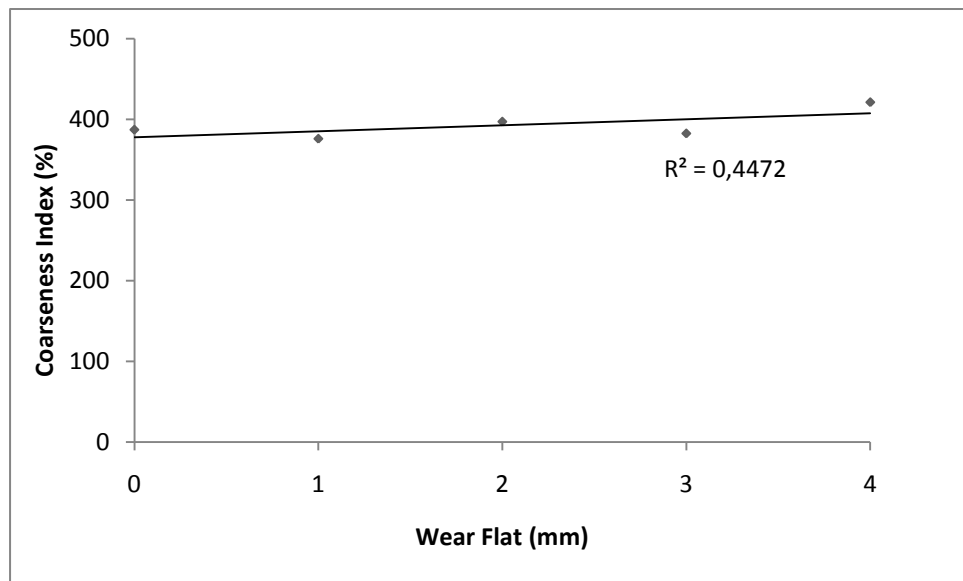


(b)

Figure 4.32. Effect of Wear Flat on Size Distribution (a) and Coarseness Index (b) for Marl 2

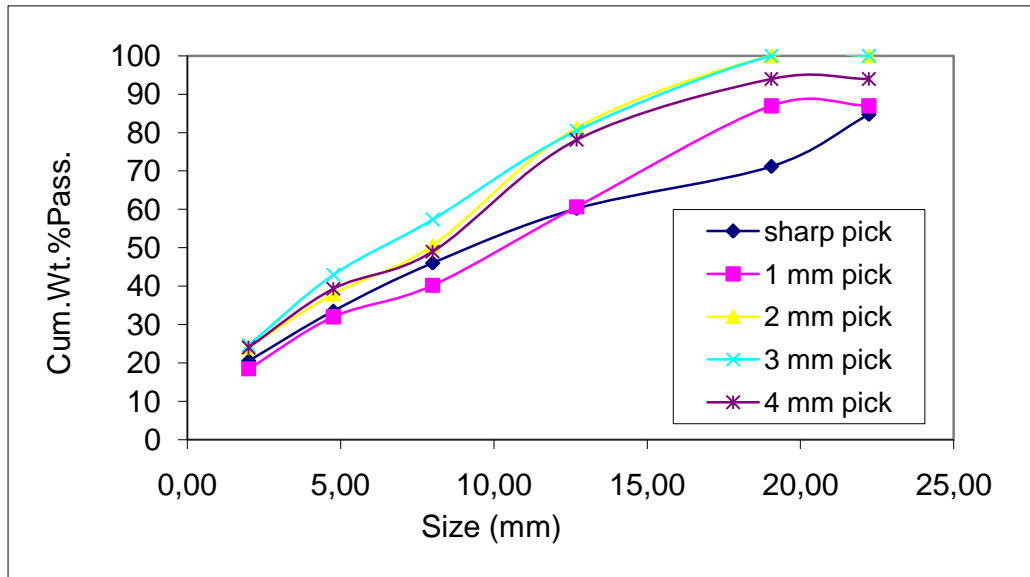


(a)

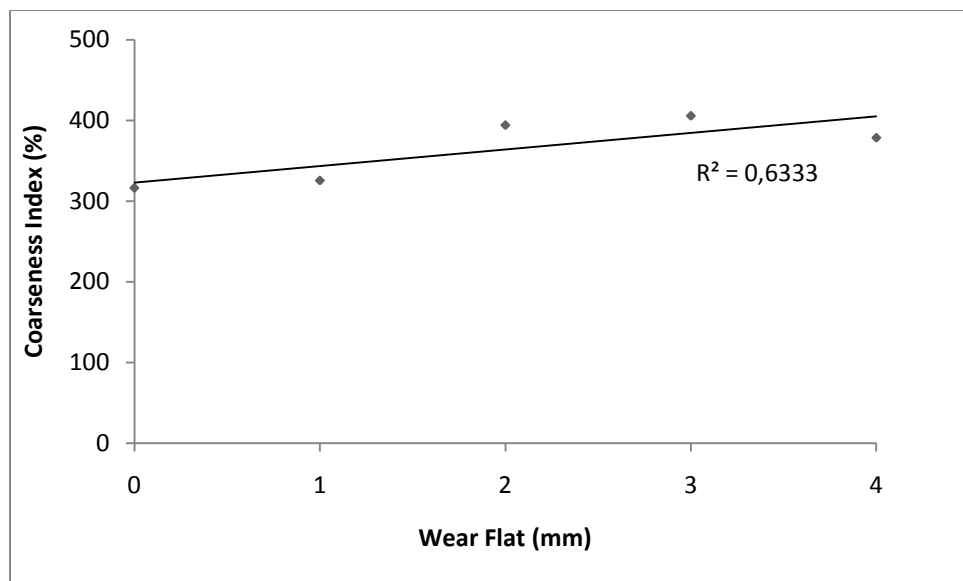


(b)

Figure 4.33. Effect of Wear Flat on Size Distribution (a) and Coarseness Index (b) for Altered Tuff

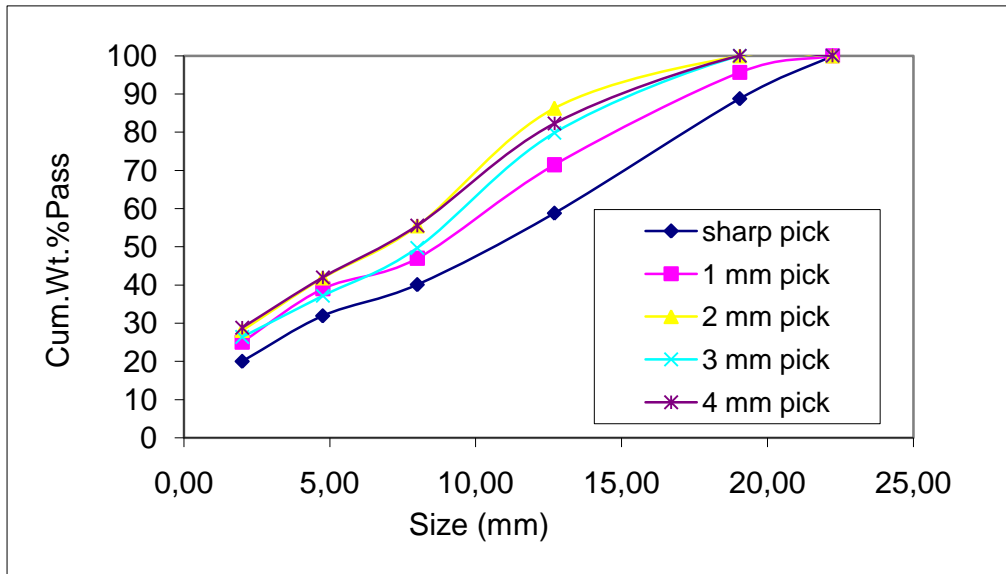


(a)

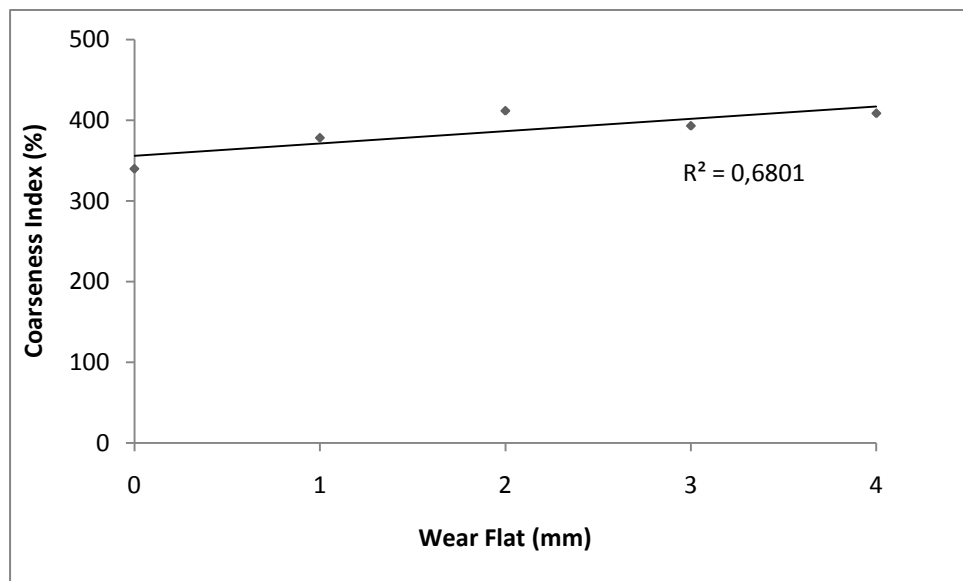


(b)

Figure 4.34. Effect of Wear Flat on Size Distribution (a) and Coarseness Index (b) for Lithic Tuff 1

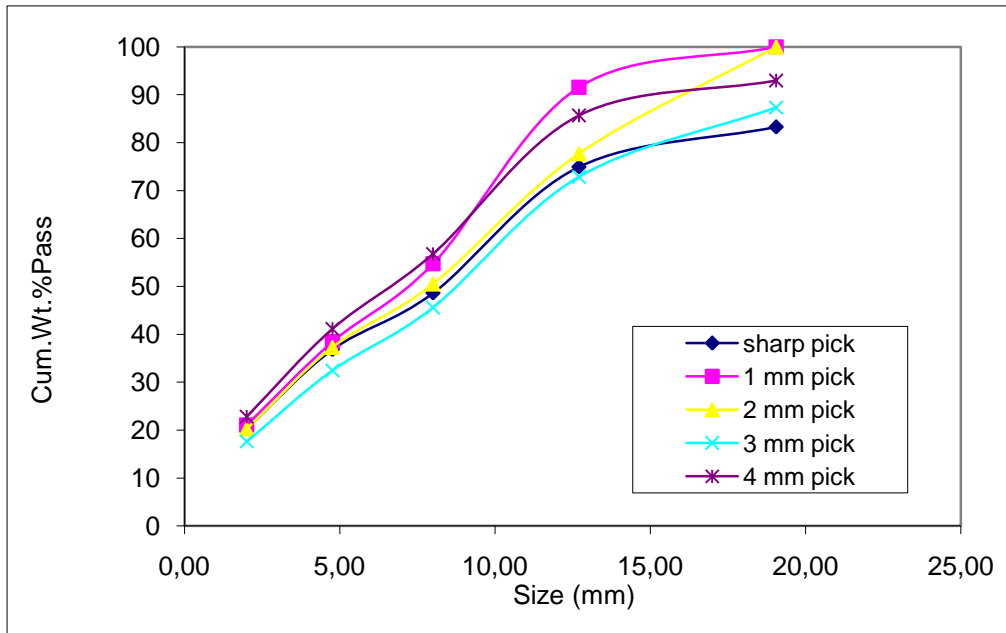


(a)

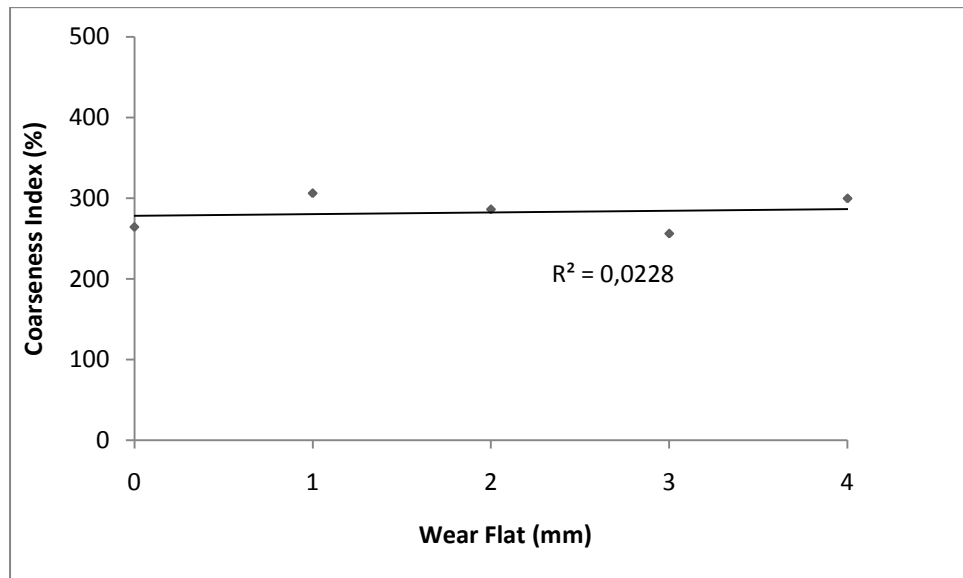


(b)

Figure 4.35. Effect of Wear Flat on Size Distribution (a) and Coarseness Index (b) for Lithic Tuff 2

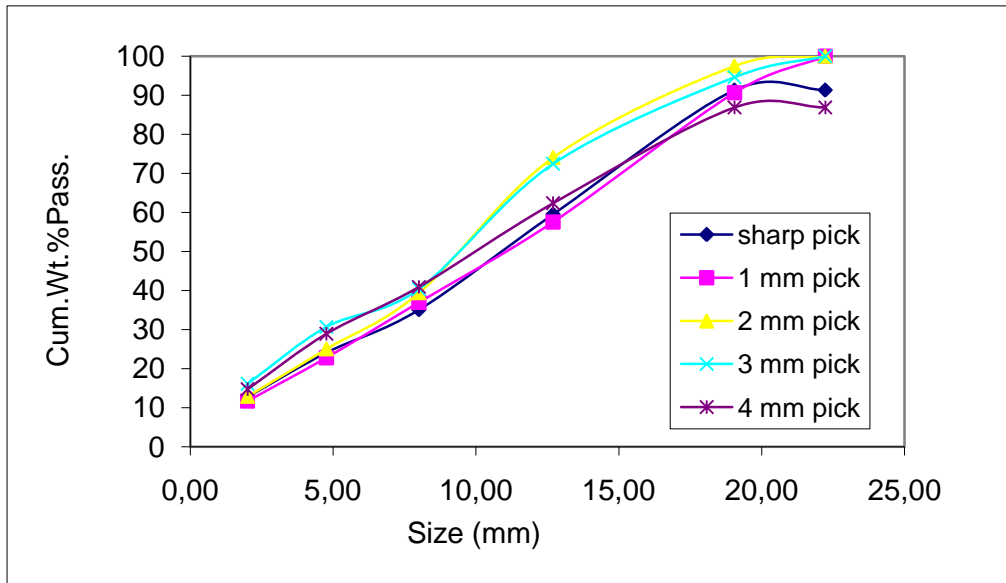


(a)

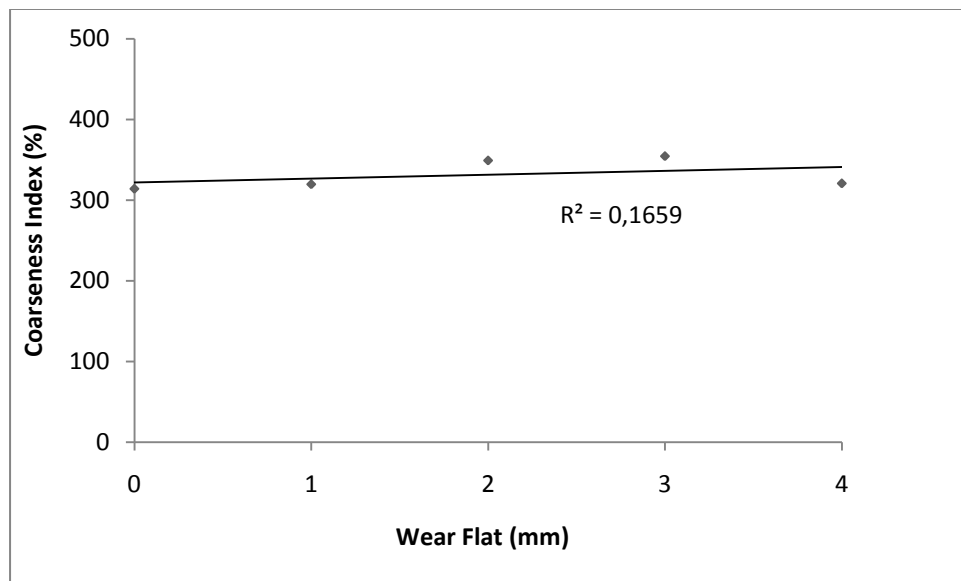


(b)

Figure 4.36. Effect of Wear Flat on Size Distribution (a) and Coarseness Index (b) for Claystone

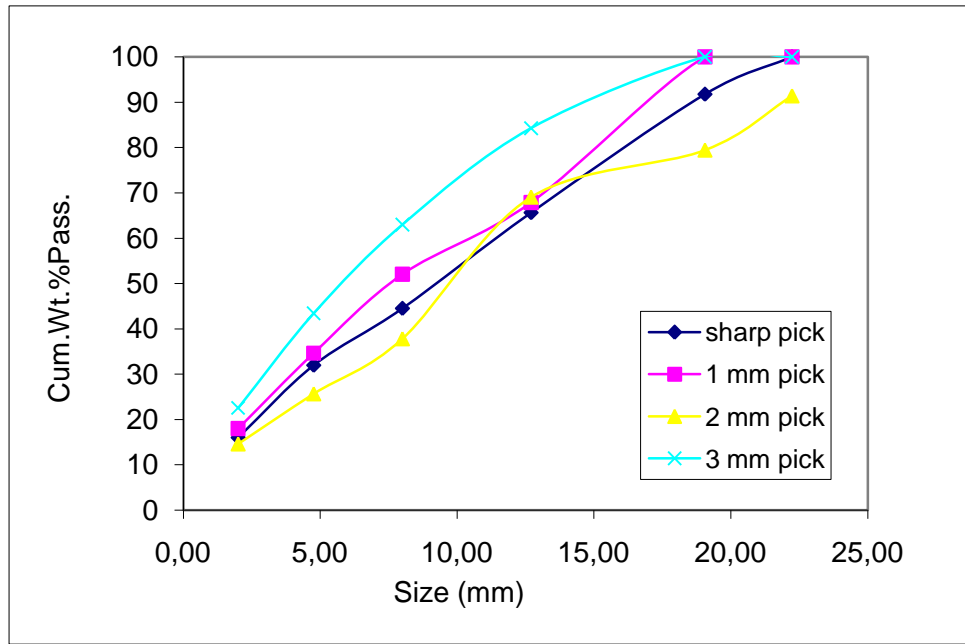


(a)

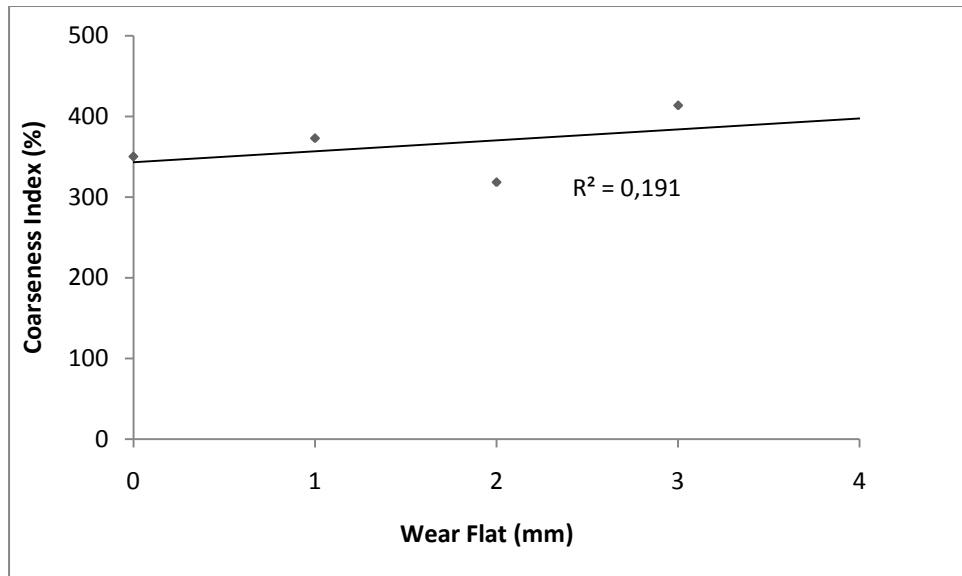


(b)

Figure 4.37. Effect of Wear Flat on Size Distribution (a) and Coarseness Index (b) for Siltstone 1

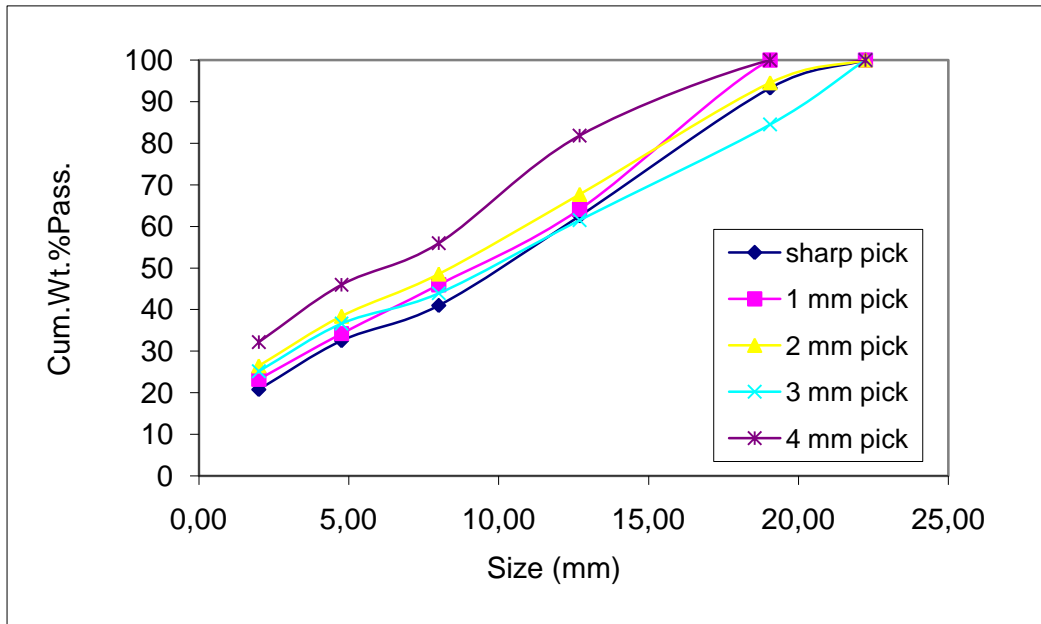


(a)

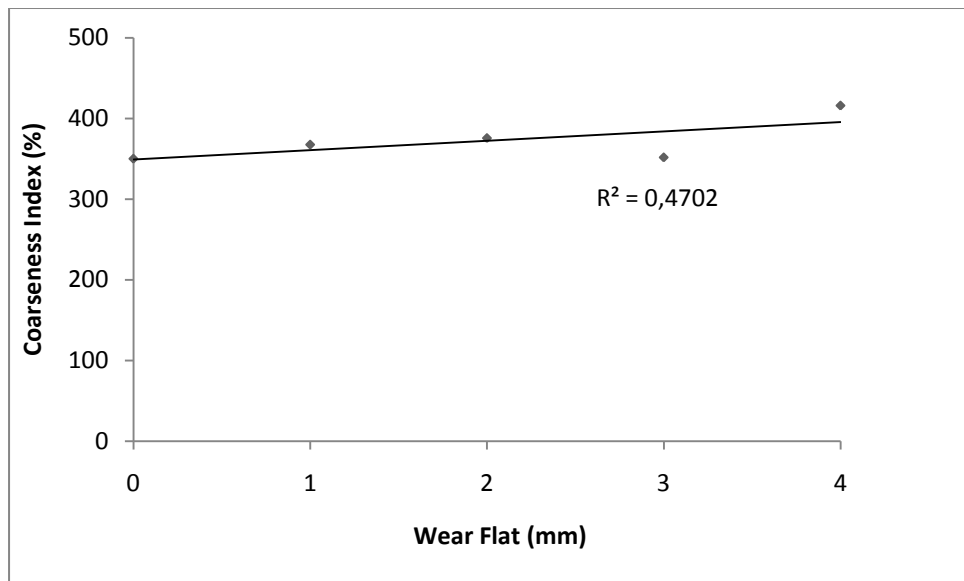


(b)

Figure 4.38. Effect of Wear Flat on Size Distribution (a) and Coarseness Index (b) for Siltstone 2

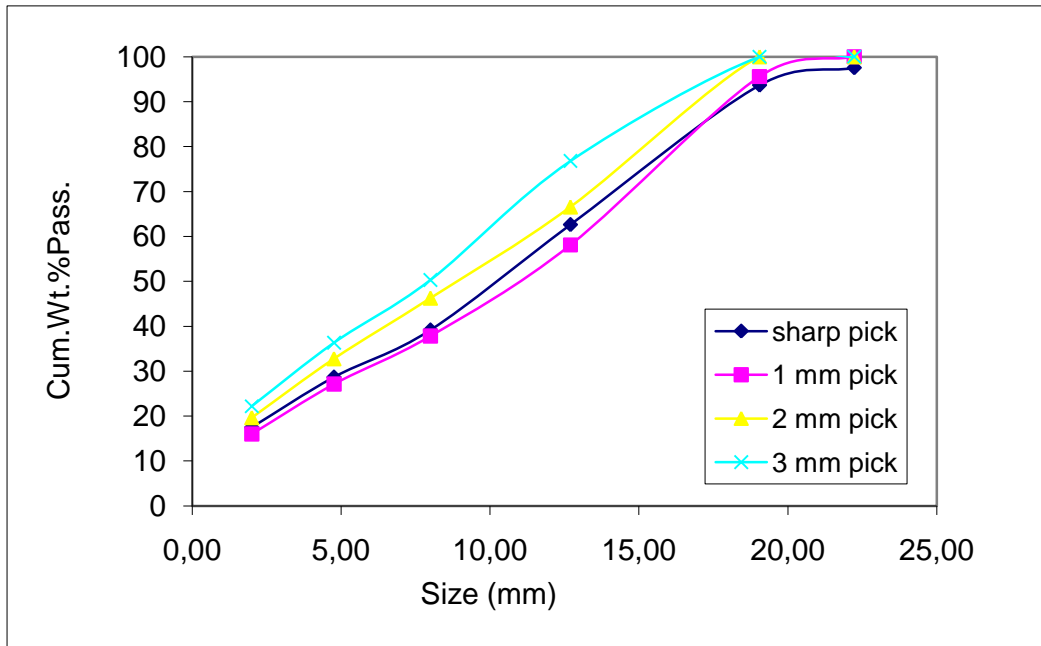


(a)

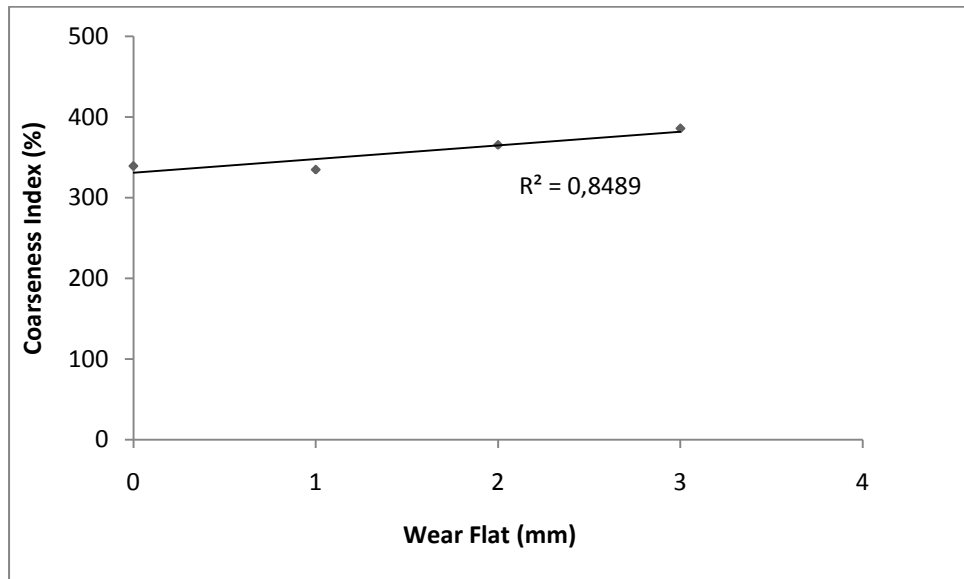


(b)

Figure 4.39. Effect of Wear Flat on Size Distribution (a) and Coarseness Index (b) for Andesite



(a)



(b)

Figure 4.40. Effect of Wear Flat on Size Distribution (a) and Coarseness Index (b) for Travertine

4.13. Rock Property Value Limits Causing Poor Cutting Performance at Different Wear Flats

Limits for different rock properties causing poor cutting performance at different wear flats have been established by evaluating Figures 4.2, 4.5, 4.8, 4.11, 4.14 and 4.17. Table 4.6 shows the critical rock property limits above which the cutting specific energy exceeds 25 MJ/m³ and poor cutting performance is expected with sharp and blunted picks having 1 mm, 2 mm, 3 mm and 4 mm wear flats.

Table 4.6. Critical Limits for Various Rock Properties

W_F (mm)	UCS (MPa)	BTS (MPa)	I_s	SH	SCH	D (gr/cm³)
0	57.00	10.00	3.00	48.00	53.00	2.70
1	35.00	6.00	2.00	30.00	40.00	2.20
2	32.00	5.00	1.75	25.00	35.00	1.90
3	22.00	3.30	1.30	17.00	30.00	1.80
4	20.00	3.00	1.20	15.00	27.00	1.70

CHAPTER 5

EVALUATION OF RESULTS AND ESTABLISHING MODELS BY STATISTICAL ANALYSES

Statistical analyses for the researches dealing with the empirical experiments are the most important methods to investigate the results and find out the best models to predict the variables. In this study, there are dependent and independent variables. The dependent variable is laboratory specific energy (MJ/m³) and the independent variables are wear flat(mm), uniaxial compressive strength (MPa), brazilian tensile strength (MPa), cone indenter number, shore hardness, schmidthammer hardness and density (gr/cm³). The best relationships between these variables were examined and the most suitable models to predict the results have been determined.

In order to determine the best models, some statistical analyses were applied and the general form of the second order regression model with interaction terms were applied to the dataset. This technique was used with the analyse of variance (ANOVA). The correlation and determination coefficients were compared and the optimum models have been established.

When the experimenter is relatively close to the optimum, a model that incorporates curvature is usually required to approximate the response. In most cases, the second-order model is adequate. The following formula is generally used to find the optimum set of operating conditions for the variables to establish the models (Montgomery, 1997).

$$y = \sum_{i=1}^k \beta_i x_i + \sum_{i=1}^k \beta_{ii} x_i^2 + \sum_{i<j} \beta_{ij} x_i x_j \quad (5.1)$$

The general form of the second order regression model with interaction terms technique is based on the elimination of the independent variables which are not available for the 0.05 confidence interval value. The significant values bigger than the 0.05 are dismissed and the new running process is applied. This is continued until the all significant values are smaller than the 0.05 confidence interval value.

All combinations have been tried and the best nine models have been established as prediction equations.

The SPSS 13.0 version software was used in this study. Initially the dataset was created and the data belonging to the variables were entered into the programme. There are totally seven different kind of independent variables and one dependent variable. The correlations between the variables were analyzed.

5.1. MODEL 1

This model includes the variables shown below;

Dependent Variable;

SE_L: Laboratory Specific Energy (MJ/m³)

Independent Variables;

W_F: Wear Flat (0 mm, 1 mm, 2 mm, 3 mm, 4 mm)

UCS: Uniaxial Compressive Strength (MPa)

I_S: Standard Cone Indenter Number

SCH: Schmidth Hammer Hardness

SH: Shore Hardness

Tables 5.1, 5.2 and 5.3 give the summary of the first statistical model, analysis of variance (ANOVA) for the first model and the coefficients of the first model.

Table 5.1. Summary of the First Statistical Model

Model	R	R Square ^a	Adjusted R Square	Std. Error of the Estimate
1	,986 ^b	,973	,968	5,19811

For regression through the origin (the no-intercept model), R Square measures the proportion of the variability in the dependent variable about the origin explained by regression. This cannot be compared to R Square for models which include an intercept.

Table 5.2. Analysis of Variance (ANOVA) for First Model

Model		Sum of Squares	df	Mean Square	F	Sig.
1	Regression	81089,409	14	5792,101	214,361	,000 ^a
	Residual	2269,708	84	27,020		
	Total	83359,118 ^b	98			

This total sum of squares is not corrected for the constant because the constant is zero for regression through the origin.

Table 5.3. Coefficients of First Model

Model		Unstandardized Coefficients		Standardized Coefficients	t	Sig.
		B	Std. Error	Beta		
1	WF	-13,009	1,803	-1,074	-7,216	,000
	UCS	-,721	,194	-,699	-3,721	,000
	SCH	1,102	,206	1,234	5,345	,000
	WF.WF	,961	,319	,270	3,018	,003
	UCS.UCS	-,058	,007	-2,425	-8,021	,000
	SCH.SCH	-,043	,008	-1,843	-5,502	,000
	SH.SH	,070	,011	1,698	6,294	,000
	WF.Is	4,982	,815	,617	6,111	,000
	WF.SCH	,389	,067	1,034	5,801	,000
	WF.SH	-,181	,052	-,330	-3,473	,001
	UCS.Is	1,704	,210	3,424	8,124	,000
	UCS.SH	,117	,020	3,049	5,931	,000
	Is.SCH	,558	,211	1,203	2,647	,010
	Is.SH	-3,519	,418	-5,179	-8,418	,000

The formula according to the results of general form of the second order regression model with interaction terms for the first model is below;

$$\begin{aligned} SE_L = & -13.009 W_F - 0.721 UCS + 1.102 SCH + 0.961 W_F^2 - 0.058 UCS^2 \\ & -0.043 SCH^2 + 0.070 SH^2 + 4.982 W_F * I_S + 0.389 W_F * SCH \\ & -0.181 W_F * SH + 1.704 UCS * I_S + 0.117 UCS * SH + 0.558 I_S * SCH \\ & -3.519 I_S * SH \end{aligned}$$

5.2. MODEL 2

This model includes the variables shown below;

Dependent Variable;

SE_L: Laboratory Specific Energy (MJ/m³)

Independent Variables;

W_F: Wear Flat (0 mm, 1 mm, 2 mm, 3 mm, 4 mm)

BTS: Brazilian Tensile Strength (MPa)

I_S: Standard Cone Indenter Number

SCH: Schmidth Hammer Hardness

D: Density (gr/cm³)

Tables 5.4, 5.5 and 5.6 give the summary of the second statistical model, analysis of variance (ANOVA) for the second model and the coefficients of the second model.

Table 5.4. Summary of the Second Statistical Model

Model	R	R Square ^a	Adjusted R Square	Std. Error of the Estimate
1	,985 ^b	,971	,966	5,41244

For regression through the origin (the no-intercept model), R Square measures the proportion of the variability in the dependent variable about the origin explained by regression. This cannot be compared to R Square for models which include an intercept.

Table 5.5. Analysis of Variance (ANOVA) for Second Model

Model		Sum of Squares	df	Mean Square	F	Sig.
1	Regression	80927,670	15	5395,178	184,170	,000 ^a
	Residual	2431,447	83	29,295		
	Total	83359,118 ^b	98			

This total sum of squares is not corrected for the constant because the constant is zero for regression through the origin.

Table 5.6. Coefficients of Second Model

Model		Unstandardized Coefficients		Standardized Coefficients	t	Sig.
		B	Std. Error	Beta		
1	WF	-10,321	1,896	-,852	-5,444	,000
	BTS	22,296	5,623	3,540	3,965	,000
	Is	-53,368	8,227	-2,911	-6,487	,000
	SCH	2,087	,620	2,337	3,363	,001
	D	-46,207	14,169	-2,939	-3,261	,002
	WF.WF	,844	,332	,237	2,540	,013
	BTS.BTS	-,658	,331	-,779	-1,990	,050
	Is.Is	27,690	4,571	3,609	6,058	,000
	D.D	41,094	8,678	5,154	4,736	,000
	WF.Is	4,965	,865	,615	5,740	,000
	WF.SCH	,206	,061	,548	3,359	,001
	BTS.Is	-10,962	2,714	-3,932	-4,039	,000
	BTS.SCH	,600	,073	3,824	8,169	,000
	BTS.D	-9,802	3,075	-3,198	-3,188	,002
	SCH.D	-1,863	,397	-4,106	-4,698	,000

The formula according to the results of general form of the second order regression model with interaction terms for the second model is below;

$$\begin{aligned} SE_L = & -10.321 W_F + 22.296 BTS - 53.368 I_S + 2.087 SCH - 46.207 D + 0.844 W_F^2 \\ & - 0.658 BTS^2 + 27.690 I_S^2 + 41.094 D^2 + 4.965 W_F * I_S + 0.206 W_F * SCH \\ & - 10.962 BTS * I_S + 0.600 BTS * SCH - 9.802 BTS * D - 1.863 SCH * D \end{aligned}$$

5.3. MODEL 3

This model includes the variables shown below;

Dependent Variable;

SE_L: Laboratory Specific Energy (MJ/m³)

Independent Variables;

W_F: Wear Flat (0 mm, 1 mm, 2 mm, 3 mm, 4 mm)

BTS: Brazilian Tensile Strength (MPa)

I_S: Standard Cone Indenter Number

SCH: Schmidth Hammer Hardness

SH: Shore Hardness

D: Density (gr/cm³)

Tables 5.7, 5.8 and 5.9 give the summary of the third statistical model, analysis of variance (ANOVA) for the third model and the coefficients of the third model.

Table 5.7. Summary of the Third Statistical Model

Model	R	R Square ^a	Adjusted R Square	Std. Error of the Estimate
1	,983 ^b	,966	,962	5,70513

For regression through the origin (the no-intercept model), R Square measures the proportion of the variability in the dependent variable about the origin explained by regression. This cannot be compared to R Square for models which include an intercept.

Table 5.8. Analysis of Variance (ANOVA) for Third Model

Model		Sum of Squares	df	Mean Square	F	Sig.
1	Regression	80527,397	11	7320,672	224,916	,000 ^a
	Residual	2831,720	87	32,549		
	Total	83359,118 ^b	98			

This total sum of squares is not corrected for the constant because the constant is zero for regression through the origin.

Table 5.9. Coefficients of Third Model

Model		Unstandardized Coefficients		Standardized Coefficients	t	Sig.
		B	Std. Error	Beta		
1	WF	-6,537	1,595	-,540	-4,097	,000
	BTS	28,303	5,860	4,494	4,830	,000
	Is	-93,862	14,323	-5,120	-6,553	,000
	WF.WF	,833	,343	,234	2,432	,017
	SH.SH	,027	,004	,644	6,229	,000
	D.D	3,757	,848	,471	4,431	,000
	WF.Is	6,930	,550	,858	12,594	,000
	BTS.SCH	,222	,027	1,412	8,147	,000
	BTS.SH	-,258	,049	-1,154	-5,289	,000
	BTS.D	-15,750	3,040	-5,138	-5,181	,000
	Is.D	43,429	7,193	4,958	6,038	,000

The formula according to the results of general form of the second order regression model with interaction terms for the third model is below;

$$\begin{aligned} SE_L = & -6.537 W_F + 28.303 BTS - 93.862 I_S + 0.833 W_F^2 + 0.027 SH^2 + 3.757 D^2 \\ & + 6.930 W_F * I_S + 0.222 BTS * SCH - 0.258 BTS * SH \\ & - 15.750 BTS * D + 43.429 I_S * D \end{aligned}$$

5.4. MODEL 4

This model includes the variables shown below;

Dependent Variable;

SE_L : Laboratory Specific Energy (MJ/m³)

Independent Variables;

W_F : Wear Flat (0 mm, 1 mm, 2 mm, 3 mm, 4 mm)

UCS: Uniaxial Compressive Strength (MPa)

I_S : Standard Cone Indenter Number

SH: Shore Hardness

D: Density (gr/cm³)

Tables 5.10, 5.11 and 5.12 give the summary of the fourth statistical model, analysis of variance (ANOVA) for the fourth model and the coefficients of the fourth model.

Table 5.10. Summary of the Fourth Statistical Model

Model	R	R Square ^a	Adjusted R Square	Std. Error of the Estimate
1	,979 ^b	,958	,954	6,25558

For regression through the origin (the no-intercept model), R Square measures the proportion of the variability in the dependent variable about the origin explained by regression. This cannot be compared to R Square for models which include an intercept.

Table 5.11. Analysis of Variance (ANOVA) for Fourth Model

Model		Sum of Squares	df	Mean Square	F	Sig.
1	Regression	79876,346	9	8875,150	226,799	,000 ^a
	Residual	3482,772	89	39,132		
	Total	83359,118 ^b	98			

This total sum of squares is not corrected for the constant because the constant is zero for regression through the origin.

Table 5.12. Coefficients of Fourth Model

Model		Unstandardized Coefficients		Standardized Coefficients	t	Sig.
		B	Std. Error	Beta		
1	WF	-7,204	1,753	-,595	-4,110	,000
	SH	-,702	,213	-,532	-3,295	,001
	D	5,334	1,460	,339	3,654	,000
	WF.WF	,932	,377	,262	2,477	,015
	UCS.UCS	-,025	,004	-1,045	-6,157	,000
	SH.SH	,094	,012	2,276	7,722	,000
	WF.Is	7,028	,596	,870	11,789	,000
	UCS.Is	1,457	,195	2,926	7,452	,000
	Is.SH	-2,266	,320	-0,335	-6,913	,000

The formula according to the results of general form of the second order regression model with interaction terms for the fourth model is below;

$$SE_L = -7.204W_F - 0.702SH + 5.334D + 0.932WF^2 - 0.025UCS^2 + 0.094SH^2 + 7.028WF * I_S \\ + 1.457UCS * I_S - 2.266I_S * SH$$

5.5. MODEL 5

This model includes the variables shown below;

Dependent Variable;

SE_L: Laboratory Specific Energy (MJ/m³)

Independent Variables;

W_F: Wear Flat (0 mm, 1 mm, 2 mm, 3 mm, 4 mm)

UCS: Uniaxial Compressive Strength (MPa)

I_S: Standard Cone Indenter Number

SH: Shore Hardness

Tables 5.13, 5.14 and 5.15 give the summary of the fifth statistical model, analysis of variance (ANOVA) for the fifth model and the coefficients of the fifth model.

Table 5.13. Summary of the Fifth Statistical Model

Model	R	R Square ^a	Adjusted R Square	Std. Error of the Estimate
1	,976 ^b	,953	,950	6,53030

For regression through the origin (the no-intercept model), R Square measures the proportion of the variability in the dependent variable about the origin explained by regression. This cannot be compared to R Square for models which include an intercept.

Table 5.14. Analysis of Variance (ANOVA) for Fifth Model

Model		Sum of Squares	df	Mean Square	F	Sig.
1	Regression	79478,433	7	11354,062	266,247	,000 ^a
	Residual	3880,684	91	42,645		
	Total	83359,118 ^b	98			

This total sum of squares is not corrected for the constant because the constant is zero for regression through the origin.

Table 5.15. Coefficients of Fifth Model

Model		Unstandardized Coefficients		Standardized Coefficients	t	Sig.
		B	Std. Error	Beta		
1	WF	-3,352	,662	-,277	-5,061	,000
	UCS.UCS	-,043	,008	-1,796	-5,417	,000
	SH.SH	,065	,012	1,575	5,373	,000
	WF.Is	6,867	,551	,850	12,470	,000
	UCS.Is	1,571	,214	3,156	7,350	,000
	UCS.SH	,046	,016	1,189	2,839	,006
	Is.SH	-2,506	,370	-3,688	-6,775	,000

The formula according to the results of general form of the second order regression model with interaction terms for the fifth model is below;

$$SE_L = -3.352W_F - 0.043UCS^2 + 0.065SH^2 + 6.867W_F * I_S + 1.571UCS * I_S \\ + 0.046UCS * SH - 2.506I_S * SH$$

5.6. MODEL 6

This model includes the variables shown below;

Dependent Variable;

SE_L: Laboratory Specific Energy (MJ/m³)

Independent Variables;

W_F: Wear Flat (0 mm, 1 mm, 2 mm, 3 mm, 4 mm)

BTS: Brazilian Tensile Strength (MPa)

I_S: Standard Cone Indenter Number

SCH: Schmidt Hammer Hardness

SH: Shore Hardness

Tables 5.16, 5.17 and 5.18 give the summary of the sixth statistical model, analysis of variance (ANOVA) for the sixth model and the coefficients of the sixth model.

Table 5.16. Summary of the Sixth Statistical Model

Model	R	R Square ^a	Adjusted R Square	Std. Error of the Estimate
1	,976 ^b	,952	,946	6,79812

For regression through the origin (the no-intercept model), R Square measures the proportion of the variability in the dependent variable about the origin explained by regression. This cannot be compared to R Square for models which include an intercept.

Table 5.17. Analysis of Variance (ANOVA) for Sixth Model

Model		Sum of Squares	df	Mean Square	F	Sig.
1	Regression	79338,462	11	7212,587	156,068	,000 ^a
	Residual	4020,656	87	46,214		
	Total	83359,118 ^b	98			

This total sum of squares is not corrected for the constant because the constant is zero for regression through the origin.

Table 5.18. Coefficients of Sixth Model

Model		Unstandardized Coefficients		Standardized Coefficients	t	Sig.
		B	Std. Error	Beta		
1	WF	-10,264	2,268	-,847	-4,525	,000
	SCH	1,294	,318	1,449	4,067	,000
	SH	-1,736	,417	-1,316	-4,163	,000
	WF.WF	,830	,415	,233	2,001	,048
	SCH.SCH	-,056	,013	-2,383	-4,455	,000
	WF.Is	5,092	,991	,631	5,136	,000
	WF.SCH	,199	,070	,529	2,838	,006
	BTS.SCH	,228	,048	1,453	4,725	,000
	BTS.SH	-,379	,074	-1,693	-5,098	,000
	Is.SH	,311	,114	,458	2,739	,007
	SCH.SH	,084	,018	2,476	4,609	,000

The formula according to the results of general form of the second order regression model with interaction terms for the sixth model is below;

$$\begin{aligned} SE_L = & -10.264W_F + 1.294SCH - 1.736SH + 0.830W_F^2 - 0.056SCH^2 + 5.092W_F * I_S \\ & + 0.199W_F * SCH + 0.228BTS * SCH - 0.379BTS * SH \\ & + 0.311I_S * SH + 0.084SCH * SH \end{aligned}$$

5.7. MODEL 7

This model includes the variables shown below;

Dependent Variable;

SE_L: Laboratory Specific Energy (MJ/m³)

Independent Variables;

W_F: Wear Flat (0 mm, 1 mm, 2 mm, 3 mm, 4 mm)

BTS: Brazilian Tensile Strength (MPa)

I_S: Standard Cone Indenter Number

SH: Shore Hardness

D: Density (gr/cm³)

Tables 5.19, 5.20 and 5.21 give the summary of the seventh statistical model, analysis of variance (ANOVA) for the seventh model and the coefficients of the seventh model.

Table 5.19. Summary of the Seventh Statistical Model

Model	R	R Square ^a	Adjusted R Square	Std. Error of the Estimate
1	,974 ^b	,949	,945	6,85529

For regression through the origin (the no-intercept model), R Square measures the proportion of the variability in the dependent variable about the origin explained by regression. This cannot be compared to R Square for models which include an intercept.

Table 5.20. Analysis of Variance (ANOVA) for Seventh Model

Model		Sum of Squares	df	Mean Square	F	Sig.
1	Regression	79129,565	8	9891,196	210,473	,000 ^a
	Residual	4229,553	90	46,995		
	Total	83359,118 ^b	98			

This total sum of squares is not corrected for the constant because the constant is zero for regression through the origin.

Table 5.21. Coefficients of Seventh Model

Model		Unstandardized Coefficients		Standardized Coefficients	t	Sig.
		B	Std. Error	Beta		
1	WF	-2,769	,866	-,229	-3,197	,002
	Is	-29,226	5,781	-1,594	-5,055	,000
	BTS.BTS	1,538	,247	1,821	6,225	,000
	D.D	6,767	1,333	,849	5,076	,000
	WF.Is	6,585	,606	,816	10,875	,000
	BTS.Is	-1,932	,686	-,693	-2,815	,006
	BTS.SH	-,606	,086	-2,707	-7,068	,000
	Is.SH	1,933	,248	2,845	7,784	,000

The formula according to the results of general form of the second order regression model with interaction terms for the Seventh model is below;

$$SE_L = -2.769W_F - 29.226I_S + 1.538BTS^2 + 6.767D^2 + 6.585WF * I_S - 1.932BTS * I_S \\ - 0.606BTS * SH + 1.933I_S * SH$$

5.8. MODEL 8

This model includes the variables shown below;

Dependent Variable;

SE_L: Laboratory Specific Energy (MJ/m³)

Independent Variables;

W_F: Wear Flat (0 mm, 1 mm, 2 mm, 3 mm, 4 mm)

UCS: Uniaxial Compressive Strength (MPa)

I_S: Standard Cone Indenter Number

SCH: Schmidt Hammer Hardness

D: Density (gr/cm³)

Tables 5.22, 5.23 and 5.24 give the summary of the eighth statistical model, analysis of variance (ANOVA) for the eighth model and the coefficients of the eighth model.

Table 5.22. Summary of the Eighth Statistical Model

Model	R	R Square ^a	Adjusted R Square	Std. Error of the Estimate
1	,965 ^b	,932	,928	7,83459

For regression through the origin (the no-intercept model), R Square measures the proportion of the variability in the dependent variable about the origin explained by regression. This cannot be compared to R Square for models which include an intercept.

Table 5.23. Analysis of Variance (ANOVA) for Eighth Model

Model		Sum of Squares	df	Mean Square	F	Sig.
1	Regression	77650,708	5	15530,142	253,013	,000 ^a
	Residual	5708,410	93	61,381		
	Total	83359,118 ^b	98			

This total sum of squares is not corrected for the constant because the constant is zero for regression through the origin.

Table 5.24. Coefficients of Eighth Model

Model		Unstandardized Coefficients		Standardized Coefficients	t	Sig.
		B	Std. Error	Beta		
1	WF	-2,352	,881	-,194	-2,671	,009
	UCS	-,740	,290	-,717	-2,549	,012
	WF.Is	6,140	,866	,760	9,216	,000
	UCS.D	,491	,151	,973	3,246	,002
	Is.SCH	,075	,040	,163	1,901	,060

The formula according to the results of general form of the second order regression model with interaction terms for the eighth model is below;

$$SE_L = -2.352W_F - 0.740UCS + 6.140W_F * I_S + 0.491UCS * D + 0.075I_S * SCH$$

5.9. MODEL 9

This model includes the variables shown below;

Dependent Variable;

SE_L: Laboratory Specific Energy (MJ/m³)

Independent Variables;

W_F: Wear Flat (0 mm, 1 mm, 2 mm, 3 mm, 4 mm)

BTS: Brazilian Tensile Strength (MPa)

I_S: Standard Cone Indenter Number

D: Density (gr/cm³)

Tables 5.25, 5.26 and 5.27 give the summary of the ninth statistical model, analysis of variance (ANOVA) for the ninth model and the coefficients of the ninth model.

Table 5.25. Summary of the Ninth Statistical Model

Model	R	R Square ^a	Adjusted R Square	Std. Error of the Estimate
1	,960 ^b	,921	,916	8,45999

For regression through the origin (the no-intercept model), R Square measures the proportion of the variability in the dependent variable about the origin explained by regression. This cannot be compared to R Square for models which include an intercept.

Table 5.26. Analysis of Variance (ANOVA) for Ninth Model

Model		Sum of Squares	df	Mean Square	F	Sig.
1	Regression	76774,540	6	12795,757	178,783	,000 ^a
	Residual	6584,577	92	71,571		
	Total	83359,118 ^b	98			

This total sum of squares is not corrected for the constant because the constant is zero for regression through the origin.

Table 5.27. Coefficients of Ninth Model

Model		Unstandardized Coefficients		Standardized Coefficients	t	Sig.
		B	Std. Error	Beta		
1	WF	-2,795	1,029	-,231	-2,716	,008
	BTS	23,075	8,299	3,664	2,780	,007
	Is	-61,530	19,927	-3,357	-3,088	,003
	WF.Is	6,765	,737	,838	9,183	,000
	BTS.D	-11,770	4,288	-3,840	-2,745	,007
	Is.D	34,400	10,196	3,927	3,374	,001

The formula according to the results of general form of the second order regression model with interaction terms for the ninth model is below;

$$SE_L = -2.795 W_F + 23.075 BTS - 61.530 I_S + 6.765 W_F * I_S - 11.770 BTS * D \\ + 34.400 I_S * D$$

5.10. COMPARISON OF MODELS

Comparisons of the results of nine prediction models with the actual laboratory cutting specific energies are given in Figures 5.1, 5.2 and 5.3. It can be seen that very good correlation exists between the predicted and actual laboratory cutting specific energy and the correlation coefficient varies from 0.9476 for the Model 1 to 0.8359 for the Model 9.

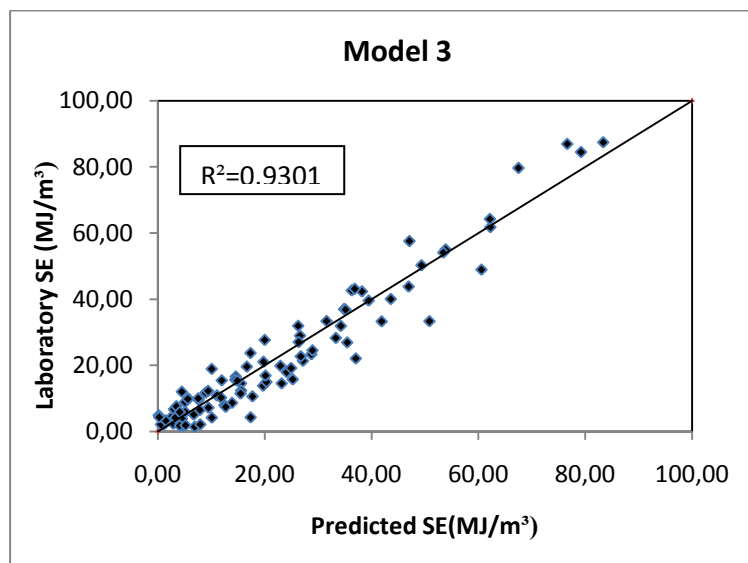
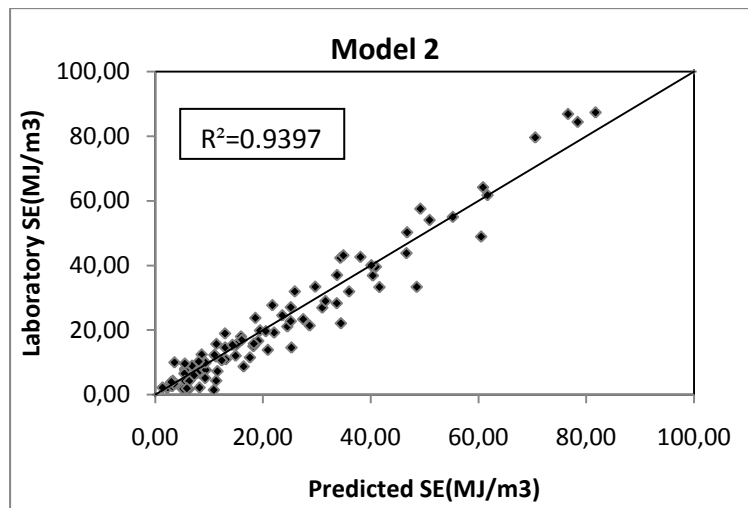
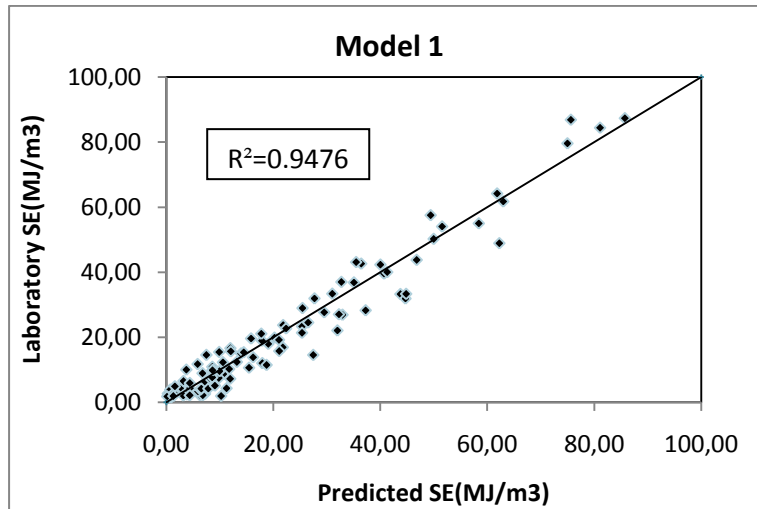


Figure 5.1. Comparisons of The Predicted and Laboratory Cutting Specific Energies for Statistical Models 1, 2, 3.

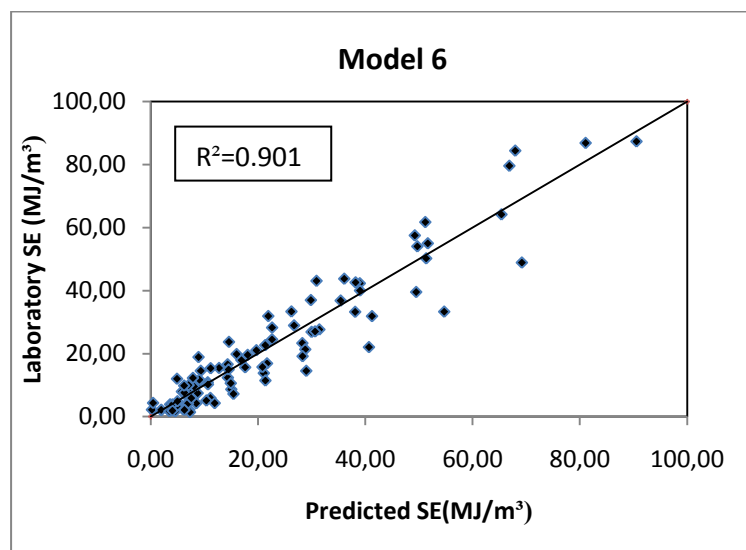
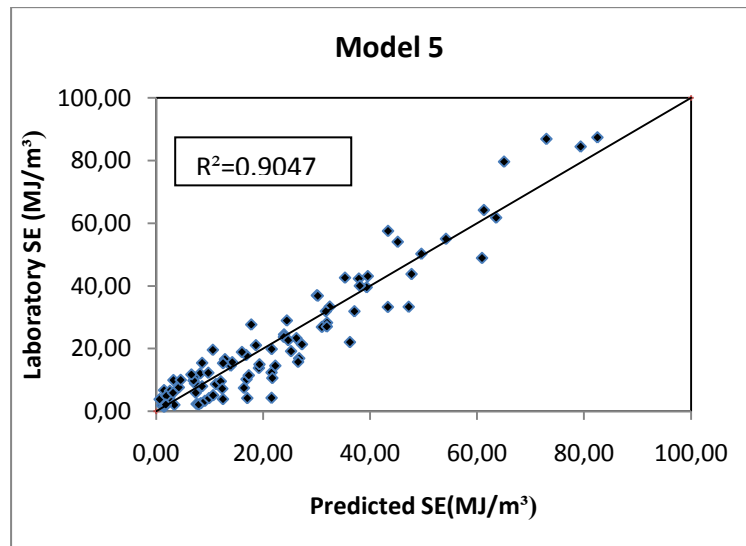
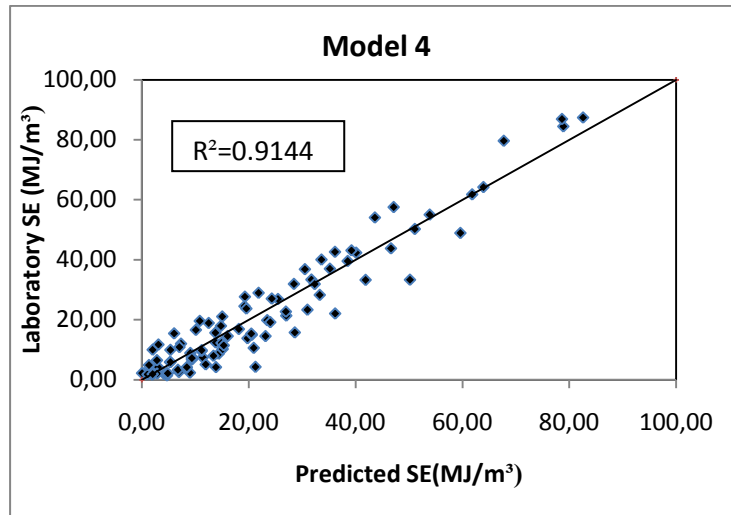


Figure 5.2. Comparisons of The Predicted and Laboratory Cutting Specific Energies for Statistical Models 4, 5, 6.

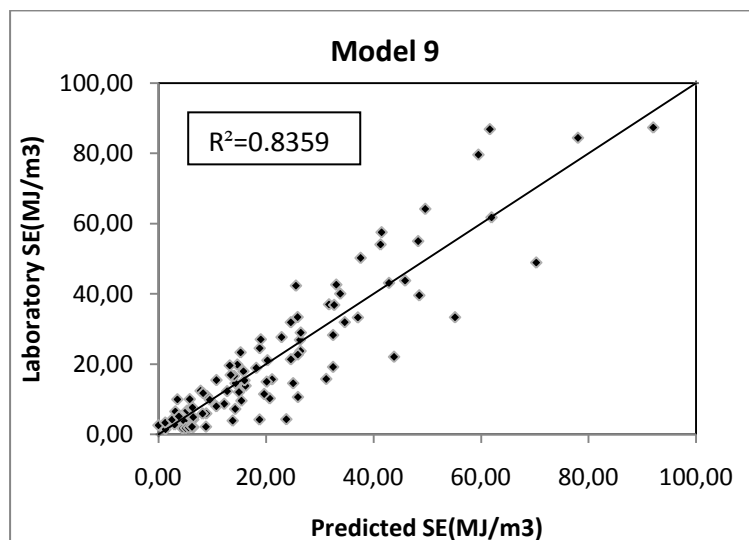
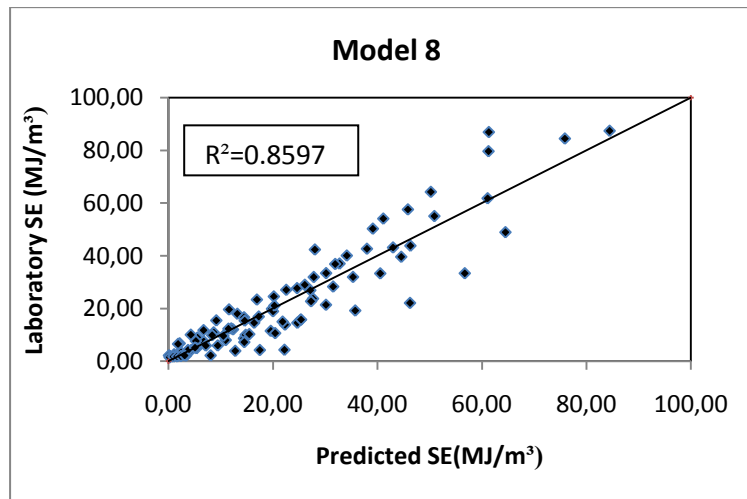
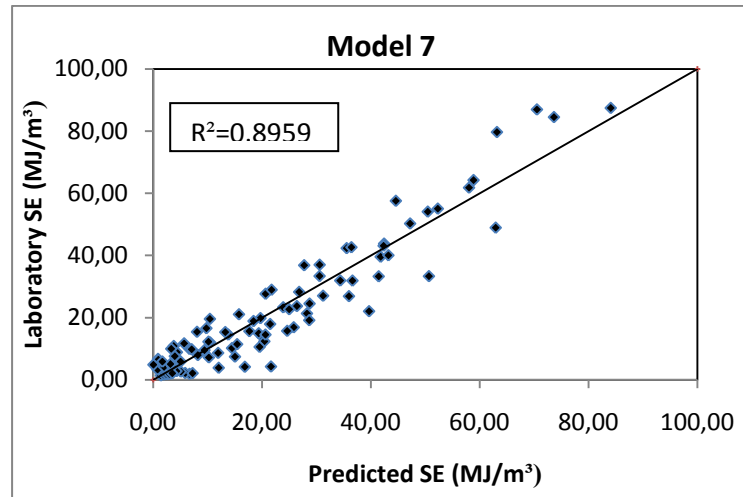


Figure 5.3. Comparisons of The Predicted and Laboratory Cutting Specific Energies for Statistical Models 7, 8, 9.

The laboratory specific energies and predicted laboratory specific energies (MJ/m³) for nine different models and for all rock types are given in Table 5.28.

Table 5.28. Laboratory and Predicted Specific Energy Results for Nine Different Statistical Models and for All Rock Types (M=Model)

Type of Rock	Wear Flat W_F (mm)	Laboratory Specific Energy (MJ/m ³)	Predicted Specific Energy (MJ/m ³)								
			M1	M2	M3	M4	M5	M6	M7	M8	M9
Limestone 1	0	6.74	7.64	7.88	3.02	9.36	1.49	7.93	0.86	2.13	5.33
	1	7.64	8.59	9.37	3.48	9.34	4.25	6.24	3.95	5.25	6.33
	2	9.85	8.63	9.33	5.61	11.19	7.01	6.22	7.05	8.36	9.56
	3	12.29	10.59	10.98	9.41	14.90	9.77	7.86	10.14	11.47	12.78
	4	15.37	14.48	14.32	14.87	20.47	12.53	11.16	13.23	14.58	16.01
Limestone 2	0	8.68	10.68	16.39	13.89	14.37	11.19	15.01	11.91	14.45	12.24
	1	13.83	16.23	20.89	19.69	19.76	19.23	21.07	20.07	22.29	16.21
	2	21.37	25.38	28.64	27.15	27.02	27.28	28.80	28.23	30.13	24.64
	3	42.63	36.45	38.07	36.28	36.14	35.33	38.18	36.40	37.97	33.08
	4	57.55	49.44	49.19	47.08	47.13	43.37	49.22	44.56	45.81	41.51
Limestone 3	0	1.93	10.25	4.97	4.77	4.19	1.11	3.47	6.65	0.28	1.18
	1	2.22	1.11	-1.45	1.14	0.03	-0.19	0.22	5.86	-0.23	-0.82
	2	2.67	0.29	-2.93	-0.82	-2.27	-1.48	-1.37	5.06	-0.74	-1.58
	3	2.84	1.40	-2.72	-1.11	-2.71	-2.77	-1.30	4.27	-1.25	-2.35
	4	4.35	4.43	-0.82	0.26	-1.28	-4.06	0.43	3.48	-1.76	-3.11
Limestone 4	0	4.24	2.63	3.26	2.44	3.02	2.47	8.47	-0.19	4.35	6.48
	1	5.93	7.05	7.19	5.12	5.26	7.42	11.11	5.01	9.42	8.89
	2	7.23	11.94	11.53	9.47	9.35	12.38	15.41	10.21	14.50	14.28
	3	11.48	18.75	17.56	15.48	15.31	17.34	21.37	15.40	19.58	19.67
	4	14.55	27.48	25.27	23.16	23.14	22.29	28.99	20.60	24.66	25.06
Clayey limestone	0	2.36	3.92	2.17	2.90	8.98	7.59	5.99	-1.57	-0.25	-0.97
	1	2.58	7.23	3.14	1.36	6.92	8.36	4.59	-0.39	1.08	0.01
	2	3.33	5.93	3.49	1.48	6.73	9.13	4.85	0.79	2.41	1.27
	3	4.2	6.54	5.53	3.26	8.40	9.89	6.78	1.97	3.74	2.54
	4	5.12	9.08	9.25	6.72	11.94	10.66	10.36	3.16	5.07	3.80

Table 5.28. Laboratory and Predicted Specific Energy Results for Nine Different Statistical Models and for All Rock Types (continued) (M=Model)

Type of Rock	Wear Flat W_F (mm)	Laboratory Specific Energy (MJ/m ³)	Predicted Specific Energy (MJ/m ³)								
			M1	M2	M3	M4	M5	M6	M7	M8	M9
Mudstone 1	0	17.96	19.07	15.91	24.11	14.79	16.84	16.90	21.47	13.17	15.82
	1	24.53	26.52	23.57	28.94	19.20	23.93	22.61	28.71	20.15	18.84
	2	26.91	32.95	30.99	35.44	25.47	31.02	29.98	35.95	27.14	26.33
	3	40.05	41.31	40.10	43.60	33.61	38.10	39.00	43.19	34.12	33.82
	4	54.07	51.58	50.90	53.42	43.61	45.19	49.69	50.43	41.10	41.31
Mudstone 2	0	12.03	17.95	14.91	4.49	7.31	8.22	4.89	10.45	12.34	14.99
	1	18.92	17.90	12.94	10.08	12.50	16.06	8.90	18.41	19.99	18.20
	2	23.73	21.85	18.57	17.34	19.55	23.90	14.57	26.38	27.65	26.43
	3	31.94	27.71	25.89	26.26	28.46	31.74	21.91	34.34	35.30	34.66
	4	43.12	35.50	34.90	36.85	39.23	39.59	30.90	42.31	42.96	42.89
Mudstone 3	0	7.99	8.53	5.53	12.46	13.39	8.59	5.81	8.18	10.94	10.77
	1	14.56	7.49	12.97	15.56	16.05	13.96	9.33	13.78	16.39	14.34
	2	14.98	13.98	18.21	20.32	20.57	19.33	14.51	19.37	21.84	20.14
	3	22.71	22.40	25.13	26.75	26.95	24.70	21.35	24.96	27.28	25.93
	4	37.01	32.74	33.73	34.84	35.19	30.07	29.85	30.56	32.73	31.73
Mudstone 4	0	19.86	20.23	19.44	22.93	23.46	21.62	16.00	19.68	19.80	14.68
	1	33.39	31.04	29.68	31.57	31.73	32.48	26.22	30.55	30.16	25.89
	2	33.28	43.78	41.60	41.88	41.87	43.34	38.10	41.41	40.52	37.10
	3	55.03	58.44	55.21	53.85	53.88	54.21	51.64	52.27	50.87	48.31
	4	79.64	75.02	70.51	67.49	67.75	65.07	66.84	63.13	61.23	59.52
Mudstone-Siltstone	0	8.92	6.77	6.82	5.08	9.07	7.28	7.13	4.33	5.54	-1.77
	1	9.58	9.95	5.49	7.62	11.16	12.10	8.06	9.40	10.50	15.44
	2	10.24	11.75	8.07	11.83	15.11	16.92	10.66	14.47	15.45	20.70
	3	10.62	15.47	12.34	17.71	20.93	21.74	14.91	19.53	20.41	25.95
	4	15.77	21.12	18.30	25.25	28.61	26.55	20.83	24.60	25.36	31.21

Table 5.28. Laboratory and Predicted Specific Energy Results for Nine Different Statistical Models and for All Rock Types (continued) (M=Model)

Type of Rock	Wear Flat W_F (mm)	Laboratory Specific Energy (MJ/m ³)	Predicted Specific Energy (MJ/m ³)								
			M1	M2	M3	M4	M5	M6	M7	M8	M9
Marl 1	0	2.07	3.17	2.15	-1.70	2.83	3.42	1.94	2.41	3.35	6.49
	1	2.17	6.82	1.35	0.57	4.64	7.97	1.94	7.21	8.06	8.84
	2	3.9	6.38	2.98	4.50	8.32	12.51	3.61	12.02	12.77	13.82
	3	4.21	7.86	6.29	10.10	13.85	17.06	6.93	16.82	17.48	18.81
	4	4.3	11.26	11.30	17.36	21.26	21.60	11.91	21.62	22.19	23.79
Marl 2	0	2.18	6.29	2.30	-1.66	0.41	-1.83	7.16	-4.90	0.09	0.57
	1	2.79	1.78	-3.13	-2.72	-1.15	-0.58	4.77	-3.26	1.85	3.00
	2	3.86	0.73	-3.84	-2.11	-0.85	0.67	4.04	-1.62	3.61	4.74
	3	4.9	1.60	-2.86	0.16	1.32	1.92	4.97	0.03	5.37	6.47
	4	5.9	4.39	-0.19	4.10	5.35	3.17	7.55	1.67	7.14	8.21
Altered Tuff	0	10.9	8.60	13.08	11.07	7.02	7.11	10.62	3.76	8.64	9.03
	1	16.62	11.98	19.09	14.58	10.10	12.89	14.32	9.75	14.46	14.08
	2	21.08	17.76	24.50	19.76	15.04	18.67	19.69	15.74	20.27	20.28
	3	28.97	25.47	31.59	26.61	21.84	24.45	26.72	21.73	26.08	26.48
	4	36.85	35.09	40.37	35.12	30.51	30.23	35.40	27.72	31.90	32.69
Lithic Tuff 1	0	7.47	9.82	5.57	12.69	11.39	16.44	8.74	15.00	6.75	6.07
	1	12.4	13.19	8.60	15.58	13.83	21.60	14.37	20.40	12.01	7.85
	2	16.91	21.78	16.03	20.14	18.14	26.76	21.67	25.80	17.27	13.45
	3	27.05	32.29	25.15	26.36	24.31	31.92	30.63	31.19	22.53	19.04
	4	31.91	44.72	35.96	34.25	32.34	37.09	41.24	36.59	27.79	24.63
Lithic Tuff 2	0	6.52	3.21	5.40	7.85	2.81	2.60	6.71	0.93	1.84	3.15
	1	10.02	3.74	9.15	7.55	2.02	4.60	7.05	3.30	4.27	5.83
	2	11.74	5.85	11.25	8.92	3.09	6.61	9.06	5.67	6.71	8.31
	3	15.45	9.89	15.04	11.96	6.03	8.61	12.73	8.03	9.15	10.79
	4	19.61	15.85	20.51	16.65	10.83	10.62	18.06	10.40	11.59	13.27

Table 5.28. Laboratory and Predicted Specific Energy Results for Nine Different Statistical Models and for All Rock Types (continued) (M=Model)

Type of Rock	Wear Flat W_F (mm)	Laboratory Specific Energy (MJ/m ³)	Predicted Specific Energy (MJ/m ³)								
			M1	M2	M3	M4	M5	M6	M7	M8	M9
Claystone	0	1.44	0.83	10.87	6.90	4.69	1.50	7.31	1.40	0.22	1.31
	1	1.71	0.94	6.21	4.66	1.93	1.58	4.56	1.92	0.94	4.49
	2	1.79	0.17	5.19	4.09	1.04	1.66	3.47	2.45	1.66	5.08
	3	1.92	1.31	5.86	5.18	2.01	1.74	4.04	2.97	2.38	5.66
	4	2.15	4.38	8.21	7.94	4.84	1.82	6.27	3.50	3.10	6.25
Siltstone 1	0	9.96	8.73	3.57	5.71	5.33	3.25	8.54	6.66	14.77	3.53
	1	15.67	12.06	11.34	14.49	13.75	14.25	17.59	17.65	25.25	21.14
	2	19.19	21.07	22.05	24.93	24.03	25.25	28.30	28.65	35.73	32.49
	3	22.08	32.00	34.44	37.05	36.17	36.25	40.67	39.64	46.21	43.83
	4	33.34	44.85	48.52	50.82	50.18	47.25	54.70	50.63	56.69	55.17
Siltstone 2	0	27.68	29.53	21.73	20.00	19.28	17.80	31.43	20.63	24.60	22.91
	1	39.58	40.72	40.93	39.45	38.52	39.38	49.47	41.77	44.53	48.52
	2	48.92	62.28	60.47	60.57	59.62	60.95	69.18	62.90	64.47	70.28
	3	87.39	85.76	81.70	83.35	82.59	82.53	90.54	84.04	84.41	92.04
Andesite	0	23.34	25.39	27.45	28.73	30.98	26.24	28.25	23.87	16.91	15.28
	1	42.34	40.04	34.34	38.20	40.10	37.93	38.97	35.52	28.01	25.58
	2	50.25	50.00	46.73	49.34	51.09	49.61	51.34	47.18	39.10	37.61
	3	64.21	61.87	60.82	62.14	63.93	61.30	65.37	58.83	50.20	49.63
	4	86.9	75.66	76.59	76.61	78.65	72.99	81.06	70.48	61.29	61.65
Travertine	0	28.28	37.28	33.68	33.31	33.29	31.97	22.62	26.79	31.51	32.49
	1	43.79	46.82	46.61	46.94	46.63	47.78	36.07	42.40	46.28	45.88
	2	61.78	63.01	61.65	62.23	61.83	63.58	51.17	58.00	61.06	61.96
	3	84.45	81.12	78.38	79.20	78.89	79.39	67.94	73.60	75.84	78.04

CHAPTER 6

CONCLUSIONS AND RECOMMENDATIONS

In this study, effect of cutting tool wear on its cutting performance was investigated. Although the laboratory cutting specific energy obtained by standard cutting test is known to give good indication of the ease of cutting and the cutting performance of a roadheader, the predicted performance can only be achieved if sharp cutting tools are used. Cutting tools on the other hand, get blunted sometimes very quickly depending on the type of rock being cut, causing a decrease in cutting performance and an increase in cutting forces. Increased pick forces cause not only the reduction in cutting rate but can damage the tool itself and machine by creating high vibration and high variation in the cutter head torque. Therefore it is important to establish the critical wear rate at which the blunted tool should be replaced. The critical wear rate, on the other hand, changes depending on the mechanical properties of the rock to be cut. Therefore it is important to establish the critical wear rates in relation to rock properties. Critical wear rates have been determined by considering the critical laboratory cutting specific energy 25 MJ/m^3 above which poor cutting performance is expected.

The major conclusions derived from this study and the recommendations can be summarized as follow:

- 1) A significant correlation exists between the laboratory cutting specific energy, mean cutting force and the uniaxial compressive strength. Specific energy and cutting force rise slightly with increasing wear rate for low strength rocks, but the increase is very rapid for higher strength rocks. Specific energy increases 4-5 times with the pick having 4 mm wear flat for higher strength rocks as compared to sharp picks. Mean cutting force also increases 2-3 times with 3-4 mm wear flats as compared to sharp picks.

2) Since the critical limit of specific energy is considered to be 25 MJ/m^3 (Table 2.4) above which poor and difficult cutting condition is expected, this limit is not exceeded even with 4 mm wear flat up to an uniaxial compressive strength of 20 MPa. The limit is exceeded even with 1 mm wear flat when the UCS exceeds 35 MPa. Therefore it can be concluded that, the critical wear flat rate decreases as the UCS of the rock increases.

3) Rather low correlation exists between the cutting specific energy, mean cutting force and the Brazilian tensile strength. But in general, specific energy and cutting force increase slightly for low tensile strengths and rapidly as the tensile strength increases. Specific energy increases about 4 times and the cutting force increases about 2-3 times with larger wear flats as compared to sharp picks for higher strength rocks.

4) Specific energy remains below 25 MJ/m^3 even with 4 mm wear flat for rocks having less than about 3 MPa tensile strength, but the critical limit is exceeded even with 1 mm wear flat when the tensile strength exceeds 6 MPa.

5) Rather high correlation exists between the specific energy, cutting force and the cone indenter hardness. Both specific energy and cutting force increase rapidly with increasing standard cone indenter number. Specific energy and cutting force increase about 3-4 times with 4 mm wear flat as compared to sharp pick at a standard cone indenter hardness number of about 2.

6) Specific energy remains below 25 MJ/m^3 even with 4 mm wear flat if the cone indenter hardness remains below 1.2, but the critical limit is exceeded even with 1 mm wear flat when the cone indenter hardness exceeds 2.

7) Rather low correlation exists between the specific energy, cutting force and the Shore hardness. But in general, both the specific energy and the cutting force increase rapidly with increasing Shore hardness. The increase is about 4 times in specific energy and about 2-3 times in cutting force as compared to sharp picks for higher shore hardness values.

8) Specific energy does not increase above 25 MJ/m^3 even with 4 mm wear flat if the Shore hardness remains below 15, whereas the limit is exceeded even with 1 mm wear flat when the Shore hardness is above 30.

9) Rather good correlation exists between the specific energy, cutting force and the Schmidt hammer hardness. The specific energy and the cutting force increase rapidly as the Schmidt hammer hardness and the wear rate increase. The increase is about 3-4 times in specific energy and about 2-3 times in cutting force as compared to sharp picks at higher Schmidt hammer values.

10) Critical specific energy is not exceeded even with 4 mm wear flat for Schmidt hammer values less than about 25-30, whereas it is exceeded even with 1 mm wear flat when the Schmidt hammer value is above 40.

11) Although the correlation is low, the specific energy and the cutting force increase rapidly as the rock density and the wear flat increase. The increase is about 3-4 times in specific energy and about 2 times in cutting force with 4 mm wear flat as compared to sharp picks for rocks with higher densities.

12) Specific energy remains below critical limit even with 4 mm wear flat for the densities below 1.7 gr/cm^3 , whereas it is exceeded even with 1 mm wear flat when the density is above 2.2 gr/cm^3 .

13) No correlation has been determined between the mineral grain size, specific energy and cutting force.

14) Breakout angles of the rock samples studied varied between 42° and 74° . Breakout angle causes a reduction in the specific energy by producing more product. Due to this reason, comparatively low specific energies have been obtained for some rock types in spite of the significant differences in cutting forces and rock properties.

15) No definite relationship has been observed between the wear flat and the rate of degradation. Although coarseness index increases slightly for some rock types with increasing wear flat representing a higher rate of degradation, the result is not consistent and the same effect has not been observed for all rock types. Therefore the increase in specific energy with blunt tools can be explained by the increase in cutting forces though the increased rate of degradation may be an additional cause for some rock types.

16) Nine models have been developed by statistical analysis to predict the laboratory cutting specific energy from different rock properties and wear flat rates. Using the models, the laboratory cutting specific energy can be estimated with correlation coefficients varying from 0.9476 to 0.8359. The models can also be used to estimate the critical wear flat rates for a certain specific energy for a particular rock.

17) Working life of worn cutting tools can be extended effectively if possible increases in the specific energy and the cutting force are determined in relation to the type of rock to be cut.

18) Prediction charts produced (Figures 4.2, 4.5, 4.8, 4.11, 4.14, 4.17) can be used to estimate the time for a pick renewal by establishing wear flat rates causing greater than 25 MJ/m³ specific energy at different rock property values.

The study has been carried out on soft to medium strength rocks because there is a risk of a cutting tool or dynamometer failure and a breakdown in the cutting set up due to very high cutting forces which may develop while cutting with large wear flats. Cutting tests can be applied on higher strength rocks if the forces developing are carefully checked and found to be safe. Other rock properties such as matrix material, texture coefficient can also be included in the studies. Field studies can be carried out to determine the effect of pick blunting on cutting head vibration.

REFERENCES

- ATKINSON, T., CASSAPI, V.B. and SINGH, R.N. 'Assessment of Abrasive Wear Resistance Potential in Rock Excavation Machinery'. International Journal of Mining and Geological Engineering, Technical Note, 1986. 3. P.151-163
- BALCI, C. and BILGIN, N. 'Mekanize Kazı Makinalarının Seçiminde Küçük ve Tam Boyutlu Kazı deneylerinin Karşılaştırılması'. İTÜ, Maden Fakültesi, Maden Mühendisliği Bölümü, Haziran 2005.
- BALCI, C., DEMİRCİN, M.A., COPUR, H. and TUNCDEMİR, H. 'Estimation of Optimum Specific Energy Based on Rock Properties for Assessment of Roadheader Performance'. The Journal of the South African Institute of Mining and Metallurgy, December 2004.
- BARKER, J.S., POMEROY, C.D. and WHITTAKER, B.N., 'The MRE Large Pick Shearer Drum'. The Mining Engineer, February 1966, p.323.
- BILGIN, N., DEMİRCİN, M.A., COPUR, H., BALCI, C., TUNCDEMİR, H. and AKCİN, N. 'Dominant Rock Properties Affecting the Performance of Conical Picks and the Comparison of Some Experimental and Theoretical Results'. International Journal of Rock Mechanics and Mining Sciences. İstanbul Technical University, Mining Engineering Department, 2005.
- BILGIN, N., YAZICI, S., ESKİKAYA, Ş., "A Model to Predict the Performance of Roadheaders and Impact Hammers in Tunnel Drivages", EUROCK '96, pp. 710-721, Torino, September 2-5, 1996.
- BILGIN, N. 'Investigations into the Mechanical Cutting Characteristics of Some Medium and High Strength Rocks'. Ph.D. Thesis, University of Newcastle upon Tyne, June 1977.

- BILGIN, N., KUZU, C., ESKİKAYA, Ş., OZDEMİR, L. ‘Cutting Performance of Jackhammers and Roadheaders in İstanbul Metro Drivages’. Presented at World Tunnel Congress, Vienna, 1997.
- BÖLÜKBAŞI, N. ‘Studies on the Design and Operation of Some Longwall Mining Systems Using A^{1/4} Scale Model’. Ph.D. Thesis, university of New Castle Upon Tyne, Nov.,1973.
- BÖLÜKBAŞI, N. ‘O.A.L. Beypazarı Bölgesi Kayaçlarının Kazılabilirlik Tayini’. ODTÜ, Maden Mühendisliği Bölümü, Ankara, 1989.
- BÖLÜKBAŞI, N. ‘Yeraltı Kömür ve Ayak Kazı Mekanizasyonu’, TKİ Genel Müdürlüğü Seminerleri No.4, Mining Eng.Dept. METU, Ankara, August, 1986.
- ÇOPUR, H., ÖZDEMİR, L., ROSTAMI, J., “Roadheader Applications in Mining and Tunneling Industries”, The Mining Engineer, pp. 38-42, March, 1998.
- DALZIEL,J.A. and DAVIES, E. ‘Initiation of Cracks in Coal Specimens by Blunted Wedges’. The Engineer, 217, 1964.pp.217-220.
- DAWIHL, W. and MAL, M. K. ‘Contribution to the Study of the Deformation Behaviour and Structure of Wc-Tic-Tac-Co Alloys’. Cobalt, 26, March 1965, p.25.
- DOEG, H.H. ‘Cemented Hard Metals-Their Bases With Particular Reference to the Tungsten CarbideCobalt System’. J.South African Inst. Min.Metall.60,12,July 1960.p.663.
- EKEMAR, C.S.G., IGGSTROM, S.A.O. and HEDEN, G.K.A. ‘The Influence of Some Metallurgical Parameters of Cemented Carbide on the Sensitivity on the Thermal Fatigue Cracking at Cutting Edges’. BISRA-ISI Conference on Materials for Metal Cutting,Scarborough, April 14-16, 1970, p.103.

- ESKİKAYA, Ş., BILGIN, N., DINCER, T., OZDEMIR, L., 'A Model to Predict Cutting Performance of Rapid Excavation Systems'. 7th Symposium on Mine Planning and Equipment Selection, Calgary, pp.575-579. Balkema, Rotterdam, October, 1998.
- EVANS, I. 'Relative Efficiencies of Picks and Discs for Cutting Rocks'. Advances in Rock Mechanics, Proc.3, Conf. Int. Soc. for Rock Mechanics, Denver, U.S.A., vol.2-B, National Academy of Sciences, 1974, p.1399.
- EVANS, I. 'A Theory of The Basic Mechanics of Coal Ploughing'. Int. Symp. Of Mining Research, vol.2, Pergamon, 1962, p.761.
- EVANS, I. and POMEROY, C.D., 'The Strength, Fracture and Workability of Coal'. Pergamon, London 1966.
- EYYUBOĞLU, E.M. 'Effect of Cutting Head Design on Roadheading Machine Performance at Çayırhan Lignite Mine'. Ph.D. Thesis, METU, 145p.2000.
- EXNER, H.E. and GURLAND, J. 'A Review of Parameters Influencing Some Mechanical Properties of Tungsten Carbide-Cobalt Alloys'. Powder Metallurgy, 13,25,1970. p.13.
- FOWELL, R.J. and PYCROFT, A.S. 'Rock Machinability Studies For The Assessment of Selective Tunnelling Machine Performance'. 21st National Rock Mechanics Symp. USA, Miss.pp.149-158,1980.
- FOWELL, R.J. 'A Simple Method for Assessing the Machineability of Rocks'. Tunnels and Tunnelling. July 1970.
- FOWELL, R.J. 'Studies on the Application of Percussively Activated Tools to Reef Slotting in Some South African Quartzites'. Ph.D.Thesis, University of Newcastle upon Tyne, December 1973.

- FOWELL, R.J. and JOHNSON, S.T. 'Rock Classification and Assessment for Rapid Excavation'. Proc. Of the Symp. On Strata Mech. Newcastle Upon Tyne, pp.241-244, 1982.
- FOWELL, R.J. and McFEAT-SMITH, I. 'Factors Influencing The Cutting Performance of a Selective Tunnelling Machine'. Proceedings of Tunnelling Symposium, 76. Department of Mining Engineering, University of Newcastle upon Tyne, England, 1976, p.301.
- FOWELL, R.J., RICHARDSON G. And GOLLICK M.J. 'Prediction of Boom Tunnelling Machine Excavation Rates'. Nelson pp.Laubach S.editors. Proceedings of the Symposium on Rock Mechanics Models and Measurements Challenges form Industry,1994.p.243-51
- FOWELL, R.J. and PYCROFT, A.S., 'Rock Machineability Studies for the assessment of the selective tunneling'.Elsevier, Newcastle Upon Tyne,1982,p.241-244.
- GEHRING, K. H., "A cutting comparison", Tunnels & Tunneling, pp. 27-30, November, 1989.
- GÖKTAN, R. M. and GÜNEŞ, N., "A Comperative Study of Schmidt Hammer Testing Procedure with Reference to Rock Cutting", International Journal of Rock Mechanics & Mining Sciences, Vol. 42, pp. 466-472, 2005.
- GURLAND, J. 'A Study of the Effect of Carbon Content on the Structure and Properties of Sintered Wc-Co Alloys'. Journal of Metals, Feb.1954,p.285.
- HARA, A. and YAZU, S. 'On the Strength Recovery Phenomena by Annealing Cemented Carbides Contraining Cracks'. Nippon Kinzoku Gakkai-Si,32,1,January 1968, p.61.

- HARLE, M.R. 'An Investigation of Some Fundamental Aspects of Three Dimensional Chip Formation in Rock Cutting'. M.Sc. Dissertation, University of Newcastle upon Tyne, August 1973.
- HEKİMOĞLU, O.Z., 'Studies in the Excavation of Selected Rock Materials with Mechanical Tools'. Ph.D Thesis, University of Newcastle Upon Tyne, 342p.,1984.
- HURT, K.G. and MACANDREW, K.M. 'Cutting Efficiency and Life of Rock Cutting Picks', Mining Science and Technology, 2 (1985),pp.139-151.
- ISRM, (International Society for Rock Mechanics). 'Rock Characterization Testing and Monitoring', ISRM Suggested Methods, Brown, E.T.(Editor),Pergamon Press,211p.2007.
- IVENSEN, V.A., CHISTYAKOVA, V.A. and EIDUK, O.N. 'Changes in Properties of Wc-Co Hard Alloys During Deformation and the Restoration of these Properties During Annealing -1 Effects of Deformation in Uniaxial Compression on Some Physical and Mechanical Properties of Hard Alloys'. Sov.Powder Metall. Met.Cer. 12,9,Sept.1973, p.722.
- JACKSON, I, F., and HARTMAN, H., L. 'An Investigation of Hard Metal Inserts for Cutting Slate'. Transactions American Society of Mining Engineers,September, 1962, p.255.
- JOHNSON, S.N. and MORGANS, W.T.A. 'A Laboratory Study of Abrasive Wear in Cutting Tools: III: The Cutting Performance of Tungsten Carbide and Other Tool Materials as Wear Progresses'. National Coal Board, MRDE Report No.1. October 1969.
- KELEŞ, S. 'Cutting Performance Assessment of a Medium Weight Roadheader at Çayırhan Coal Mine'. M.Sc. Thesis, Middle East Technical University, 58p.,2005

- KENNY, P. and JOHNSON, S.N. 'The Effect of Wear on the Performance of Mineral-Cutting Tools'. Colliery Guardian, June 1976, p.246.
- KENNY, P. and JOHNSON, S.N. 'An Investigation of the Abrasive Wear of Mineral Cutting Tools', 36, 1976, p.337.
- LARDNER, E. 'Review of Current Hardmetal Technology'. Conf.Materials for Metal Cutting. The Iron and Steel Institute. 1970.p.122.
- LARDNER, E. 'Isostatically Hot Pressed Hard Metal'. The Production Engineer, March-April,1974, p.113-118.
- LATIN, A. 'The Properties of Tungsten Carbide-Cobalt Alloys Used for Mineral Cutting Tools'. Metallurgia, 64, Nov., Dec. 1961, p.211,267.
- LATIN,A., 'Studies of the Wear and Fracture of Cemented Carbides as used in Coal Mining Tools'. MRE Report no. 2025, National Coal Board, 1955.
- LATIN, A. and WILLIAMS, S.R. 'Further Studies of the Wear and Fructure of Cemented Carbides as used in Coal Mining Tools'. MRE Report no. 2106, National Coal Board, 1958.
- MAHER, D.J. 'An Investigation into the Effects of Wear on Rock Cutting Systems'. M.Sc.Dissertation, University of Newcastle Upon Tyne, August,1973.
- McFEAT-SMITH, I. 'Correlation of Rock Properties and Tunnel Machine Performance in Selected Sedimentary Rocks'. Ph.D. Thesis, University of Newcastle upon Tyne, June 1975.
- McFEAT-SMITH, I. and FOWELL, R.J. 'Correlation of Rock Properties and the Cutting Performance of Tunnelling Machines'. Proceedings Conference on Rock Engineering, 4-7 April 1977, Newcastle upon Tyne, p.581.
- MERCHANT, M.E. 'Basic Mechanics of the Metal Cutting Process'. J.Applied Mechanics, 11, 1945, p.A.168.

- MONTGOMERY, W.E. 'Carbides, Their Properties Testing and Grade Selection'.
ASTME Nat.Eng.Conference, Philadelphia, ASTME Paper MR
68-172, May 1968a.
- MONTGOMERY, R.S. 'The Mechanism of Percussive Wear of Tungsten Carbide
Composites'. Wear, 12, 5, Nov. 1968b, p.309.
- MONTGOMERY, R.S. 'Percussive Wear Properties of Cemented Carbides'.
Transactions of the Mining Society of A.I.M.E. 244, June 1969,
p.153.
- MONTGOMERY, D.C. 'Design and Analyses of Experiments'. 5th Edition, Arizona
State University, 1997.
- MRDE, 'NCB Cone Indenter'. Handbook No.5, Burton on Trent, 12p. 1977.
- NEIL, D.M., ROSTAMI, J., OZDEMİR, L. and GERTSCH, R. 'Production
Estimating Techniques for Underground Mining Using
Roadheaders'. SME, AIME Annual Meeting, Albuquerque, New
Mexico, 1994.
- NISHIMATSU, Y. 'The Mechanics of Rock Cutting'. Int.J.Rock Mechanics. Min.
Sci., 9, 1972, p.261.
- OSBURN, H.J. 'Some Consideration of the Metallurgy of Rock Cutting Tools'.
M.Sc.Dissertation, University of Newcastle upon Tyne.
September, 1968.
- OSBURN, H.J. 'Wear of Rock Cutting Tools'. Powder Metallurgy, 12,24,1969,
p.471.
- PARIKH, N.I. 'Modes of Fracture and Slip in Cemented Carbides'.
J.Amer.Cer.Soc.40,10,1957,p.335.
- PEARSE, G. 'Machines for Mining Headings'. Mining Magazine, pp 33-49,
July,1987.

- PHILLIPS, H.R. 'Rock Cutting Mechanics Related to the Design of Primary Excavation Systems'. Ph.D. Thesis, University of Newcastle upon Tyne, October 1975.
- POOLE, R.W., FARMER, I.W., 'Geotechnical Factors Effecting Tunneling Machine Performance in Coal Measures Rock'. Tunnels and Tunneling, pp.27-30. December 1978.
- RISPIN, A. 'An Investigation Into the Application of Linear Cutting Tools to the Machining of Strong and Abrasive Rock Materials'. Ph.D. Thesis, University of Newcastle upon Tyne, October 1970.
- ROBBINS, R.J., 'Mechanised Tunnelling – Progress and Expectations'. Twelfth Sir Julius Wernher Memorial Lecture, Tunnelling, The Institution of Mining and Metallurgy, 1976.
- ROXBOROUGH, F.F. and RISPIN, A. 'The Mechanical Cutting Characteristics of the Lower Chalk'. Report to T.R.R.L., May 1972, Department of Mining Engineering, University of Newcastle upon Tyne.
- ROXBOROUGH, F.F. and RISPIN, A. 'The Mechanical Cutting Characteristics of the Lower Chalk'. Tunnels and Tunneling. January 1973. p.45.
- ROXBOROUGH, F.F. 'Cutting Rock with Picks'. The Mining Engineer, June 1973, p.445.
- ROXBOROUGH, F.F. and PHILLIPS, H.R. 'Experimental Studies on the Excavation of Rocks Using Picks'. Advances in Rock Mechanics, Proc. of the 3rd ISRM Congress, Denver, 1974.
- ROXBOROUGH, F.F. and PHILLIPS, H.R. 'The Mechanical Properties and Cutting Characteristics of the Bunter Sandstone'. Report to the TRRL, Department of Mining Engineering, University of Newcastle upon Tyne, March 1975.
- SCHNEIDER, H., 'Criteria for Selecting a Boom-Type Roadheading'. Mining Magazine, pp.183-187, September 1988.

- SHAW, M.C. 'Metal Cutting Principles'. Clarendon Press-Oxford, 1977.
- SPAUN,G. and THURO,K. 'Drillability in Hard Rock Drill and Blast Tunnelling, Felsbau, 14, 103-109, 1996.
- SPEIGHT, H.E. and FOWELL, R.J. 'The Influence of Operational Parameters of Roadheader Productivity and Efficiency With Particular Reference to Cutting Pick Wear'. Dosco Overseas Engineering, Newark, University of Newcastle upon Tyne, 1984.
- SUZUKI, H., HAYASHI, K. 'Effects of the Carbon Content on the Properties of Wc-Tic-Co Alloys'. Transactions of the Japan Institute of Metals, 7, 3, July,1966, p.199.
- THURO, K. And PLINNINGER, R.J., 'Geological Limits in Roadheader Excavation-Four Case Studies'. 8th International IAEG Congress, Balkema, Rotterdam, 21-25 September 1998.
- THURO, K., PLINNINGER, R.J., "Roadheader Excavation Performance – Geological and Geotechnical Influences", 9th ISRM Congress Paris, Theme 3: Rock Dynamics and Tectonophysics/Rock Cutting and Drilling, 25-28 August, 1999.
- TUCKER, R.H., 'Improvement of Potential in Mining Development and Tunneling Systems in the National Coal Board'.The Mining Engineer, pp.663-669, June 1985.
- ULUSAY, R and HUDSON, J.A., 'The Complete ISRM Suggested Methods for Rock Characterization, Testing and Monitoring, 1974-2006.

VITA

PERSONAL INFORMATION

Surname, Name : Dođruöz, Cihan
Nationality : Turkish (TC)
Date of Birth and Place : 04.01.1980, Ankara
Marital Status : Single
Phone : +9 0 312 566 21 74
 +9 0 312 210 26 56
 +9 0 533 542 08 16
E-mail : dogruoz@metu.edu.tr
 cihandogruoz@hotmail.com
Web : www.cihandogruoz.com
Driving Licence : Class B



EDUCATION

2005-2010 Middle East Technical University (METU), Mining Eng. Dept.,
Philosophy of Doctorate (PhD), Ankara.
2004-2005 Middle East Technical University (METU), Mining Eng. Dept.,
Scientific Preperation, Ankara
2003-2004 Middle East Technical University (METU), Foreign Languages
Department, Ankara
2000-2003 Dumlupınar University, Master of Science (MS), Kütahya
1996-2000 Dumlupınar University, Mining Eng. Dept.(BS), Kütahya
1993-1996 Seyranbađları High School, Ankara

WORK EXPERIENCE

2000-2001 Orhan Marble Ind.Trade Ltd.Co., Afyon ,Turkey
Export Manager
2001-2003 Dumlupınar University, Mining Eng. Dept.
Research and Teaching Assistant (Mine Mechanization, Mine Survey)
2003 - 2010 Middle East Technical University (METU), Mining Eng. Dept.
Research and Teaching Assistant (Mine Mechanization, Mine Survey)

PARTICIPATED PROJECTS

- Valuation of Seyitömer Lignite Basin by Surpac Vision
- Electronic Commerce and Its Importance for the Development of Turkish Mining Sector
- Geothermal Energy, Turkey Potential and Environmental Evaluation
- Entrance to the Kırdar Quarry Bench Stability
- Total Quality Management System of Orhan Marble Factory

FIELD OF PROFESSIONAL INTERESTS

- Mine Mechanization
- Mine Excavation
- Mine Survey
- Cement Production
- Concrete